coatings

MDPI

Review

Green Synthesis of Metal and Metal Oxide Nanoparticles Using Different Plants' Parts for Antimicrobial Activity and Anticancer Activity: A Review Article

Aysha Bukhari [1], Irfan Ijaz [1,*], Ezaz Gilani [1], Ammara Nazir [1], Hina Zain [2], Ramsha Saeed [3], Saleh S. Alarfaji [4], Sajjad Hussain [1], Rizwana Aftab [1] and Yasra Naseer [3]

1 School of Chemistry, Faculty of Basic Scieneces and Mathematics, Minhaj University Lahore, Lahore 54700, Pakistan; ayshabukhari.che@mul.edu.pk (A.B.); ezazgilani.chem@mul.edu.pk (E.G.); Ammaranazir.chem@mul.edu.pk (A.N.); sajjaduet07@yahoo.com (S.H.); Rizab2008@hotmail.com (R.A.)
2 Department of Allied Health Sciences, Superior University Lahore, Lahore 54700, Pakistan; Hina.zain@superior.edu.pk
3 Department of Chemistry, Forman Christian College Lahore, Lahore 54700, Pakistan; Ramsha.sd@gmail.com (R.S.); yasra.naseer@gmail.com (Y.N.)
4 Department of Chemistry, Faculty of Science, King Khalid University, Abha 61413, Saudi Arabia; ssalarvagi@kku.edu.sa
* Correspondence: iffichemixt266@gmail.com

check for updates

Citation: Bukhari, A.; Ijaz, I.; Gilani, E.; Nazir, A.; Zain, H.; Saeed, R.; Alarfaji, S.S.; Hussain, S.; Aftab, R.; Naseer, Y. Green Synthesis of Metal and Metal Oxide Nanoparticles Using Different Plants' Parts for Antimicrobial Activity and Anticancer Activity: A Review Article. *Coatings* **2021**, *11*, 1374. https://doi.org/10.3390/coatings11111374

Academic Editor: Grzegorz Dercz

Received: 19 August 2021
Accepted: 12 October 2021
Published: 9 November 2021

Abstract: Nanotechnology emerged as a scientific innovation in the 21st century. Metallic nanoparticles (metal or metal oxide nanoparticles) have attained remarkable popularity due to their interesting biological, physical, chemical, magnetic, and optical properties. Metal-based nanoparticles can be prepared by utilizing different biological, physical, and chemical methods. The biological method is preferred as it provides a green, simple, facile, ecofriendly, rapid, and cost-effective route for the green synthesis of nanoparticles. Plants have complex phytochemical constituents such as carbohydrates, amino acids, phenolics, flavonoids, terpenoids, and proteins, which can behave as reducing and stabilizing agents. However, the mechanism of green synthesis by using plants is still highly debatable. In this report, we summarized basic principles or mechanisms of green synthesis especially for metal or metal oxide (i.e., ZnO, Au, Ag, and TiO_2, Fe, Fe_2O_3, Cu, CuO, Co) nanoparticles. Finally, we explored the medical applications of plant-based nanoparticles in terms of antibacterial, antifungal, and anticancer activity.

Keywords: ecofriendly synthesis; seed; nanotechnology; biological activity

1. Introduction

Technology and science are moving at the highest rate for developing green technology. Nanotechnology is one of the most interesting topics utilized to produce and employ materials having interatomic structural characteristics. Nanotechnology emerged as scientific innovation in the 21st century. Nanoparticles can be defined as particles having the size in the range of 1–100 nm and exhibited dimensions on a scale of one-billionth of a meter [1–3]. Nanoparticles are advanced materials in technology and science and have various applications in agriculture [4,5], medical [6], electronic [7], chemical [8], and pharmaceutical [9] fields. The biosynthesis of nanoparticles with desired morphology (shape, size, and crystalline nature) has been one of the basic aims in chemistry that can be utilized for various applications, e.g., catalysis, biomedical, lower-cost electrode, and biosensor [10–12]. Except for their unique chemical and physical properties, nanoparticles behaved as a bridge between molecular or atomic structure and bulk materials. Thus, they are the best candidate for many important applications such as biotechnology, trace substance identifications, medical, and electrochemistry [13–16]. Different synthetic approaches have been used for the fabrication of nanoparticles with desired the morphology

and size. Although these approaches have resulted in superior nanoparticles, still a basic understanding of the improved fabricating process is required that could be utilized at the commercial and industrial levels. To achieve nanoparticles of desired morphology, two different basic approaches of synthesis (such as bottom-up and top-down methods) have been studied in the existing literature, shown in Figure 1. Conventionally, nanoparticles are synthesized through a diverse range of preparation methods such as ball milling, sputtering, lithographic techniques, and etching [17]. The utilization of the bottom-up approach (in which nanoparticles are prepared from simpler substances) also involves various protocols such as sol–gel process, molecular/atomic condensation, chemicals' vapor deposition, laser pyrolysis, and spray pyrolysis, shown in Figure 1 [18]. New fields, i.e., green synthetic methods, are attaining remarkable attention in current development and research on materials science. Mainly, green synthesis of nanoparticles, prepared through regulation, clean-up, control, and remediation processes will uplift their ecofriendliness. Some fundamental principles of bio-synthesis can therefore be described by various components such as reduction of pollution, utilization of non-toxic solvent, prevention of waste, and renewable feed-stock [19]. Biosynthesis is essential to avoid the formation of harmful by-products through an environmentally friendly and sustainable approach. Biosynthesis of metal and metal oxide nanoparticles has been adopted to accommodate several biological entities such as plant extracts, bacteria, and algae. Among the existing green approaches of preparation for metal and metal oxide nanoparticles, using the plant is a rapid, easy, and simple process to synthesize nanoparticles at a large level as compared to algae-, fungi-, and bacteria-based prepared nanoparticles The prepared green nanomaterials have a great application in the pharmaceutical industry such as novel pharmaceuticals preparation, drug delivery personification procedures, and synthesis of functional nanodevices [20].

Here, we summarized the current research on the biosynthesis of metallics and their oxide nanoparticles with their advantages as compared to physical and chemical synthetic approaches. Additionally, we also described the essential role of various biological components (amino acid, carbohydrate, flavonoid, terpenoid, protein, and polyphenol) and solvent systems in the synthesis of metal and metal oxide nanoparticles. The objective of this review was to promote green synthesis, which is simple, cost-effective, and ecofriendly, so the novelty of this review article lies in explaining the recently reported (2019–2021) green synthetic methods of metal and metal oxide nanoparticles from plants and their capacity as antimicrobial and antibacterial agents.

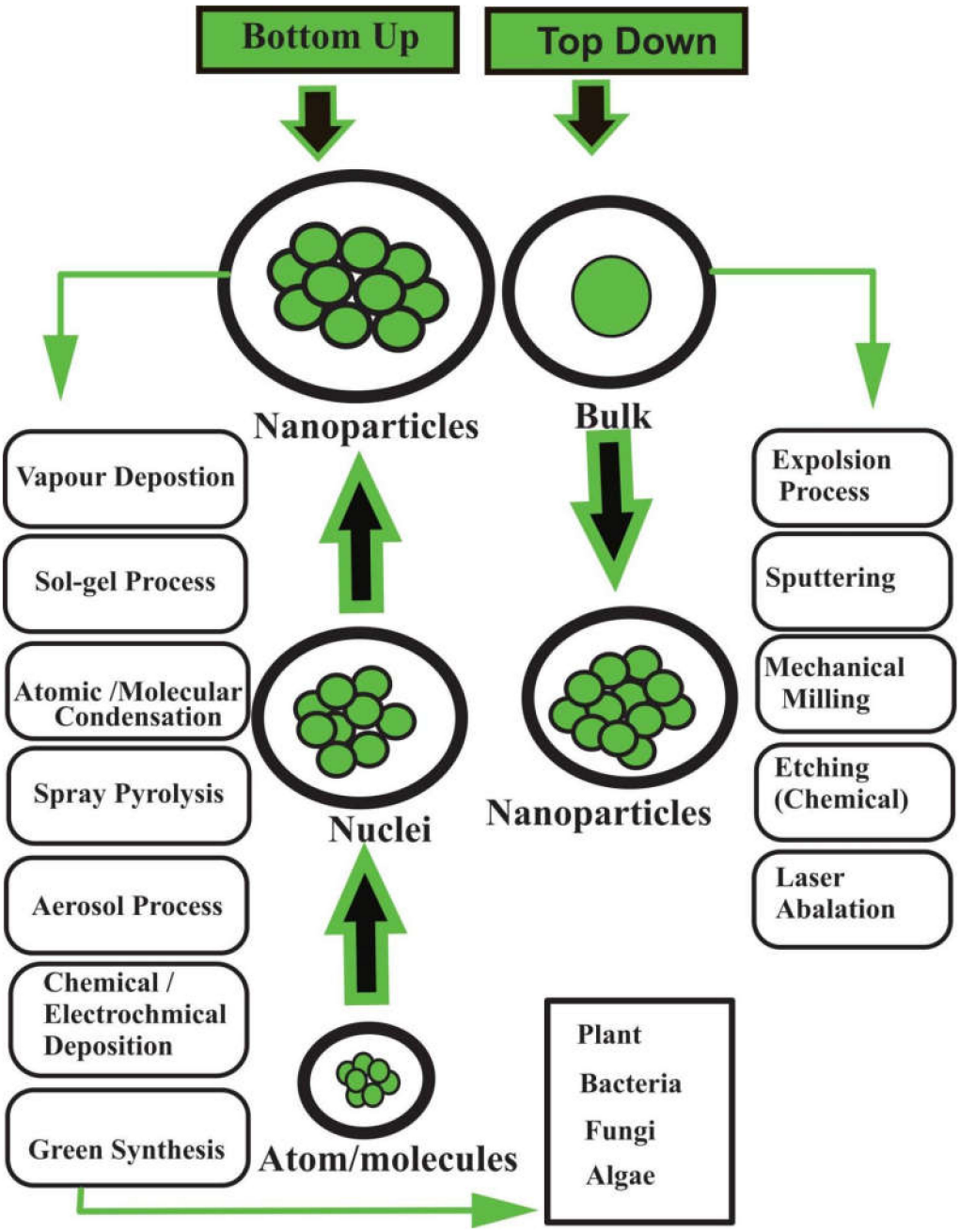

Figure 1. Top-up and bottom-down synthetic methods of metal and metal oxide nanoparticles.

2. Green Chemistry and Sustainable Principle

Green chemistry for sustainable development has been reported for less than 15 years [21]. Sustainable development can be termed as the development that accounts for and includes the needs of presently fulfilling and the capability of incoming generations [22]. Sustainable development has unique importance for industrial chemistry because it is concerned with pollution and the use of natural sources [23]. Chemistry has been considered a toxic branch of science, and, normally, the word chemical is associated with toxicity and hazards [24]. Generally, there are many methods to reduce risk by using protection, which is known as protective gear. When these methods fail, the risk of toxicity and hazards is increased. Due to high toxicity and hazards, the outcome can be more harmful, like injuries and deaths [25,26]. Therefore, safe, sustainable methods and procedures help to decrease toxicity and hazard to reduce the danger of accidents and damages [27,28].

3. Synthesis of Metal and Metal Oxide Nanoparticles Using Plants

In biological synthesis (using different organisms such as plants, bacteria, fungi, algae, and actinomycetes) of metal or metal oxide nanoparticles, ecofriendly accepted "green chemistry" ideas have been employed [29]. Biological synthesis of nanoparticles via biological organisms is summarized as a green substitute for the synthesis of nanoparticles having desired properties. In biological synthesis, both types of organisms (i.e., unicellular and multicellular) are permitted to react [30]. Plants are well-known chemical factories of nature that are inexpensive and ecofriendly. Plants have shown remarkable potential in heavy metals' detoxification and collection, by which environmental contamination and pollutants' problems can be resolved because the traces of these heavy metals are also hazardous. There are many benefits for nanoparticles' synthesis via plant extract as compared to other biosyntheses such as by bacteria, fungi, actinomycetes, and algae [31]. One advantage of plant-mediated NPs is that the kinetics for this method are sufficiently higher than other biological methods. Different parts of plants, i.e., leaf, stem, seed, fruit, and roots, have been extensively used for the biosynthesis of nanoparticles because of the presence of remarkable phytochemicals [32]. For the synthesis of nanoparticles, specific parts of the plant are washed with tap or distilled water, after squeezing, filtering, and adding respective salt solutions, whose nanoparticles we wish to synthesize. The color of the solution begins to change, thus revealing the synthesis of nanoparticles, which we can separate easily.

4. Role of Capping Agents in the Synthesis of Metal and Metal Oxide Nanoparticles

Capping agents play an essential role in the synthesis of nanoparticles' formation. The main role of the capping agent is to stabilize and functionalize the nanoparticles. By using a capping agent, we can impart the useful or desired properties to nanoparticles by controlling size and protecting the surface area and morphology. Various surfactants have been used as a capping agent for changing the desired morphology of nanoparticles, but these surfactants are very tough to remove. Moreover, these surfactants are toxic to our ecosystems [33]. Due to these limitations, there is a need to use ecofriendly capping agents and develop a green route at a commercial and non-commercial level for nanoparticles' formation.

5. Role of Phytochemicals in the Synthesis of Metal and Metal Oxide Nanoparticles

The biosynthesis of nanoparticles compromises three main ingredients, e.g., solvent medium, reducing agents, and stabilizing agents [34–36]. To prepare plant-mediated nanoparticles, the photo component of plant extract serves as a reducing and stabilizing agent. Now, researchers have focused on plant-mediated nanoparticles' biosynthesis due to more advantages over conventional physical and chemical synthetic procedures [37–44].

5.1. Role of Amino Acid in Green Synthesis of Nanoparticles

Synthesis of nanoparticles using bio-molecules has recently attained much interest because of their non-hazardous nature and because they do not involve harsh methods. Amino acid serves as an excellent capping and reducing agent to prepare nanoparticles having a specific structure. Maruyama and coworkers prepared gold nanoparticles with a size range of 4–7 nm by amino acid as a capping agent. There are 20 different types of amino acids. Among these different types, they used L-histidine, which reduced tetraauric acid to gold nanoparticles. The concentration of amino acid (L-histidine) affects the size of nanoparticles. The size of nanoparticles is decreased with an increase in the concentration of amino acids [45]. Qing-Hua Xu reported a single-step formation of gold nanoparticles by using two amino acids (glutamic and histidine) [46]. Meghana Ramani synthesized ZnO nanoparticles of different shapes and sizes by using three types of amino acids such as l-glutamine, l-alanine, and l-threonine. These amino acids played an important role as a capping agent. The surface modification of ZnO nanoparticles due to a capping agent was confirmed by FTIR spectroscopy [47].

5.2. Role of Protein in Green Synthesis of Nanoparticles

In the biosynthesis of nanoparticles, the vital role of proteins cannot be ignored. Proteins can offer a vital role of reduction, by which they donate e (electron) to the Ag+ ion that leads to the synthesis of silver nanoparticles. Recent studies report the potential role of proteins in the formation of silver nanoparticles by using *Capsicum annum* [48]. The absorption spectra of UV-Vis (ultraviolet-visible spectroscopy) showed a strong absorption peak at 210 nm, which the authors attributed to the existence of a peptide bond. While the peak was around 280 nm, the UV-Vis absorption spectrum showed the existence of amino acids, e.g., phenylalanine and tyrosine, that tend to react with silver ion. In another study, casein was utilized as a stabilizing and reducing agent in the synthesis of silver nanoparticles [49]. For the confirmation of the role of protein in the process of formation of nanoparticles, sodium dodecyl sulfate-polyacrylamide gel electrophoresis (SDS-PAGE) analysis of leaf extracts of *Olax scandens* and concentrated supernatants of *O. scandens*-based silver nanoparticles was performed. The results illustrated that some low-molecular-weight peptide bonds present in the extract of leaf were absent in the obtained nanoparticles. Such proteins of low-molecular-weight have been utilized in biosynthesis phenomena. NPs unite with proteins and form a dynamic nanoparticle-protein corona [50]. Similar results were studied in the soya been-mediated synthesis of gold nanoparticles [51].

5.3. Role of Carbohydrates or Saccharides in Green Synthesis of Nanoparticles

The recent study also showed the role of carbohydrates of saccharides in the synthesis of nanoparticles. Raveendran and coworkers utilized sugar and starch as nanoparticles-reducing or -stabilizing agents, respectively. In another study, glucose and hemicellulose were utilized for the synthesis of nanoparticles [52,53]. Polysaccharides are the major class of carbohydrates' molecules with repeating units of mono- and disaccharides that linked each other by a glycosidic bond. Polysaccharides served as a capping agent in the synthesis of nanoparticles. These are the advantages of polysaccharides as a reducing agent:

- Low cost
- Stable
- Safe
- Nontoxic
- Hydrophilic

The green synthesis is performed in the presence of water as a solvent, therefore removing the use of a toxic solvent [54,55]. One of the unique characteristics of polysaccharides is that they sharply accelerate the kinetics of sol-gel methods because of their catalytic effect [56]. Shu-Juan Bao reported an eco-friendly, bio-mimetic method for the synthesis of TiO_2 nanomaterials. Polysaccharides not only have been found to modify the size, shape, and structure of TiO_2 but have induced various phases; rutile phase has been achieved in the presence of chitosan and the anatase phase has been achieved in the presence of starch.

Dextran is a branched polysaccharide that consists of many glucose molecules with a chain of different lengths. Gold nanoparticles were synthesized using natural honey that served as a reducing agent. Fructose in the honey was considered to serve as a reducing agent, while proteins were responsible for the stabilization of nanoparticles [57]. Gold nanoparticles were synthesized using amino cellulose that acted as capping as well as reducing agents.

5.4. Role of Phenolics Acid in Green Synthesis of Nanoparticles

Phenolic acid is a very essential phytochemical that belongs to the polyphenols' family. It is composed of two important functional groups, i.e., carboxylic acid and phenolic ring. Various types of phenolic acid, i.e., ellagic acid, caffeic acid, protocatechuic acid, and gallic acid, are reported as reducing agents for the preparation of metal nanoparticles [58]. It is reported that silver nanoparticles can be prepared upon the formation of a transitional complex of Ag^+ with gallic acid. Consequently, through oxidation phenomena, it converts to quinine that forms silver nanoparticles [59,60].

5.5. Role of Flavonoid in Green Synthesis of Nanoparticles

Flavonoid is the component of plants' pigment that compromises a class of secondary metabolites because of their diversity and biological synthesis in plants [61]. Up until now, 7000 different flavonoid molecules have been reported. Flavonoids can be present in various forms, e.g., flavonol, isoflavones, anthocyanidins, flavones, flavanones, and flavan3-ol. Flavonoids are considered a basic bio-reducing agent of plant extract and their reducing ability is due to their ability to donate hydrogen ions or electrons [62]. Various articles have been published on the electron or hydrogen ion-releasing capability of flavonoids utilized for the preparation of nanoparticles [63–65]. Thus, flavonoids in an extract of the plant are currently utilized as a necessary tool for the primary assessment of untapped plants for the preparation of nanoparticles [66]. In another report, it was reported the production of free hydrogen ions during keto-enol conversion of flavonoids, e.g., rosmarinic acid and luteolin can be intended to reduce silver ions for the synthesis of silver nanoparticles [67]. In another report, it was reported hydrogen ions of flavonoids during the reduction of metal salt can oxidize to the carbonyl group [68]. In an extract of *Ocimum basilicum*, the transformation of enol- to keto- is a key factor in the biosynthesis of silver nanoparticles [69].

5.6. Role of Terpenoids in Green Synthesis of Nanoparticles

Terpenoids or isoprenoids are very important phytochemical that belongs to naturally synthesized terpenes. They are derivatives of essential oil, which are a mixture of secondary metabolites induced by plants. Previous studies have described the importance of these metabolites in the preparation of silver nanoparticles [70]. It was reported that two important terpenoids, e.g., sesquiterpenoids and monoterpenoids, are basic constituents for the silver nanoparticles' synthesis [71]. Various reports showed the importance of essential oil of different plants' species in the synthesis of silver nanoparticles such as *Cocos nucifera* [72], rosemary [73], *Ricinus communis* [74], and *Anacardium occidentale* [75].

6. Synthesis of Metal or Metal Oxides' Nanoparticles by Using Plants

In this review article, we summarized the basic principles or mechanisms of the green synthesis method, especially for metal or metal oxide (i.e., ZnO, Au, Ag, TiO_2, Fe, Fe_2O_3, Cu, CuO, Co) nanoparticles.

6.1. Zinc Oxide Nanoparticles

Recently, Zinc oxide nanoparticles have emerged as one of the most significant metal oxide nanoparticles due to carrying specific differences in morphology (size, shape, and crystalline nature), applications, low toxicity, economic benefits, and bio-compatibility [76–78]. Zinc oxide nanoparticles can be prepared from various parts of a plant such as a leaf, Stem, root, flower, seed, and fruit.

6.1.1. Synthesis of ZnO Nanoparticles Using Leaf: (2019–2021)

To date, numerous leaves' extracts have been used for the synthesis of ZnO nanoparticles, as shown in Table 1.

Walnut aqueous leaf extract was utilized for the bio-synthesis of ZnO nanoparticles with a size range of 15 to 40 nm and evaluated against *E. coli* (ZOI = 7 to 9 mm) and *S. aureus* (Gram-positive bacterial stain) [79]. Demissie, Meron Girma, et al. reported *Lippia adoensis* aqueous leaf extract inspired preparation of ZnO nanoparticles and investigated against Staphylococcus *aureus* (ZOI = 6–14 mm), *Enterococcus faecalis* (ZOI = 6–10 mm), *Escherichia coli* (ZOI = 6–12 mm), and *Klebsiella pneumoniae* (ZOI = 6–12 mm) [80]. *Cayratia pedata*-based ZnO nanoparticles were also synthesized by Jayachandran et al. The mechanism of *Cayratia pedata*-based nanoparticles' synthesis is shown in Figure 2 [81].

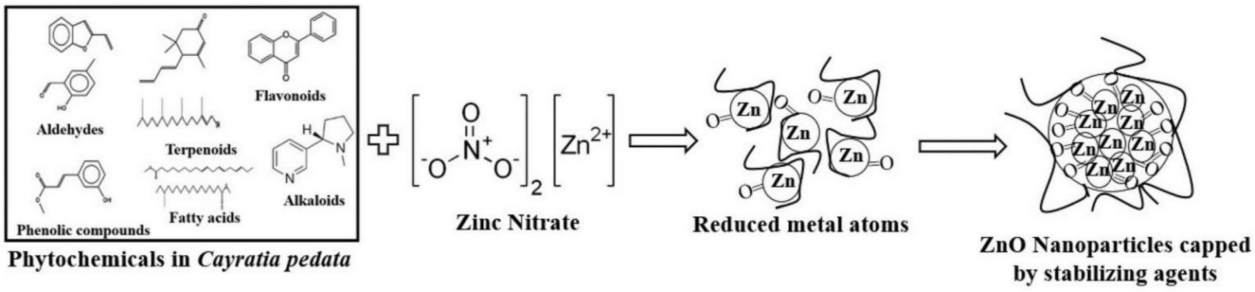

Figure 2. The mechanism of *Cayratia pedata-based* nanoparticles' synthesis (reused from Ref. [81], an Open Access Article, (CC BY NC AD)).

Piper betle aqueous leaf extract was applied for the synthesis of ZnO nanoparticles with an average size of 112 nm. *S. aureus* (ZOI = 2–3 mm) and *E. coli* (ZOI = 1–4 mm) are main causes of surgical site infection (SSI). Globally, SSI accounts for 2.5% to 41.9%, and an even higher rate in developing countries. Surgical site infection affects not only the health of patients but also the development of the country. The anti-bacterial agents are a significantly effective solution to lower this rate and Piper betle-mediated ZnO nanoparticles were proven to show excellent antibacterial activity against *S. aureus* and *E. coli* [82]. *Becium grandiflorum* was reported for the biosynthesis of ZnO nanoparticles and evaluated antimicrobial activity against *S. aureus* (ZOI = 7 mm), *E. coli* (ZOI = 6 mm), *K. pneumonia* (ZOI = 8 mm), and *P. aeruginosa* (ZOI = 11mm) bacteria, shown in Figure 3. Methyl blue dye from an aqueous solution was effectively removed by synthesized ZnO nanoparticles [83].

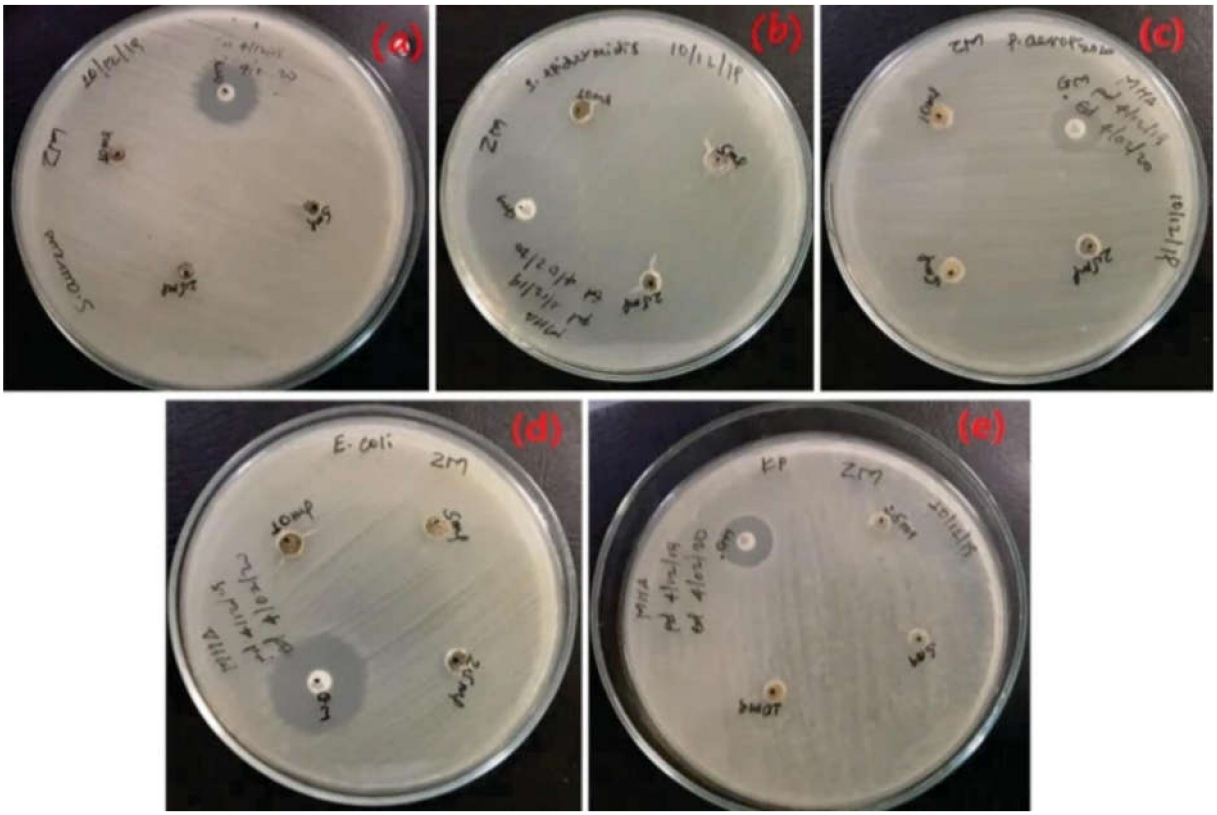

Figure 3. Antimicrobial activities of ZnO NPs against (**a**) *Staphylococcus aureus*, (**b**) *Staphylococcus epidermidis*, (**c**) *Pseudomonas aeruginosa*, (**d**) *Escherichia coli*, and (**e**) *Klebsiella pneumonia* (reused from Ref. [83], an Open Access Article, Creative Commons Attribution 4.0 (CC BY 4.0)).

In another study, ZnO nanoparticles were prepared from aqueous leaf extract of *Achyranthes aspera* and evaluated for antibacterial activity against *S. gallinarum* and *S. enteritidis* using the agar wall diffusion method. The author also observed that *Achyranthes aspera*-mediated ZnO nanoparticles showed zone of inhibition (ZOI) of 31 mm against *S. enteritidis* and *S. gallinarum* showed 30 mm [84]. Spherical-shaped ZnO nanoparticles with a size range of 30–55 nm were fabricated using an aqueous leaf extract of *Arthrospira platensis*. The results showed that antimicrobial activities of *Arthrospira platensis*-mediated nanoparticles were dose-dependent. Their application as an anti-microbial agent was studied and formed clear zones of 24.1 ± 0.3, 21.1 ± 0.06, 19.1 ± 0.3, 19.9 ± 0.1, and 21.6 ± 0.6 mm, at 200 ppm against *B. subtilis*, *S. aureus*, *P. aeruginosa*, *E. coli*, and *C. albicans*, respectively. These antibacterial activities were reduced as synthesized ZnO concentration decreased. ZnO nanoparticles showed significantly higher cytotoxic efficacy against cancerous cells than normal cell lines [85]. Hexagonal-shaped ZnO nanoparticles with a crystallite size of 17 nm were produced from ethanol leaf extract of *Sambucus ebulus*. The synthesized ZnO nanoparticles showed acceptable photo-catalytic degradation of Methylene blue dye. *Sambucus ebulus*-mediated ZnO nanoparticles explain efficient antioxidant and antibacterial activity [86]. Droepenu, Eric Kwabena, et al. reported the biosynthesis of ZnO nanoparticles using *Anacardium occidentale* and tested against *S. aureus* (ZOI = 1.06 ± 0.14 mm), *E. aquaticum* (ZOI = 1.99 ± 0.11 mm), *K. pneumoniae* (ZOI = 2.08 ± 0.03 mm), *E. coli* (ZOI = 1.49 ± 0.09 mm), and *A. baumanii* (ZOI = 2.99 ± 0.01 mm) [87].

From 2020 to 2019, several publications reported ZnO nanoparticles synthesized using leaf extract of various plants, e.g., *Eucalyptus globulus Labill* [88], *Cassia fistula* and *Melia azadarach* [89], *Euphorbia hirta* [90], saffron leaf [91], *Azadirachta Indica* [92], *Aquilegia pubiflora* [93], Broccoli extract [94], *Costus igneus* [95], *Pandanus odorifer* [96], and *Solanum torvum* [97].

Table 1. Synthesis of ZnO nanoparticles from leaf extract.

Sr. No	Reducing Agent	Part of Plant	Size	Shape	Biological Activities	Year of Publication	Ref.
1	Walnut leaf	Leaf	15–40 nm	Triangular	*E. coli* (ZOI = 7–9 mm) and *S. aureus*	2021	[79]
2	*Lippia adoensis*	Leaf	22.6–26.8 nm	Predominantly spherical	*S. aureus* (ZOI = 6–14 mm), *E. faecalis* (ZOI = 6–10 mm), *E. coli* (ZOI = 6–12 mm) and *K. pneumonia* (ZOI = 6–12 mm)	2021	[80]
3	*Cayratia pedata*	Leaf	52.24 nm.	-	Utilized in the immobilization of the enzyme (Glucose oxidase)	2021	[81]
4	Piper betle	Leaf	112 nm	Hexagonal shape and spherical	*S. aureus* (ZOI = 2–3 mm) and *E. coli* (ZOI = 1–4 mm)	2021	[82]
5	*Becium grandiflorum*	Leaf	20 nm	-	*S. aureus* (ZOI = 7 mm) *E. coli*, (ZOI = 6 mm), *K. pneumonia* (ZOI = 8 mm), and *P. aeruginosa* (ZOI = 11 mm) Degradation of methylene blue (69% degraded after 200 min)	2021	[83]
6	*Achyranthes aspera*	Leaf	28.63–61.42 nm	Hexagonal	*S. gallinarum* (MIC ≥ 0.195 mg ± 0.00) and *S. enteritidis* (MIC ≥ 0.390mg ± 0.00)	2021	[84]
7	*Arthrospira platensis*	Leaf	30–55 nm	Spherical	*subtilis* (ZOI = 24.1 ± 0.3 mm), *S. aureus* (ZOI = 21.1 ± 0.06 mm), *P. aeruginosa* (ZOI = 19.1 ± 0.3 mm), *E. coli* (ZOI = 19.9 ± 0.1 mm), and C. *albicans* (ZOI = 21.6 ± 0.6 mm) Showed significantly high cytotoxic efficacy against cancerous cell	2021	[85]
8	*Sambucus ebulus*	Leaf	17 nm	Hexagonal	*cereus*, *S. aureus*, and *E. coli* Photo-catalytic degradation of Methylene blue ((80% degraded after 200 min)	2020	[86]

Table 1. *Cont.*

Sr. No	Reducing Agent	Part of Plant	Size	Shape	Biological Activities	Year of Publication	Ref.
9	*Anacardium occidentale*	Leaf	107.03 ± 1.54 nm and 206.58 ± 1.86 nm	Spherical	*S. aureus* (ZOI = 1.06 ± 0.14 mm), *E. aquaticum* (ZOI = 1.99 ± 0.11 mm), *K. pneumoniae* (ZOI = 2.08 ± 0.03 mm), *E. coli* (ZOI = 1.49 ± 0.09 mm), and *A. baumanii* (ZOI = 2.99 ± 0.01 mm)	2021	[87]
10	*Eucalyptus globulus Labill.*	Leaf	27–35 nm	-	-	2020	[88]
11	*Cassia fistula* and *Melia azadarach*	Leaf	3–68 nm	-	*Cassia fistula* *E. coli* (ZOI = 21 ± 0.68 mm at 10 µL) and (ZOI = 44 ± 3.00 mm at 200 µL) and *S. aureus* (ZOI = 14 ± 0.54 mm at 10 µL) and (ZOI = 32 ± 2.30 mm at 200 µL) *Melia azadarach* *E. coli* (ZOI = 20 ± 0.56 mm at 10 µL) and (ZOI = 40 ± 0.48 mm at 200 µL) and *S. aureus* (ZOI = 21 ± 0.68 mm at 10 µL and (ZOI = 38 ± 0.55 mm at 200 µL)	2020	[89]
12	*Euphorbia hirta*	Leaf	5–20 nm in diameter	-	-	2020	[90]
13	saffron leaf	Leaf	Less than 50 nm in diameter	Spherical	At 25 (µg/disc) Concen of ZnOPs *S. Typhimurium* (ZOI = 12 ± 0.27 mm), *L. monocytogenes* (ZOI = -), and *E. faecalis* (ZOI = 11 ± 0.39 mm). At 50 (µg/disc) Concen of ZnOPs *S. Typhimurium* (ZOI = 23 ± 0.29 mm), *L. monocytogenes* (ZOI = -), and *E. faecalis* (ZOI = 14 ± 0.30 mm). At 50 (µg/disc) Concen of ZnOPs *S. Typhimurium* (ZOI = 26 ± 0.27 mm), *L. monocytogenes* (ZOI = -), and *E. faecalis* (ZOI = 18 ± 0.39 mm). Free radical scavenging activity was reported in DPPH and FRAP (64%). Degradation of methylene blue (69% degraded after 200 min).	2020	[91]
14	*Azadirachta Indica*	Leaf	25.97 nm	Hexagonal	*E. coli* (ZOI = 9.3 mm), Degradation of methylene blue (Degraded 35.5%. 45.7%, 63.9%, 72.1%, and 80.2% at 40, 80, 120, 160, and 200 min, respectively).	2020	[92]
15	*Aquilegia pubiflora*	Leaf	34.23 nm	Spherical or elliptical	*aeruginosa* (ZOI = 10.3 ± 0.19 mm) and *F. solani* (ZOI = 13 ± 14 mm) Antiparasitic potential.	2020	[93]
16	Broccoli extract	Leaf	4–17 nm	Hexagonal	Catalytic activity against methylene blue (74%) and phenol red (71%).	2019	[94]
17	*Costus igneus*	Leaf	26.55 nm	Hexagonal	At 40 (µg/mL) Concen of ZnOPs *S. mutans* (ZOI = 2.83 ± 0.15 mm), *L. fusiformis* (ZOI = 4.73 ± 0.25 mm), *P. vulgaris* (ZOI = 4.13 ± 0.14 mm), and *V. parahaemolyticus* (ZOI = 4.2 ± 0.1 mm). At 50 (µg/mL) Concen of ZnOPs *S. mutans* (ZOI = 4.83 ± 0.15 mm), *L. fusiformis* (ZOI = 6.6 ± 0.1 mm), *P. vulgaris* (ZOI = 5.3 ± 0.2 mm), and *V. parahaemolyticus* (ZOI = 5.13 ± 0.17 mm). At 70 (µg/mL) Concen of ZnOPs *S. mutans* (ZOI = 5.86 ± 0.18 mm), *L. fusiformis* (ZOI = 8.53 ± 0.20 mm), *P. vulgaris* (ZOI = 6.33 ± 0.15 mm), and *V. parahaemolyticus* (ZOI = 6.56 ± 0.11 mm). Antidiabetic activity. Free radical scavenging activity was reported in DPPH (75%)	2019	[95]
18	*Pandanus odorifer*	Leaf	90 nm	Spherical	*B. subtilis* (ZOI = 26 mm) and *Gram-negative E. coli* (ZOI = 24 mm).	2019	[96]
19	*Solanum torvum*	Leaf	34–40 nm	Spherical	Decreased serum uric acid level. Could affect hepatic and renal performance in rats.	2019	[97]

6.1.2. Synthesis of ZnO Nanoparticles Using Roots and Root Hairs (2020–2021)

Roots and roots' extracts are also well established for the synthesis of ZnO nanoparticles. To date, different roots' extracts have been used for the synthesis of ZnO nanoparticles, as shown in Table 2. In 2021, the synthesis of spherical ZnO nanoparticles with an average size of 11.34 nm using *Rubus Fairholmianus root* (Dimethyl sulfoxide) extract was reported and tested against *S. aureus* (MIC = 157.22 μg/mL) [98]. In another study, aqueous root hair extract of P*hoenix dactylifera* was utilized for the synthesis of ZnO nanoparticles with a size range of 30.87 to 47.89 nm. ZnO nanoparticles were found to be 45% more cytotoxic than well-known chemotherapeutic drugs (doxorubicin). Especially Triple-negative breast cancer cells were found to be weaker to P*hoenix dactylifera*-mediated nanoparticles than doxorubicin. *Phoenix dactylifera*-mediated were observed to be 82.26% cytotoxic to lungs cancer cells. *Phoenix dactylifera*-mediated ZnO nanoparticles exhibited promising antibacterial action against *K. pneumoniae* (ZOI = 2.4 cm), *S. aureus* (ZOI = 3.0 cm), *Salmonella typhi* (ZOI = 2.8 cm), and *E. coli* (ZOI = 2.7 cm) [99]. Liu, Di, et al. reported *Raphanus sativus-mediated ZnO nanoparticles exhibited antibacterial activity against S. aureus* (ZOI = 21.23 ± 1.16 mm) and *E. Faecalis* (ZOI = 11.23 ± 0.58 mm) [100]. Recently, *Sphagneticola trilobata L* was also reported to synthesize ZnO nanoparticles, which were mainly irregular in shape [101]. *Moringa oleifera* was applied for the formation of hexagonal-shaped ZnO nanoparticles with a size of ~25 nm. The prepared ZnO nanoparticles were tested for their antibacterial action against *B. Subtilis* (ZOI = 12.5 mm) and *E. coli* (ZOI = 11.6 cm) [102].

Table 2. Different roots and root hairs' extracts have been used for the synthesis of ZnO nanoparticles.

Sr. No	Reducing Agent	Part of Plant	Size	Shape	Biological Activities	Year of Publication	Ref.
1	*Rubus Fairholmianus*	Root	11.44 nm	Spherical	*S. aureus* (MIC = 157.22 μg/mL)	2021	[98]
2	*Phoenix dactylifera*	Root hair	30.87–47.89 nm	-	*K. pneumoniae* (ZOI = 2.4 cm), *S. aureus* (ZOI = 3.0 cm), *Salmonella typhi* (ZOI = 2.8 cm), *E. coli* (ZOI = 2.7 cm), and *P. aeruginosa* (ZOI = 1.6 cm) Anticancer cytotoxicity	2021	[99]
3	*Raphanus sativus*	Root	15 and 25 nm	Hexagonal	*S. aureus* (ZOI = 21.23 ± 1.16 mm) and *E. faecalis* (ZOI = 11.23 ± 0.58 mm)	2020	[100]
4	*Sphagneticola trilobata L*	Root	-	Irregular	-	2020	[101]
5	*Moringa oleifera*	Root	~25 nm	Hexagonal	*B. Subtilis* (ZOI = 12.5 mm) and *E. coli* (ZOI = 11.6 cm)	2020	[102]

6.1.3. Synthesis of ZnO Nanoparticles Using Stem and Stem Bark: (2019–2021)

Biosynthesis of ZnO nanoparticles using stem or stem bark has gained immense attention recently. Synthesis of ZnO nanoparticles using stem and stem bark is shown in Table 3. *Amygdalus scoparia*-mediated ZnO nanoparticles were synthesized by Jobie, Fatemeh Norouzi, et al., who investigated their antibacterial action against *B. subtilis* (ZOI = 25 mm), *S. aureus* (ZOI = 28 mm), *S. typhimurium* (ZOI = 21 mm), *E. coli* (ZOI = 28 mm), *E. aerogenes* (ZOI = 22 mm), *K. aerogenes* (ZOI = 21 mm), *P. oryzae* (ZOI = 18 mm), *C. glabrata* (ZOI = 16 mm), *F. thapsinum* (ZOI = 16 mm), *C. albicans* (ZOI = 16 mm), *F. semitectum* (ZOI = 18 mm), and *C. neoformans* (ZOI = 18 mm). Synthesized ZnO nanoparticles exhibited excellent photocatalytic activity, shown in Figure 4.

Prepared ZnO nanoparticles exhibited an excellent inhibitory effect on cancer line cells, whereas they had no hazardous effect on normal line cells. *Amygdalus scoparia*-mediated ZnO-cured diabetic rats illustrated an excellently higher level of insulin and lower alanine transaminase (ALT), aspartate aminotransferase (AST), and blood glucose as compared to a Streptozotocin (STZ)-induced diabetic group and other cured groups [103]. *Cinnamomum verum* bark was reported for the formation of ZnO nanoparticles and tested against *S. aureus* (MIC = 125 μg/mL) and *E. coli* (MIC = 62.5 μg/mL) [104]. Hexagonally shaped ZnO nanoparticles were synthesized by using aqueous root extract of *Mussaenda*

frondosa with a size range of 5–20 nm, and its antimicrobial efficiency was evaluated against *S. aureus* (ZOI = 21.51 mm), *B. subtilis* (ZOI = 19.13 mm), and *P. aeruginosa* (ZOI = 20.31 mm). This study reported photocatalytic activity and biological applications such as antidiabetic, anticancerous, antioxidant, anti-inflammatory, and antimicrobial activity [105]. *Albizia lebbeck* aqueous stem bark extracts were utilized for the formation of ZnO nanoparticles and tested against *S. aureus* (ZOI = 4.50 ± 0.30 mm), *B. cereus* (ZOI = 8.83 ± 0.42 mm), *S. typhi* (ZOI = 91.3 ± 0.41mm), *K. pneumoniae* (ZOI = 7.30 ± 0.29 mm), and *E. coli* (ZOI = 10.57 ± 0.320 mm). The *Albizia lebbeck* stem bark extracts-mediated ZnO nanoparticles exhibited strong antioxidant and cytotoxicity against breast cancer cell lines [106].

Table 3. Synthesis of ZnO nanoparticles using stem and stem bark.

Sr. No	Reducing Agent	Part of Plant	Size	Shape	Biological Activities	Year of Publication	Ref.
1	*Amygdalus scoparia*	Stem	-	-	At 100 (µg/mL) Concen of ZnOPs *B. Subtilis* (ZOI = 25 mm), *S. aureus* (ZOI = 28 mm), *S. typhimurium* (ZOI = 21 mm), *E. coli* (ZOI = 28 mm), *E. aerogenes* (ZOI = 22 mm), *K. aerogenes* (ZOI = 21 mm), *P. oryzae* (ZOI = 18 mm), *C. glabrata* (ZOI = 16 mm), *F. thapsinum* (ZOI = 16 mm), *C. albicans* (ZOI = 16 mm), *F. semitectum* (ZOI = 18 mm), and *C. neoformans* (ZOI = 18 mm) Exhibited excellent photocatalytic activity Exhibited excellent inhibitory effect on cancer line	2021	[103]
2	*Cinnamomum verum*	Stem bark	-	Hexagonal	*aureus* (MIC = 125 µg/mL) and *E. coli* (MIC = 62.5 µg/mL)	2020	[104]
3	*Mussaenda frondose*	Stem bark	5–20 nm	Hexagonal	*S. aureus* (ZOI = 21.51 mm), *B. subtilis* (ZOI = 19.13 mm), and *P. aeruginosa* (ZOI = 20.31 mm). Photocatalytic activity and biological applications such as antidiabetic, anticancerous, anti-inflammatory, and antimicrobial activity	2020	[105]
4	*Albizia lebbeck*	Stem bark	-	-	Tested against *S. aureus* (ZOI = 4.50 ± 0.30 mm), *B. cereus* (ZOI = 8.83 ± 0.42 mm), *S. typhi* (ZOI = 91.3 ± 0.41mm), *K. pneumonia* (ZOI = 7.30 ± 0.29 mm), and *E. coli* (ZOI = 10.57 ± 0.320). Free radical scavenging activity was reported in H_2O_2 (IC50 0f 48.5, 48.7, and 60.2 µg/mL for 0.1 M, 0.05 M, and 0.05 M, respectively) and cytotoxicity against breast MD-MB and MCF-7 cancer cell lines	2019	[106]

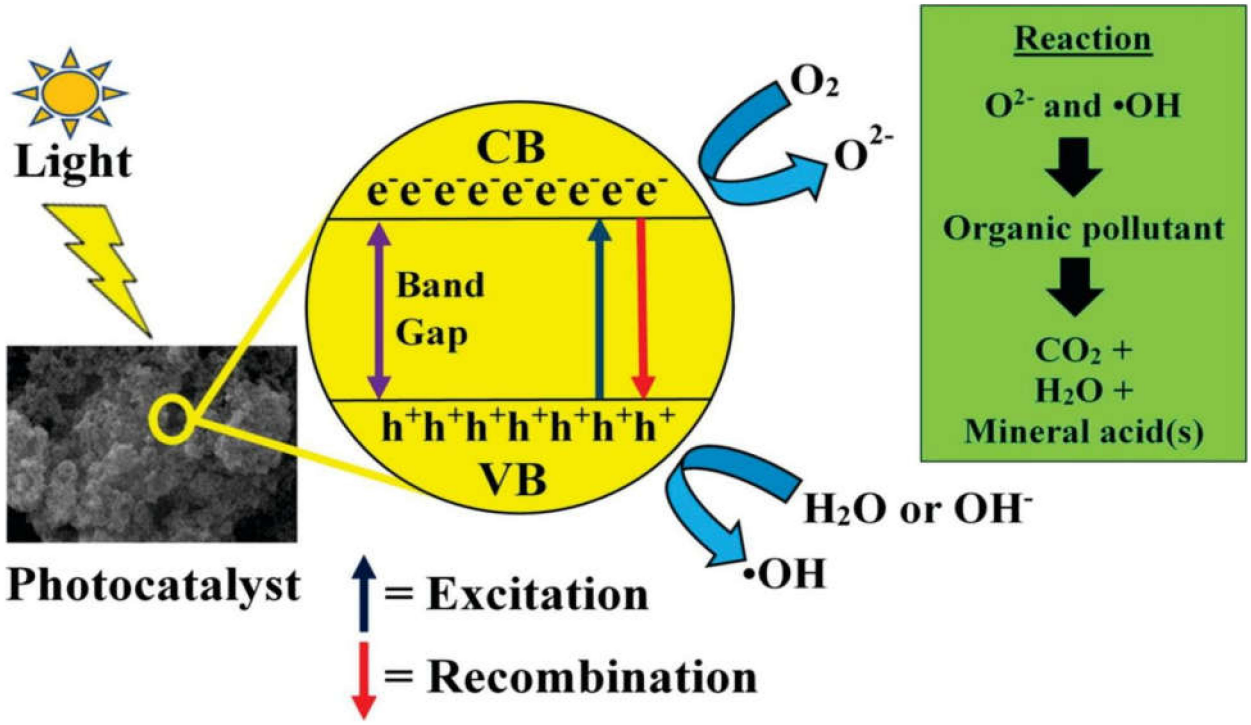

Figure 4. Synthesized ZnO nanoparticles exhibited excellent photocatalytic activity. Reused with permission from [103].

6.1.4. Synthesis of ZnO Nanoparticles Using Flower Extract: (2019–2021)

Flowers were also used in the biosynthesis of ZnO nanoparticles, as shown in Table 4. Biological synthesis of flake-structured ZnO nanoparticles was achieved by using *Cassia auriculata.* The prepared ZnO nanoparticles were used against various bacterial strains to evaluate their antimicrobial efficiency against *S. pneumonia, S. aureus, E. coli, and K. pneumonia* (the size of the zone observed ranged from 18 mm to 25 mm against the abovementioned pathogens) and anticancer agent against MG-63 cell. The cell adhesion assay was carried out to investigate the anticancer efficiency of *Cassia auriculata*-mediated ZnO nanoparticles against MG-63 cells [107]. In another study, the antimicrobial efficacy of *Punica granatum* flower-mediated ZnO nanoparticles was assessed against *S. diarizonae* (ZOI = 10.00 mm), *B. cereus* (ZOI = 12.33 ± 0.58 mm), *S. aureus* (ZOI = 10.50 ± 0.87 mm), *P. aeruginosa* (ZOI = 10.00 ± 1.00 mm), *S. pneumonia* (ZOI = 14.00 ± 1.00 mm), *K. pneumonia* (ZOI = 11.00 ± 1.00 mm), *E. faecalis* (ZOI = 9.67 ± 0.58 mm), *S. typhi* (ZOI = 8.67 ± 1.15 mm), *E. coli* (ZOI = 10.00 ± 1.00 mm), *L. monocytogenes* (ZOI = 14.33 ± 0.58 mm), *E. faecium* (ZOI = 15.83 ± 0.76 mm), *A. hydrophila* (ZOI = 13.83 ± 0.29 mm), and *M. catarrhalis* (ZOI = 12.00 ± 1.00 mm) [108]. *Moringa Oleifera* aqueous flower extract was used for the production of ZnO nanoparticles with a size of 13.2 nm [109]. *Matricaria chamomilla L* promoted the preparation of ZnO nanoparticles with an average size of 62 nm, reported by Ogunyemi, Solabomi Olaitan, et al. [110]. Hexagonally and Triangularly shaped ZnO nanoparticles with size range 30 to 40 nm synthesized by using the flower of *Syzygium aromaticum* were reported by Lakshmeesha, Thimappa Ramachandrappa, et al. [111].

Table 4. Synthesis of ZnO nanoparticles using flowers.

Sr. No	Reducing Agent	Part of Plant	Size	Shape	Biological Activities	Year of Publication	Ref.
1	*Cassia auriculata*	Flower	-	Flake structured	*S. pneumonia*, *S. aureus*, *E. coli*, and *K. pneumonia* (the size of zone observed ranged from 18 mm to 25 mm against the abovementioned pathogens) Anticancer agent against MG-63 cells (15 and 20 µg)	2021	[107]
2	*Punica granatum*	Flower	-	Irregular shaped	At 100 (µg/mL) Concen of ZnOPs *S. diarizonae* (ZOI = 10.00 mm), *B. cereus* (ZOI = 12.33 ± 0.58 mm), *S. aureus* (ZOI = 10.50 ± 0.87 mm), *P. aeruginosa* (ZOI = 10.00 ± 1.00 mm), *S. pneumonia* (ZOI = 14.00 ± 1.00 mm), *K. pneumonia* (ZOI = 11.00 ± 1.00 mm), *E. faecalis* (ZOI = 9.67 ± 0.58 mm), *S. typhi* (ZOI = 8.67 ± 1.15 mm), *E. coli* (ZOI = 10.00 ± 1.00 mm), *L. monocytogenes* (ZOI = 14.33 ± 0.58 mm), *E. faecium* (ZOI = 15.83 ± 0.76 mm), *A. hydrophila* (ZOI = 13.83 ± 0.29 mm), and *M. catarrhalis* (ZOI = 12.00 ± 1.00 mm)	2020	[108]
3	*Moringa Oleifera*	-	13.2 nm	-	-	2020	[109]
4	*Matricaria chamomillaL*	Flower	62.4 nm	-	*Pv. Oryzae* (ZOI = 2.2 cm)	2019	[110]
5	*Syzygium aromaticum*	Flower	30–40 nm	Triangular and hexagonal	Potential application in agriculture and food industries	2019	[111]

6.1.5. Synthesis of ZnO Nanoparticles Using Seed (2020–2019)

The aqueous seed extract of the different plants has been widely used as a reducing and capping agent for the biosynthesis of ZnO nanoparticles, as shown in Table 5. Ware, Umavathi, Saraswathi, et al. reported the ecofriendly synthesis of ZnO nanoparticles using seed extract of *Parthenium hysterophorus* with a size of 10 nm [112]. In another study, Lettuce aqueous seed extract was utilized as a reducing agent for the formation of ZnO nanoparticles with an average size of 50 nm, and its effect on the process of seed germination was investigated [113]. Ngom, I. et al. reported the formation of ZnO nanoparticles using seed extract of *Moringa Oleifera* [114]. Longan aqueous seed extract was employed for the production of pure hexagonal-phase ZnO nanoparticles with a size range of 10–100 nm. The photocatalytic activity of Longan seed-mediated ZnO nanoparticles was evaluated through de-colorization of Orange II, methylene blue (MB), and methyl orange [115]. *Trigonella foenum-graecum* aqueous seed extract was also successfully applied for the biosynthesis of irregular spherical and flake-shaped ZnO nanoparticles with a size range of 70 nm to 90 nm. The photocatalytic activity of trigonal *Trigonella foenum-graecum*-mediated ZnO nanoparticles was evaluated through de-colorization of methylene blue [116].

Table 5. Synthesis of ZnO nanoparticles using Seed.

Sr. No	Reducing Agent	Part of Plant	Size	Shape	Biological Activities	Year of Publication	Ref.
1	*Parthenium hysterophorus*	Seed	10 nm	Hexagonal	-	2020	[112]
2	Lettuce	Seed	50 nm	-	Effect on the process of seed germination	2020	[113]
3	Eriobotrya japonica	Seed	50 nm	-	-	2020	[114]
4	Longan seed	Seed	10–100 nm	Hexagonal	Evaluated through de-colorization of Orange II (70%), methylene blue (MB 90%), and methyl orange (80%)	2019	[115]
5	*Trigonella foenum-graecum*	Seed	70–90 nm	Irregular spherical and flake	Potential application in agriculture and food industries	2019	[116]

6.1.6. Synthesis of ZnO Nanoparticles Using Fruit and Fruit Peel: (2019–2021)

ZnO nanoparticles synthesized using fruit and fruit extract are shown in Table 6. Khan, Mujahid, et al. reported the synthesis of hexagonal ZnO nanoparticles with an average size of 58 nm using an aqueous extract of *Passiflora foetida* fruit peels. *Passiflora foetida*-based ZnO nanoparticles showed remarkable efficiency toward Rhodamine B and MB dye (91.06%) and MB dye (93.25%), respectively [117]. Aqueous fruit extracts of *Myristica fragrans* were used to prepare elliptical- and spherical-shaped ZnO nanoparticles with a mean size of 41.23 nm and tested against *E. coli* (ZOI = 15 ± 1.54 mm), *K. pneumoniae* (ZOI = 27 ± 1.73 mm), *P. aeruginosa* (ZOI = 17 ± 1.66 mm), and *S. aureus* (ZOI = 21 ± mm). Prepared nanoparticles exhibited excellent larvicidal activity against *Aedes aegypti.* Similarly, significant leishmanicidal activity was also examined against *amastigote* and *promastigote* parasites. The biologically prepared ZnO nanoparticles exhibited excellent antioxidant and biocompatible nanoparticles. Photocatalytic activities of prepared ZnO nanoparticles were evaluated through decolorizations of methylene blue [118]. Hexagonal ZnO nanoparticles with an average size of 33.1 ± 11.7 nm were derived from aqueous peel extract of *citrus sinensis* and tested against *E. coli* and *S. aureus.* The toxicity of *citrus sinensis*-based ZnO nanoparticles toward human umbilical vein endothelial cells was dose-dependent. The feasibility of human umbilical vein endothelial cells (HUVECs) increased when reacted with 6.25 mg/L of prepared ZnO nanoparticles. However, feasibility lowered sharply, to around 20%, when the concentration of prepared ZnO nanoparticles increased to 25 mg/L or higher. It showed that prepared ZnO nanoparticles enhance the growth of HUVECs at low concentrations [119]. Aqueous fruit extract of orange was utilized for the formation of spherical ZnO nanoparticles with a size range of 10–20 nm and was evaluated against *E. coli* and *S. aureus* [120]. In another study, ZnO nanoparticles were prepared using the fruit of *Ailanthus altissima* with a size range of 5–18 nm and tested against *E. coli* and *S. aureus* [121].

Table 6. Synthesis of ZnO nanoparticles using Fruit and Fruit peel.

Sr. No	Reducing Agent	Part of Plant	Size	Shape	Biological Activities	Year of Publication	Ref.
1	*Passiflora foetida*	Fruit peel	58 nm	Hexagonal	Showed remarkable efficiency toward Rhodamine B (91.06%) and MB dye (93.25%)	2021	[117]
2	*Myristica fragrans*	Fruit	41.23 nm	Spherical	*E. coli* (ZOI = 15 ± 1.54 mm), *K. pneumoniae* (ZOI = 27 ± 1.73 mm), *P. aeruginosa* (ZOI = 17 ± 1.66 mm), and *S. aureus* (ZOI = 21 ± mm) Exhibited excellent larvicidal activity against *Aedes aegypti* Leishmanicidal activity was also examined against *amastigote* and *promastigote* parasite	2021	[118]
3	*Citrus sinensis*	Fruit peel	33.1 ± 11.7	Hexagonal	*E. coli* and *S. aureus.* Toxicity toward human umbilical vein endothelial	2020	[119]
4	Orange	Fruit	10–20 nm	Spherical	-	2020	[120]
5	*Ailanthus altissima*	Fruit	5–18 nm	-	*E. coli* and *S. aureus*	2019	[121]

6.2. Gold Nanoparticles

Among the various metal and metal oxide nanoparticles, gold nanoparticles have specific morphology (size, shape, and crystalline nature), controlled geometry, and stable nature [122]. Gold nanoparticles are utilized in light-harvesting assemblies, electronics, molecular switches, and sensing [123–126]. Gold nanoparticles are also utilized in the diagnosis, detection, and cure of various diseases [127,128]. Gold nanoparticles, with their multiple properties, gained attention and their features can be modified by altering the shape, size, and aspect ratio. Gold nanoparticles are proven to be exclusive in biomedical applications. They are used as a tool for early cancer diagnosis, heart diseases, and the presence of infectious agents. The non-toxic and biocompatible nature of gold nanoparticles makes them a good candidate for drug and gene delivery. They can modify their surface with antibodies and other drug molecules. They carry drugs that are released at the target site selectively [129,130]. Gold nanoparticles are also explored for gene delivery due to their optimal properties. It is reported that, for the enhancement of the genetic material of any plant, the DNA coated with gold nanoparticles is injected into the plant cell and results in transformation [131]. Gold nanoparticles, due to their biochemical inertness and their unique optical-electronical properties, are also broadly applied in analytical sciences. Sensory probes, conductors, electronic chips, photovoltaics, and fuel cells are advanced technical applications of gold nanoparticles. Gold nanoparticles are widely used in fluorescence, surface plasmon resonance, lateral flow immunochromatographic assay (LFICA), enzyme-linked immunosorbent assay (ELISA), and SERS immunoassays of biomolecules (Elahi, N.). The current advancement in imaging techniques such as Computed tomography, X-ray, and SERS is also based on the high-density resolution of gold nanoparticles. [132]. They are also found in many chemical reactions as a catalyst.

6.2.1. Synthesis of Gold Nanoparticles from Plant

Gold nanoparticles can be prepared from various parts of the plant such as leaf, Stem, root, flower, seed, and fruit. Synthesis and the mechanism of formation of gold nanoparticles using plant are illustrated in Figures 5 and 6, respectively.

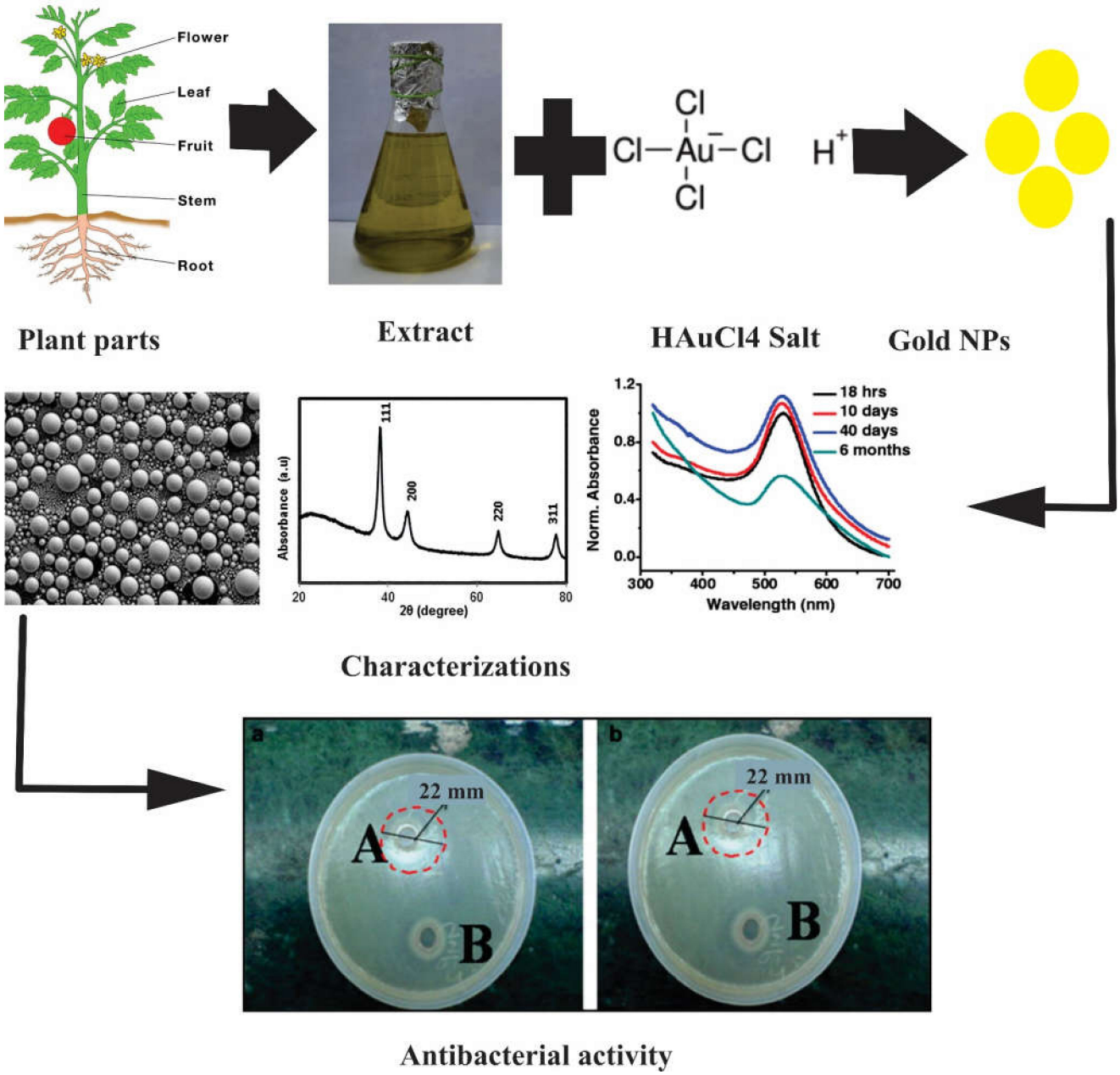

Figure 5. Schematic synthesis of gold nanoparticles using plants' parts.

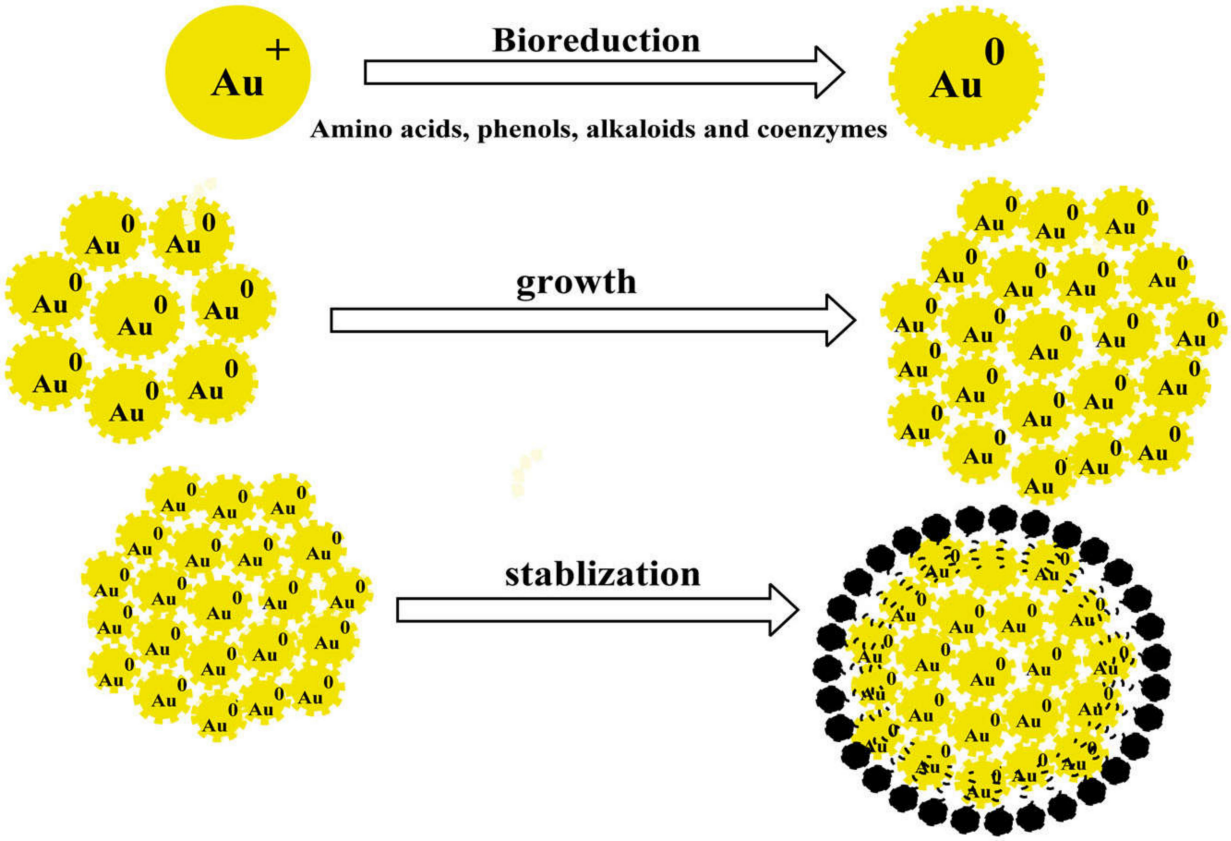

Figure 6. Mechanism for synthesis of gold nanoparticles using a plant. Reused from [133], an Open Access Article, Creative Commons Attribution 4.0 (CC BY 4.0).

6.2.2. Synthesis of Gold Nanoparticles Using Leaves: (2019–2021)

Leaves' extracts are used to synthesize gold nanoparticles, as shown in Table 7. In 2021, gold nanoparticles were derived from aqueous leaf extract of *Lantana camara*, *Populus alba*, and *Hibiscus arboreus* with a size of ~16.3 ± 0.7 nm. The antibacterial activity of prepared gold nanoparticles was tested against *E. coli* and *S. aureus* (MIC value = 100 µg/mL). The bio-synthesized gold nanoparticles were also utilized for the degradation of MB and CR dye [134]. In another report, *Limnophila rugosa* was used for the production of spherical-shaped gold nanoparticles with a mean particles' size distribution of 122 nm. *Limnophila rugosa*-capped gold nanoparticles showed tremendous catalytic activity in the reduction of different nitrophenols, e.g., 4-nitrophenol, 3-nitrophenol, and 1,4-nitrophenol [135]. Olajire, A.A. et al., reported the biological synthesis of spherical gold nanoparticles with a mean size of 18.85 ± 6.74 nm by utilizing aqueous leaf extract of *Ananas comosus.* Low-density polyethylene with 1% gold nanoparticles exhibited a degradation efficacy of 90% after 240 h [136]. Recently, a single-step and eco-friendly biosynthesis of gold nanoparticles was reported by El-Borady et al., utilizing leaf of P*hragmites australis.* The results exhibited the production of spherical-shaped gold nanoparticles with about 18 nm diameter. *Phragmites australis*-based gold nanoparticles showed tremendous anticancer efficiency with an $IC_{50.}$ Prepared gold nanoparticles also exhibited good quenching for 2,2-diphenyl-1-picrylhydrazyl free radical with scavenging % equal to 10.26. P*hragmites australis*-based gold nanoparticles also showed excellent photocatalytic activity, as they completely degraded the MB in just 60 s. *Mentha Longifolia*-mediated nanoparticles had tremendous anti-breast cancer efficiency against HS319.T, MCF7, and UACC-3133 cell lines [137]. An environmentally friendly method for the biological formation of gold nanoparticles was developed by Shah, Sumaira, et al., using ethanol leaf extract of S*ageretia theazans*. The biological activity of S*ageretia theazans*-based gold nanoparticles was evaluated against *S. au-*

reus, K. pneumonia, and *B. subtilis.* The antioxidant efficiency was investigated with DPPH scavenging activity; the maximum scavenging efficiency was observed at 100 µg/mL [138]. In another report, gold nanoparticles were bio-synthesized by reducing gold metal ions upon interlinking with aqueous leaf extract of *Coriandrum sativum.* TEM was utilized to calculate the size range of spherical gold nanoparticles, which was in the range of being 32.96 ± 5.25 nm [139]. In another study, an instantaneous, single-step, inexpensive, ecofriendly production of gold nanoparticles via aqueous leaf extract *Persicaria salicifolia was reported by* Hosny, Mohamed, et al., resulting in the production of violet-colored, spherical-shaped gold nanoparticles with diameters between 5 and 23 nm. The cytotoxicity study of *Persicaria salicifolia*-mediated gold nanoparticles using sulforhodamine-B assay showed tremendous cell capability in inhibiting the proliferation and growth of breast cancer cells (MCF7 cell line). Additionally, prepared gold nanoparticles showed antioxidant activity [140]. In 2021, gold nanoparticles were biosynthesized through the mixing of *aqueous* leaf extract of *Curcumae Kwangsiensis* with a size of ~8–25 nm. Gold nanoparticles showed tremendous antioxidant properties toward common free radicals, e.g., DPPH. Prepared gold nanoparticles had excellent anti-ovarian cancer activity against Sw-626, SK-0V, and P cell lines [141]. In another study, the aqueous extract *Centaurea behen* was utilized for the simple and environmental production of gold nanoparticles. For testing of the cytotoxicity effect of *C. behen* extract and gold nanoparticles, an MTT test was performed. *C. behen*-mediated gold nanoparticles revealed the cytotoxicity against THP-1 cell line. The IC_{50} for prepared nanoparticles was measured for about 25 µg/mL, whereas *C. behen* extract could not achieve the IC_{50}. Similarly, for testing of antioxidant property of gold nanoparticles, a DPPH test was performed. Gold nanoparticles revealed maximum DPPH scavenging efficiency of 14% [142]. Padalia, Hemali, et al., reported the biosynthesis of gold nanoparticles utilizing *Ziziphus nummularia* and their anticancer and antioxidant activities. TEM exhibited the biosynthesized gold nanoparticles to be 11–12 nm in size and spherical. The biosynthesized particles exhibited dose-dependent cytotoxicity toward the human breast cell line, fibroblast normal cell line, and breast cancer cell line. The biologically prepared gold nanoparticles showed excellent antioxidant activity toward ABTS (IC_{50} = 690 µg/mL), DPPH (IC_{50} = 520 µg/mL), and (IC_{50} = 330 µg/mL) [143].

Table 7. Synthesis of Gold nanoparticles using leaf extracts.

Sr. No	Reducing Agent	Part of Plant	Size	Shape	Biological Activities	Year of Publication	Ref.
1	*Lantana camara, Populus alba,* and *Hibiscus arboreus*	Leaf	~16.3 ± 0.7 nm	-	*E. coli* and *S. aureus* (MIC value of ~100 µg/mL.) For the degradation of MB and CR dye	2021	[134]
2	*Limnophila rugosa*	Leaf	122 nm	Spherical	Tremendous catalytic activity in the reduction of different nitrophenols	2021	[135]
3	*Ananas comosus*	Leaf	18.85 ± 6.74 nm	Spherical	Exhibited a degradation efficacy of 90% after 240 hrs	2021	[136]
4	*Phragmites australis*	Leaf	18 nm	Spherical	Showed tremendous anticancer efficiency. Exhibited good quenching for 2,2-diphenyl-1-picrylhydrazyl free radical with scavenging % equal to 10.26. Excellent photocatalytic activity, as they completely degraded the MB in just 60 sec.	2021	[137]
5	*Mentha longifolia*	Leaf	36.4 nm	Spherical	Tremendous anti-breast cancer efficiency against HS319.T (IC50 = 224 ± 0 µg/mL), MCF7 (IC50 = 264 ± 0 µg/mL) and UACC-3133 (IC50 = 201 ± 0 µg/mL) cell lines	2021	[138]
6	*Sageretia theazans*	Leaf	36 and 13 nm.	-	*S. aureus* (ZOI = 10 ± 0.54 mm), *K. pneumonia* (ZOI = 12 ± 0.2 mm), and *B. subtilis* (ZOI = 6 ± 0.4 mm). The antioxidant efficiency was investigated with DPPH scavenging activity, the maximum scavenging efficiency was observed at 100 µg/mL	2021	[139]
7	*Coriandrum sativum*	Leaf	32.96 ± 5.25 nm	Spherical	-	2021	[139]

Table 7. *Cont.*

Sr. No	Reducing Agent	Part of Plant	Size	Shape	Biological Activities	Year of Publication	Ref.
8	*Persicaria salicifolia*	Leaf	5 and 23 nm	Spherica	*Inhibiting the proliferation and growth of breast cancer cells (MCF7 cell line). Showed antioxidant activity*	2021	[140]
9	*Curcumae kwangsiensis*	Leaf	~8–25 nm	Spherical	Showed tremendous antioxidant property toward common free radical, e.g., BHT (IC50 = 153 µg/mL). Excellent anti-ovarian cancer activity against Sw-626 (IC50 = 166 µg/mL), SK-0V (IC50 = 204 µg/mL), and PA1 cell lines (IC50 = 153 µg/mL)	2021	[141]
10	*Centaurea behen*	Leaf	50 nm	Spherical	Revealed cytotoxicity against THP-1 cell line. The IC_{50} for prepared nanoparticles was measured at about 25 µg/mL. Revealed maximum DPPH scavenging efficiency of 14%	2021	[142]
11	*Ziziphus nummularia*	Leaf	11–12 nm	Spherical	Excellent antioxidant activity toward ABTS (IC50 = 690 µg/mL), DPPH (IC50 = 520 µg/mL), and SO (IC50 = 330 µg/mL).	2021	[143]
12	*Jasminum auriculatum*	Leaf	8–37 nm	Spherical	*E. coli*, *K. pneumonia*, *S. pyogenes*, *S. aureus*, and *Candida* (fungus). Showed excellent Antimicrobial commotion toward Inhibitory effect in the proliferation of the human cervical cancer cell line (IC_{50} = 104 µg/mL).	2020	[144]
13	*Vitex negundo*	Leaf	Below 100 nm	Spherical rod-shaped	*B. Subtilis* (ZOI = 14 ± 0.7 mm), *P. aeruginosa* (ZOI = 13 ± 0.6 mm), *S. aureus* (ZOI = 12 ± 0.7 mm), and *E. coli* (ZOI = 23 ± 0.6 mm). Exhibited tremendous antioxidant activities against H_2O_2 (78%) scavenging, Nitric oxide scavenging (83%), and DPPH (79%). Exhibited tremendous anti-inflammatory activity.	2020	[145]
14	*Pongamia pinnata*	Leaf	10–25 nm	-	Tested against oomycetes SR1(MIC_{80} = 1.6) and BP1120 (MIC_{80} = 0.8)	2020	[146]
15	*Lactuca indica*	Leaf	13.5 nm	Spherical	Exhibited remarkable degradation of methyl orange (2.05×10^{-3}) and 4-nitrophenol (1.3×10^{-3}).	2019	[147]
16	*Croton Caudatus*	Leaf	20 and 50 nm	Spherical	-	2019	[148]
17	*Sansevieria roxburghiana*	Leaf	-	Spherical, hexagonal, rod, and decahedral	Degradation of MB (49.62%), bromothymol blue 88.16%), acridine orange (40.44), phenol red (85.88), and Congo red (93.09).	2019	[149]
18	*Simarouba glauca*	Leaf	-	Prism and spherical	At 2.7 mL Gold solution *S. aureus* (ZOI = 2.0 mm), *B. subtilis* (ZOI = 1.0 mm), *E. coli* (ZOI = 0.6 mm), *P. vulgaris* (ZOI = 0.2 mm), *K. pneumonia* (ZOI = No), and *S. mutans* (ZOI = 1.6 mm).	2019	[150]
19	*Alcea rosea*	Leaf	4–95 nm	Triangular, spherical, hexagonal, and pentagonal	Exhibited anti-oxidant commotion against ABTS (47.16 to 64.82%) and DPPH (15.95 to 51.53%)	2019	[151]
20	*Bauhinia pupurea*	Leaf		Hexagonal, nanorod, and triangular	*B. Subtilis*, *P. aeruginosa*, *S. aureus*, Anticancer effects toward Lung carcinoma cell A549 (IC_{50} = 36.39 µg/mL). Exhibited high antioxidant efficiency against DPPH (IC_{50} = 27.21 µg/mL).	2019	[152]
21	*Coleus aromaticus*	Leaf	-	-	*epidermis* (ZOI = 27 mm) and *E. coli* (ZOI = 22 mm) Cytotoxicity toward liver cell (HepG2) cell line	2019	[153]
22	*Annona muricata*	Leaf	25.5 nm	Spherical mono-dispersed	S. aureus (40%), E. faecalis (46%), K. pneumonia (52%), and C. sporogeneses (54%), flaws (31%), C. albicans (42%), F. oxysporum (50%), and P. camemberti (66%).	2019	[154]

In 2019–2020, several publications reported gold nanoparticles synthesized using leaf extract of various plants, e.g., *Jasminum auriculatum* [144], *Vitex negundo* [145], *Pongamia pinnata* [146], *Lactuca indica* [147], *Croton Caudatus* [148], *Sansevieria roxburghiana* [149], *Simarouba glauca* [150], *Alcea rosea* [151], *Bauhinia pupurea* [152], *Coleus aromaticus* [153], and *Annona muricata* [154].

6.2.3. Synthesis of Gold Nanoparticles Using Root Extracts: (2021–2019)

The seed extract of the different plants has been widely used as a reducing and capping agent for the biosynthesis of gold nanoparticles, as shown in Table 8. Licorice aqueous root extract was utilized for the formation of circular gold nanoparticles with a size range of 2.647 nm to 16.25 nm and tested toward *P. aeruginosa* (ZOI = 25 ± 0.17), *E. coli* (ZOI = 29 ± 0.35), *S. aureus* (ZOI = 26 ± 0.29), *S. typhi* (ZOI = 26 ± 0.15), *B. subtilis* (ZOI = 25 ± 0. 15), *P. citrinum* (ZOI = 19 ± 0.21), *A. niger* (ZOI = 17 ± 0.29), *Candida albicans* (ZOI = 14 ± 0.21), *F. oxysporum* (ZOI = 18 ± 0.33), and *A. flavus* (ZOI = 16 ± 0.15). Licorice-based gold nanoparticles exhibited antioxidant activity toward DPPH and ABTS. The cytotoxicity of prepared particles was examined by utilizing the MTT approach against liver (HePG-2) and breast cancer (MCF-7) cell lines [155]. In another research, the author adopted an environmentally friendly and sustainable method to synthesize gold nanoparticles by utilizing *Phragmites australis* aqueous root extract. The cytotoxicity of prepared particles was examined by utilizing an MTT approach against human lung cancer cells (A549 cell line). Antioxidant efficiency was less than 10%. The prepared gold nanoparticles showed excellent efficiency in removing methyl orange and methyl blue [156]. In 2020, spherical gold nanoparticles were derived by a green method utilizing *Codonopsis pilosula* with the size of 20 ± 3.2 nm and tested against *E. coli* (ZOI = 7.0 ± 0.42 mm), *B. subtilis* (ZOI = 12.0 ± 0.85 mm), and *S. aureus* (ZOI = 17.0 ± 1.2 mm) [157]. Zhang, Tipeng, et al. prepared the gold nanoparticles using *Euphorbia fischeriana* aqueous root extract with the size of 20–60 nm [158]. In 2019, *Paeonia moutan* methanol root extract was used to synthesize gold nanoparticles. The cytotoxicity of prepared particles was examined by utilizing an MTT approach against the murine microglial (BV2) cells. *Paeonia moutan*-mediated gold nanoparticles hindered the inflammation in murine microglial (BV2) [159].

Table 8. Synthesis of Gold nanoparticles using root extracts.

Sr. No	Reducing Agent	Part of Plant	Size	Shape	Biological Activities	Year of Publication	Ref.
1	Licorice	Root	2.647–16.25 nm	Circular	*P. aeruginosa* (ZOI = 25 ± 0.17), *E. coli* (ZOI = 29 ± 0.35), *S. aureus* (ZOI = 26 ± 0.29), *S. typhi* (ZOI = 26 ± 0.15), *B. subtilis* (ZOI = 25 ± 0. 15), *P. citrinum (ZOI* = 19 ± 0.21), *A. niger* (ZOI = 17 ± 0.29), *Candida albicans* (ZOI = 14 ± 0.21), *F. oxysporum* (ZOI = 18 ± 0.33), and *A. flavus* (ZOI = 16 ± 0.15). Antioxidant activity toward DPPH and ABTS.	2021	[155]
2	*Phragmites australis*	Root	-	-	Cytotoxicity toward human lung cancer cells (A549 cell line). Antioxidant efficiency was less than 10%	2021	[156]
3	*Codonopsis pilosula*	Root	20 ± 3.2 nm	Spherical	*E. coli* (ZOI = 7.0 ± 0.42 mm), *B. subtilis* (ZOI = 12.0 ± 0.85 mm), and *S. aureus* (ZOI = 17.0 ± 1.2 mm).	2020	[157]
4	*Euphorbia fischeriana*	Root	20–60	-	-	2019	[158]
5	*Paeonia moutan*	Root	25.08 ± 3.73 nm	-	Hindered the inflammation in murine microglial (BV2)	2019	[159]

6.2.4. Synthesis of Gold Nanoparticles Using Stem Extracts: (2021–2019)

Recently, *Brassica oleracea var. Acephala cv galega* was utilized to biosynthesize spherical gold nanoparticles with an average diameter of 25.08 ± 3.73 nm, as shown in Table 9. Additionally, the antioxidant assay was carried out in the root extract after the formation of gold nanoparticles [160]. Khoshnamvand, M. et al., reported the synthesis of gold nanoparticles by utilizing *Apium graveolens* aqueous stem extract. The prepared particles could be utilized as a catalyst for the reduction of 4-nitophenol [161]. Gold nanoparticles were biosynthesized utilizing the stem of *Angelica aiges* by a green approach. Prepared particles degraded the Malachite and eosin dye [162].

Table 9. Synthesis of Gold nanoparticles using stem extracts.

Sr. No	Reducing Agent	Part of Plant	Size	Shape	Biological Activities	Year of Publication	Ref.
1	*Brassica oleracea var. Acephala cv galega*	Stem	25.08 ± 3.73 nm	Spherical	The antioxidant assay was carried out in the root extract after the formation of gold nanoparticles	2021	[160]
2	*Apium graveolens*	Stem	-	-	Utilized as a catalyst for reduction of 4-nitophenol	2020	[161]
3	*Angelica aiges*	Stem	-	-	Degraded the Malachite (67%) and eosin dye (64%)	2019	[162]

6.2.5. Synthesis of Gold Nanoparticles Using Flower Extracts: (2021–2019)

In 2021, saffron stigma-mediated gold nanoparticles were produced by Alhumaydhi, Fahad A., et al. and tested against *E. coli, as shown* in Table 10 [163]. In 2020, spherical gold nanoparticles were derived from *Clitoria ternatea*, having particles size of 18.16 nm [164]. *Musa acuminata* ethanol and aqueous extract were utilized for the biosynthesis of gold nanoparticles, having a size range of 12.6–15.7 nm and evaluated against *K. pneumoniae* (ZOI = 12 mm), *P. aeruginosa* (ZOI = 9 mm), *E. faecalis* (ZOI = 10 mm), *S. typhi* (ZOI = NO), *E. coli* (ZOI = 7), *S. aureus* (ZOI = 11 mm), and *P. mirabilis* (ZOI = 12 mm). Prepared gold nanoparticles exhibited antioxidant activity toward DPPH [165]. Perveen, Kahkashan, et al. reported the biosynthesis of gold nanoparticles utilizing *Elettaria cardamomum* and their anticancer and antioxidant activities are shown in Table 11. TEM exhibited the biosynthesized gold nanoparticles to be 16.63 nm in size and spherical [166].

Table 10. Synthesis of Gold nanoparticles using flower and seed extracts.

Sr. No	Reducing Agent	Part of Plant	Size	Shape	Biological Activities	Year of Publication	Ref.
1	Saffron	Flower	-	-	-	2021	[163]
2	*ClitoriaTernatea*	Flower	18.6 nm	Spherical	-	2020	[164]
3	*Musa acuminata*	Flower	12.6–15.7 nm	-	*K. pneumonia* (ZOI = 12 mm), *P. aeruginosa* (ZOI = 9 mm), *E. faecalis* (ZOI = 10 mm), *S. typhi* (ZOI = NO), *E. coli* (ZOI = 7), *S. aureus* (ZOI = *11 mm)*, and *P. mirabilis* (ZOI = 12 mm). Exhibited antioxidant activity toward DPPH (IC50 = 390 µg for ethanol and 460 µg aqueous)	2019	[165]
4	*Elettaria cardamomum*	Seed	16.6 nm	-		-	[166]

6.3. Silver Nanoparticles

The synthesis of silver nanoparticles has gained remarkable attention due to their application in climate change, contamination [167], anti-microbial activities [168,169], information storage [170], bio-medical applications [171], energy generation [172], clean water technology [173], catalysis [174], biological sensors [175,176], optoelectronics [177], Lithium-ion batteries [178], and DNA sequencing [179]. Silver nanoparticles have vast applications in biomedicine due to their unique biological properties depending on their structure and size. Silver nanoparticles possess a very wide-spectrum, high antimicrobial activity [180]. They effectively kill microbes at a very low concentration [181]. Silver nanoparticles from free radicals alter the properties of microbial membranes and ultimately cause damage. Silver nanoparticles interact with microbial DNA and inhibit microbial activities [182]. Medical applications of silver nanoparticles are not only limited to antimicrobial treatments but they are also extended to bone healing [183], wound healing, vaccine development, the anti-diabetic effect [184], etc. Recent studies also proved silver nanoparticles as efficient candidates against various cancers. The surface-to-volume ratio of silver nanoparticles affects anticancer activity. Strong anticancer activities of silver particles are reported when size is reduced to even Angstrom [185]. It is also used in the treatment to control multi-drug-resistant microorganisms [186]. Silver nanoparticles are also used as a tool in dentistry [187,188]. Apart from biomedical applications, silver nanoparticles are widely used in various analytical techniques because of their unique physicochemical properties. They play an important role in biosensor and imaging technologies [189]. Many analytical techniques are also using silver nanoparticles in instrumentation [190]. They are used as fillers in biomaterials. Silver nanoparticles' films have been recently used as an alternative food packaging material [191]. There are various methods, such as Supercritical Fluid Synthesis, Laser Ablation, Laser Pyrolysis, Ball Milling, Ultrasonic Synthesis, etc., that have been used for the synthesis of silver nanoparticles. Recently, the biological synthesis of silver nanoparticles by using biological organisms such as plants, fungi, algae, and bacteria as capping and reducing agents and their anti-microbial activity has been studied. The different biological molecules such as tannins, ketones, flavonoids, protein, and aldehydes are responsible for the synthesis of silver nanoparticles by oxidation of Ag^+ to Ag^0.

6.3.1. Synthesis of Silver Nanoparticles

Silver nanoparticles can be prepared from various parts of the plant such as leaf, stem, root, flower, seed, and fruit.

6.3.2. Synthesis of Silver Nanoparticles Using Leaf Extracts: (2019–2020)

To date, numerous leaves' extracts have been used for the synthesis of silver nanoparticles, as shown in Tables 11 and 12. Rauf, Abdur, et al. reported the formation of AgNPs using *Mentha longifolia* aqueous leaves' extracts. The round oval morphology of silver nanoparticles with a mean size of 10.23 ± 2 nm was revealed by TEM. *Mentha longifolia*-based silver nanoparticles showed tremendous antibacterial effect toward *S. aureus* (ZOI = 12 ± 0.03 mm), *B. subtilis* (ZOI = 10 ± 0.01 mm), and *K. pneumonia* (ZOI = 0) and antioxidant activities [192]. In another research, the biological fabrication of silver nanoparticles was explained by *Ocimum Americanum*, with a particle size of 48.25 nm. The biologically prepared silver nanoparticles showed anti-bacterial activity against *S. aureus* (ZOI = 18.33 ± 0.33 mm), *P. aeruginosa* (ZOI = 17.66 ± 0.66 mm), *V. cholera* (ZOI = 15.66 ± 0.88 mm), *Aeromonas sp* (ZOI = 13. 33 ± 0.33 mm), *Bacillus sp* (ZOI = 16.33 ± 0.33 mm), and *E. coli* (ZOI = 7.66 ± 0.33 mm). The anti-oxidant activity was examined by H_2O_2 and DPPH. Silver nanoparticles showed excellent photocatalytic degradation of Eosin dye [193]. By utilizing *Clerodendrum inerme* as both a capping and reducing agent, Khan, Shakeel Ahmad, et al., synthesized silver nanoparticles and evaluated them for various biological activities, e.g., anti-mycotic, i.e., *A. niger* (ZOI = 17 mm) and *A. flavus* (ZOI = 22 mm), *and antibacterial*, i.e., *B. subtilis* (ZOI = 15 mm) and *S. aureus* (ZOI = 14 mm), activities. The antioxidant and cytotoxic activities of prepared gold nanoparticles were also examined by utilizing DPPH

free radical scavenging (78.8 ± 0.19%) and the MTT process [194]. In another study, *Salvia officinalis* hexane, ethyl acetate, and ethanol leaf extract were utilized in the formation of Ag-NPs. The biologically produced silver nanoparticles exhibited less cytotoxicity toward the HeLa cells' line and exhibited excellent anti-plasmodial efficiency (IC50 = 3.6 lg/mL) [195]. A rapid and eco-friendly approach for preparing spherical silver nanoparticles with size of 27–36 nm by utilizing *Alstonia venenata* was performed. The larvicidal efficiency on early-third-instar larvae was sufficiently higher for silver nanoparticles as compared to extract. The larvicidal activity was tested toward *Culex quinquefasciatus* with IC_{50} equivalent to 14.50 lg/mL, *Anopheles stephensi* with IC_{50} equivalent to 12.28 lg/mL, and *Aedes aegypt*i with IC_{50} equivalent to 13.49 lg/mL [196]. Previous work reported the bio-fabrication of spherical silver nanoparticles with a diameter of 20–40 nm, utilizing *Sida retusa* and tested toward *S. aureus (ZOI* = 17 mm), *B. subtilis* (ZOI = 14 mm), *E. coli* (ZOI = 15 mm), and *S. typhi* (ZOI = 15 mm). [197]. In 2021, Singh, Surya P., et al. reported the formation of AgNPs from Carica papaya aqueous leaf extract and its anticancer activity toward various human cancer cells. The cytotoxic commotion was performed toward various human cell and non-tumorigenic keratinocytes' cells. Cure of DU145 cell with *C. papaya*-mediated silver nanoparticles (0.5–5.0 µg/mL) for 1 or 2 days decreased the total cell number by 21–36% [198]. In another research, the author achieved silver nanoparticles with particles' sizes of 35 ± 2 nm and 30 ± 3 nm using *Carissa carandas* aqueous leaf extract. Biologically synthesized silver nanoparticles exhibited excellent anti-oxidant activity through DPPH assay. Prepared silver nanoparticles also showed remarkable ant-bacterial activity toward human pathogenic bacteria, e.g., *E. faecalis* (ZOI = 7.0 ± 0.0 mm), *S. flexneri* (ZOI = 8.0 ± 1.0 mm), *S. typhimurium* (ZOI = 8.0 ± 1.0 mm), and *gonococci spp* (ZOI = 6.0 ± 0.0 mm) [199]. *Malva parviflora* ethanol and waterleaf extract were utilized to synthesize spherical silver nanoparticles. The biologically synthesized silver nanoparticles inhibited the growth of *F. oxysporum* (81%), *A. alternate (82%), H. rostratum* (89%), and *F. solani* (81%) [200]. *Ziziphus nummularia* aqueous leaf extract was utilized to synthesize silver nanoparticles. These silver nanoparticles exhibited efficient anti-microbial commotion against *S. aureus, C. rubrum, S. typhimurium, P. aeruginosa, C. neoformans, C. albicans,* and *C. glabrata.* Silver nanoparticles also exhibited good DPPH activity (IC_{50} = 520 mg/mL) and ABTS activity (IC_{50} = 55 mg/mL) [201]. A previous study confirmed for first time the capability of *Otostegia persica* for the bio-synthesis of silver nanoparticles. These particles exhibited excellent anti-oxidant activity compared to the Otostegia persica leaf extract. These particles also showed potential anti-bacterial activity toward *S. pyogenes* (ZOI = 14 ± 0.4 mm), *S. aureus* (ZOI = 16 ± 0.1 mm), *B. subtilis* (ZOI = 15 ± 0.3 mm), *P. aeruginosa* (ZOI = 21 ± 0.5 mm), *S. typhi* (ZOI = 19 ± 0.4 mm), and E. *coli* (ZOI = 17 ± 0.1 mm) [202]. In another study, Abdallah, Basem M., et al. aimed to produce silver nanoparticles from *Lotus lalambensis* aqueous leaf extract and their anticandidal activity toward *C. albicans* (MIC = 125 µg/mL) [203]. Spherical silver nanoparticles were produced utilizing Symplocos racemosa. Anti-microbial activity of biologically prepared silver nanoparticles was studied on P. aeruginosa (ZOI = 22 mm) [204]. Silver nanoparticles were biosynthesized by an environmentally friendly hydrothermal approach using *Aloe vera* aqueous leaf extract, used to evaluate antibacterial potency against *P. aeruginosa* (ZOI = 14.00 ± 1.00 *mm), S. aureus* (ZOI = 21.00 ± 1.00 mm), *E. coli* (ZOI = 20.00 ± 2.00 mm), and *Enterobacter sp* (ZOI = 32.00 ± 2.00 mm [205]. In another report, Seerangaraj, Vasantharaj, et al. aimed to biosynthesize spherical silver nanoparticles with particles' size of 55.65 nm by utilizing *Ruellia tuberosa.* Biologically prepared silver nanoparticles exhibited cytotoxic potency against A549 lunger cancer line with IC_{50} = 68 µg/mL. These silver nanoparticles were also degraded the Coomassie brilliant blue and crystal violet [206]. Sharma, Yashika, et al. evaluated the anti-chikungunya potency of *Psidium guajava* aqueous leaf extract and the biologically prepared silver nanoparticles [207]. Ekennia, Anthony C., et al. reported the formation of spherical silver nanoparticles using *Euphorbia sanguinea* and its photocatalytic degradation of CR (90% within 1 h) [208].

Table 11. Synthesis of Silver nanoparticles using leaf extracts (2021).

Sr. No	Reducing Agent	Part of Plant	Size	Shape	Biological Activities	Year of Publication	Ref.
1	*Mentha longifolia*	Leaf	10.23 ± 2 nm	Round oval	At 2.0 (µg/mL) Concen of AgNPs *S. aureus* (ZOI = 12 ± 0.03 mm), *B. subtilis* (ZOI = 10 ± 0.01 mm), and *K. pneumonia (ZOI = 0).*	2021	[192]
2	*Ocimum americanum*	Leaf	48.25 nm	-	At 100 (µg/mL) Concen of AgNPs *S. aureus* (ZOI = 18.33 ± 0.33 mm), *P. aeruginosa* (ZOI = 17.66 ± 0.66 mm), *V. cholera* (ZOI = 15.66 ± 0.88 mm), *Aeromonas sp* (ZOI = 13. 33 ± 0.33 mm), *bacillus sp* (ZOI = 16.33 ± 0.33 mm), and *E. coli* (ZOI = 7.66 ± 0.33 mm) Anti-oxidant activity was examined by H_2O_2 (58.71%) and DPPH (75%). Photocatalytic degradation of Eosin dye (91.17%)	2021	[193]
3	*Clerodendrum inerme*	Leaf	-	-	*A. niger* (ZOI = 17 mm), *A. flavus* (ZOI = 22 mm), and *antibacterial* i.e., *B. subtilis* (ZOI = 15 mm) and *S. aureus* (ZOI = 14 mm) The anti-oxidant and cytotoxic activities were also examined by utilizing DPPH free radical scavenging and MTT process (78.8 ± 0.19%)	2020	[194]
4	*Salvia officinalis*	Leaf	41 nm	*Spherical*	Exhibited less cytotoxicity toward HeLa cells' line and exhibited excellent anti-plasmodial efficiency (IC50 = 3.6 lg/mL)	2021	[195]
5	*Alstonia venenata*	Leaf	27–36 nm	Spherical	The larvicidal efficiency on early-third-instar larvae was sufficiently higher for silver nanoparticles as compared to extract. The larvicidal activity was tested toward *Culex quinquefasciatus* with IC_{50} equivalent to 14.50 lg/mL, *Anopheles stephensi* with IC_{50} equivalent to12.28 lg/mL, and *Aedes aegypt*i with equivalent to LC5013.49 lg/mL	2021	[196]
6	*Sida retusa*	Leaf	20–40 nm.	Spherical	*S. aureus* (ZOI = 17 mm), *B. subtilis* (ZOI = 14 mm), *E. coli* (ZOI = 15 mm), and *S. typhi* (ZOI = 15 mm)	2021	[197]
7	Carica papaya	Leaf	-	-	Anticancer activity toward various human cancer cells. The cytotoxic commotion was performed toward various human cells and non-tumorigenic keratinocytes' cells. Cure of DU145 cell with *papaya*-mediated silver nanoparticles (0.5–5.0 µg/mL) for 1 or 2 days decreased the total cell number by 21–36%	2021	[198]
8	*Carissa carandas*	Leaf	35 ± 2 nm at 25 °C and 30 ± 3 nm at 60	-	*E. faecalis* (ZOI = 7.0 ± 0.0 mm), *S. flexneri* (ZOI = 8.0 ± 1.0 mm), *S. typhimurium* (ZOI = 8.0 ± 1.0 mm), and *gonococci spp* (ZOI = 6.0 ± 0.0 mm) Exhibited excellent antioxidant activity through DPPH assay (IC50 = 68.12 ± 1.27).	2021	[199]
9	*Malva parviflora*	Leaf	50.6 nm	Spherical	Inhibited the growth of *F. oxysporum* (81%), *A. alternate* (82%), *H. rostratum* (89%), and *F. solani* (81%).	2021	[200]

Table 11. *Cont.*

Sr. No	Reducing Agent	Part of Plant	Size	Shape	Biological Activities	Year of Publication	Ref.
10	*Ziziphus nummularia*	Leaf	25.6 nm	Oval and Spherical	Exhibited good DPPH activity (IC_{50} = 520 mg/mL) and ABTS activity (IC_{50} = 55 mg/mL)	2021	[201]
11	*Otostegia persica*	Leaf	36.5 ± 2.0 nm	Spherical	*S. pyogenes* (ZOI = 14 ± 0.4 mm), *S. aureus* (ZOI = 16 ± 0.1 mm), *B. subtilis* (ZOI = 15 ± 0.3 mm), *P. aeruginosa* (ZOI = 21 ± 0.5 mm), *S. typhi* (ZOI = 19 ± 0.4 mm), and *E. coli* (ZOI = 17 ± 0.1 mm) Exhibited excellent anti-oxidant activity (84%) compared to Otostegia persica leaf extract (64%).	2021	[202]
12	*Lotus lalambensis*	Leaf	-	-	*C. albicans* (MIC = 125 µg/mL)	2021	[203]
13	*Symplocos racemosa*	Leaf	-	-	*P. aeruginosa* (ZOI = 22 mm)	2021	[204]
14	*Aloe vera*	Leaf	-	-	*P. aeruginosa* (ZOI = 14.00 ± 1.00 mm), *S. aureus* (ZOI = 21.00 ± 1.00 mm), *E. coli* (ZOI = 20.00 ± 2.00 mm), and *Enterobacter sp (ZOI* = 32.00 ± 2.00 mm)	2021	[205]
15	*Ruellia tuberosa.*	Leaf	55.65 nm	Spherical	Cytotoxic potency against A549 lung cancer line with IC_{50} = 68 µg/mL. Degraded the Coomassie brilliant blue and crystal violet absorbance (peaks of the degraded CV and CBB were recorded at 586 and 590 nm)	2021	[206]
16	*Psidium guajava*	Leaf	-	-	Anti-chikungunya potency	2021	[207]
17	*Euphorbia sanguinea*	Leaf	-	-	Photocatalytic degradation of CR (90% within 1 h)	2021	[208]

In the period of 2019–2020, several publications reported Silver nanoparticles synthesized using leaf extract of various plants, e.g., *Borago officinalis* [209], *Tragopogon collinus* [210], *Melia azedarach* [211], *Mentha aquatica* [212], *Ziziphus joazeiro* [213], *Elytraria acaulis* [214], *Hyptis suaveolens* [215], *Caesalpinia pulcherrima* [216], *Gomphrena globosa* [217], *Plumbago auriculata* [218], *Cucumis prophetarum* [219], *Polygonatum graminifolium* [220], *Cocos nucifera* [221], *Mimosa albida* [222], *Capparis zeylanica* [223], *Holoptelea integrifolia* [224], *Annona Reticulatal* [225], *Combretum erythrophyllum* [226], *Berberis vulgaris* [227], *Catharanthus roseus* [228], *Ganonerion polymorphum* [229], *Premna integrifolia L* [230], and *Piper betle* [231].

Table 12. Synthesis of Silver nanoparticles using leaf extracts (2019–2020).

Sr. No	Reducing Agent	Part of Plant	Size	Shape	Biological Activities	Year of Publication	Ref.
1	*Borago officinalis*	Leaf	40 nm	Irregular	The bio-synthesized silver nanoparticles were hazardous to *Spodoptera littoralis*	2020	[209]
2	*Tragopogon collinus*	Leaf	7 nm	-	At 6000 (µg/mL) Concen of AgNPs S. *aureus* (ZOI = 2 mm) and *E. coli* (ZOI = 4 mm) At 7000 (µg/mL) Concen of AgNPs S. *aureus* (ZOI = 5 mm) and *E. coli* (ZOI = 7 mm) At 8000 (µg/mL) Concen of AgNPs S. *aureus* (ZOI = 10 m) and *E. coli* (ZOI = 8 mm)	2020	[210]
3	*Melia azedarach*	Leaf	18–30 nm	Spherical	*Verticillium dahlia*	2020	[211]
4	*Mentha aquatica*	Leaf	41 nm	Spherical	*P. aeruginosa* (MIC = 2.2µg/mL), *E. coli* (MIC = 58µg/mL), *B. cereus* (MIC = 20), and *S. aureus* (MIC = 198µg/mL)	2020	[212]

Table 12. *Cont.*

Sr. No	Reducing Agent	Part of Plant	Size	Shape	Biological Activities	Year of Publication	Ref.
5	*Ziziphus joazeiro.*	Leaf	-	-	*E. coli* ATCC 25922 and *S. aureus* ATCC 25923	2020	[213]
6	*Elytraria acaulis*	Leaf	5–100 nm	Cuboid	*S. typhi* (ZOI = 11.5 ± 2.5 mm), *S. Epidermis* (ZOI = 14.3 ± 1.7 mm), *E. coli* (ZOI = 11.2 ± 1.6 mm), and *B. subtilis* (ZOI = 12.0 ± 2.4 mm). Anti-oxidant activity toward DPPH (84.47%) and ABTS (85.25%) Cytotoxic commotion was performed against A549 cell line (IC50 = 79.6 µg/mL)	2020	[214]
7	*Hyptis suaveolens*	Leaf	29.19–52.27 nm	-	Scavenged H2O2 (54.21–70.11%) and DPPH (77.75–83.19) Stopped coagulation of blood	2020	[215]
8	*Caesalpinia pulcherrima*	Leaf	9 nm	Spherical	Cytotoxicity toward HeLa cell line (IC50 = 4.44 mg/mL)	2020	[216]
9	*Gomphrena globosa*	Leaf	-	Spherical	*subtilis* (ZOI = 40 mm), *P. aeruginosa* (ZOI = 38 mm), *M. luteus* (ZOI = 48 mm), *E. coli* (ZOI = 53 mm), and *K. pneumonia* (ZOI = 39 mm)	2020	[217]
10	*Plumbago auriculata*	Leaf	20 to 500 nm	-	At 5 (µg/mL) Concen of AgNPs *S. aureus* (ZOI = 10 ± 1.5 mm), *B. subtilis* (ZOI = 8 ± 0.5 mm), *K. pneumonia* (ZOI = 11 ± 0.5 mm), and *E. coli* (ZOI = 10 ± 0.8 mm), At 10 (µg/mL) Concen of AgNPs *S. aureus* (ZOI = 10 ± 0.8 mm), *B. subtilis* (ZOI = 10 ± 1.7 mm), *K. pneumonia* (ZOI = 11 ± 0.8 mm), and *E. coli* (ZOI = 10 ± 0.6 mm), At 15 (µg/mL) Concen of AgNPs *S. aureus* (ZOI = 8 ± 0.7 mm), *B. subtilis* (ZOI = 8 ± 0.9 mm), *K. pneumonia* (ZOI = 12 ± 1.0 mm), and *E. coli* (ZOI = 12 ± 1.0 mm), At 20 (µg/mL) Concen of AgNPs *S. aureus* (ZOI = 10 ± 1.5 mm), *B. subtilis* (ZOI = 8 ± 1.0 mm), *K. pneumonia* (ZOI = 14 ± 1.7 mm), and *E. coli* (ZOI = 12 ± 2.5 mm), Inhibited the growth of *Culex quinquefasciatus* (45.1 µg/mL) *and Aedes aegypti*	2020	[218]
11	*Cucumis prophetarum*	Leaf	30–50 nm	-	At 20 (µg/mL) Concen of AgNPs *S. typhi* (ZOI = 15 ± 0.2 mm) and *S. aureus* (ZOI = 11 ± 0.4 mm) At 50 (µg/mL) Concen of AgNPs *S. typhi* (ZOI = 17 ± 0.5 mm) and *S. aureus* (ZOI = 14 ± 0.3 mm) At 75 (µg/mL) Concen of AgNPs *S. typhi* (ZOI = 20 ± 0.6 mm) and *S. aureus* (ZOI = 18 ± 0.4 mm) Anti-oxidant activity toward DPPH (IC50 = 29.2 µg/mL) and ABTS (IC50 = 34.5µg/mL)	2020	[219]
12	*Polygonatum graminifolium*	Leaf	3–15 nm	Spherical	*E. coli* (ZOI = 27 mm) and *S. aureus* (ZOI = 16 mm)	2020	[220]
13	*Cocos nucifera*	Leaf	14.2 nm	Cubic	*E. coli* (ZOI = 16.0 ± 0.11 mm), *B. subtilis* (ZOI = 10.0 ± 0.05 mm), *S. aureus* (ZOI = 12.0 ± 0.06 mm), and *S. typhimurium* (ZOI = 13.0 ± 0.12 mm),	2020	[221]

Table 12. *Cont.*

Sr. No	Reducing Agent	Part of Plant	Size	Shape	Biological Activities	Year of Publication	Ref.
14	*Mimosa albida*	Leaf	6.5 nm ± 3.1 nm	-	Exhibited anti-oxidant activity (IC50 = 7563 ± 967)	2020	[222]
15	*Capparis zeylanica*	Leaf	-	Spherical	*S. Paratyphi* (ZOI = 18 mm), *S. dysenteriae* (ZOI = 19 mm), *S. epidermidis* (ZOI = 22 mm), *E. faecalis* (ZOI = 20 mm), *A. niger* (ZOI = 21 mm), and *C. albicans* (ZOI = 20 mm)	2020	[223]
16	*Holoptelea integrifolia*	Leaf	32–38 nm.	Spherical	Showed antioxidant activities toward DPPH (74.59 ± 3.08%) Showed antiinflammatory (binding constant 2.60 ± 0.05 × 10^{-4}) and antidiabetic (86.66 ± 5.03%) activities.	2019	[224]
17	*Annona reticulatal*	Leaf	-	Cubic	*P. Aeruginosa* (MIC = *62.5* µg/mL*), E. coli* (MIC = *62.6* µg/mL*), S. aureus* (MIC = *31.5* µg/mL*), B. cereus* (MIC = *125* µg/mL*),* and *C. albicans* (MIC = *62.5* µg/mL)	2019	[225]
18	*Combretum erythrophyllum*	Leaf	13.62 nm	Spherical	*S. Epidermidis* (ZOI = 12 mm), *P. vulgaris* (ZOI = 11 mm), *S. aureus* (ZOI = 15 mm), and E. *coli* (ZOI = 12 mm)	2019	[226]
19	*Berberis vulgaris*	Leaf	30–70 nm	Spherical	*S. aureus* and *E. coli*	2019	[227]
20	*Catharanthus roseus*	Leaf	-	-	*P. Aeruginosa* (ZOI = 6 mm), *S. dysenteriae* (ZOI = 8 mm), *S. aureus* (ZOI = 8 mm), and *B. anthracis* (ZOI = 12 mm),	2019	[228]
21	*Ganonerion polymorphum*	Leaf	20–60 nm	Hexagonal and Spheri-cal	*B. Cereus (*99.75%) and *E. coli (*99.94%)	2019	[229]
22	*Premna integrifoliaL*	Leaf	9–35 nm	Spherical	*E. faecalis* (MIC = 60 µg/mL), *V. parahaemolyticus* (MIC = 10 µg/mL), *S. dysenteriae* (MIC = 20 µg/mL), *S. aureus* (MIC = 30 µg/mL*),* and *S. flexneri* (MIC = 70 µg/mL) Showed anti-oxidant activity (IC50 = 524.19 ± 2.63 µg/mL) and cytotoxic to cancer cell line (SiHa).	2019	[230]
23	*Piper betle*	Leaf	6–14 nm	Spherical	At 1000 (µg/mL) Concen of AgNPs*F. Solani* (ZOI = 3.13 ± 0.25 mm) and *A. brassicae* (ZOI = 67. 21 ± 3.15 mm)	2019	[231]

6.3.3. Synthesis of Silver Nanoparticles Using Root Extracts: (2021–2020)

Roots are also well established for the synthesis of silver nanoparticles, as shown in Table 13. In 2021, Gul, Anadil, et al. bio-synthesized spherical silver nanoparticles utilizing *Ricinus communis* methanolic root extract with an average size of 29 nm and used them to evaluate against *E. coli* (73%), *K. pneumonia* (60%), *S. aureus* (56%), *S. pneumonia* (60%), *A. niger* (77%), and *A. alternate* (75%). The results illustrated that the prepared nanoparticles exhibited remarkable efficiency toward Urease (IC_{50} = 36.81 ± 0.05 µg/mL) and Xanthine (IC_{50} = 3.60 ± 0.04 µg/mL) [232]. In another report, spherical silver nanoparticles with average size of 20.49 nm were prepared by utilizing *Duchesnea indica* and tested toward *E. coli* (MIC = 0.53 mg/mL), *S. typhi* (MIC = 0.01 mg/mL), *A. alternata* (MIC = 0.51 mg/mL), and *M. canis* (MIC = 0.53 mg/mL) [233]. Arshad, Hammad, et al. reported a simpler, quicker, and ecofriendly approach to prepare silver nanoparticles by utilizing *Salvadora persica* aqueous root extract and tested them toward *S. epidermidis* ATCC12228 (MIC = 0.39 µg/mL) and *E. coli (MIC* = 0.19 µg/mL) [234]. In another report, Tripathi, Deepika, et al. examined the cytotoxic efficiency of *Asparagus officinalis*-mediated silver nanoparticles toward a cervical cancer cell line (SiHa) [235]. In 2020, silver nanoparticles

were prepared through an inexpensive and ecofriendly approach by utilizing *Astragalus tribuloides Delile.* The resultant silver nanoparticles showed excellent anti-oxidant properties compared to the extract. The resultant silver nanoparticles were also used to evaluate bacterial activity toward S. aureus, S. flexneri, E. coli, and B. cereus [236]. In another research, an environmental process was used for the preparation of silver nanoparticles by *Berberis asiatica* aqueous root extract and tested against *S. typhimurium* (ZOI = 7 mm), *E. coli* (ZOI = 11 mm), *S. aureus* (ZOI = 12 mm), and *K. pneumoniae* (ZOI = 6 mm) [237].

Table 13. Synthesis of Silver nanoparticles using root extracts.

Sr. No	Reducing Agent	Part of Plant	Size	Shape	Biological Activities	Year of Publication	Ref.
1	*Ricinus communis*	Root	29 nm	Spherical	*E. coli* (73%), *K. pneumonia* (60%), *S. aureus* (56%), *S. pneumonia* (60%), *A. niger* (77%), and *A. alternate* (75%) Exhibited remarkable efficiency toward Urease (IC_{50} = 36.81 ± 0.05 µg/mL) and Xanthine (IC_{50} = 3.60 ± 0.04 µg/mL)	2021	[232]
2	*Duchesnea indica*	Root	20.49 nm	Spherical	*E. coli* (MIC = 0.53 mg/mL), *S. typhi* (MIC = 0.01 mg/mL), *A. alternate* (MIC = 0.51 mg/mL), and *M. canis* (MIC = 0.53 mg/mL)	2021	[233]
3	*Salvadora persica*	Root	37.5 nm	Rod and Spherical	*S. epidermidis* ATCC12228 (MIC = 0.39 µg/mL) and *E. coli (MIC* = 0.19 µg/mL)	2021	[234]
4	*Asparagus officinalis*	Root	-	-	Cytotoxic toward cervical cancer cell line (SiHa) (IC50 = 44 lg mL^{-1})	2021	[235]
5	*Astragalus tribuloides Delile*	Root	34.2 ± 8.0 nm	Spherical	*S. aureus* (ZOI = 18 mm), *S. flexneri* (ZOI = 27 mm), *E. coli* (ZOI = 24 mm), and *B. cereus* (ZOI = 16 mm) Excellent anti-oxidant (64% property higher than extract (47%)	2020	[236]
6	*Berberis asiatica*	Root	14 nm	Spherical	*S. typhimurium* (ZOI = 7 mm), *E. coli* (ZOI = 11 mm), *S. aureus* (ZOI = 12 mm), and *K. pneumonia* (ZOI = 6 mm)	2020	[237]

6.3.4. Synthesis of Silver Nanoparticles Using Stem and Stem Bark Extracts: (2019–2021)

Biosynthesis of ZnO nanoparticles using stem or stem bark has gained immense attention nowadays, as shown in Table 14. In 2021, the author reported an environmentally friendly preparation of silver nanoparticles using *Grewia lasiocarpa* aqueous stem extract. The spherical shape of bio-synthesized nanoparticles was shown by SEM and HR-TEM. The prepared silver nanoparticles exhibited cytotoxicity toward HeLa (IC_{50} > 1 µg/mL). The prepared silver nanoparticles were also used to evaluate bacterial activity against *S. aureus* (MIC = 15.67 ± 2.08 µg/mL) [238]. *Euphorbia nivulia* was utilized to prepare spherical silver nanoparticles with a size of 20–90 nm and tested against *K. pneumoniae* (MIC = 23.5 ± 0.5 µg/mL), *B. cereus* (MIC = 27 ± 1 µg/mL), *S. aureus* (MIC = 24.5 ± 1.5µg/mL), *P. aeruginosa* (MIC = 30.5 ± 0.5 µg/mL), *B. subtilis* (MIC = 29 ± 1 µg/mL), and *C. albicans* (MIC = 26 ± 1 µg/mL) [239]. In another study, silver nanoparticles were derived from *Boswellia dalzielii* aqueous stem extract. The anti-oxidant activity of prepared silver nanoparticles was tested using DPPH (TEAC = 300.91) [240]. A biosynthesis of spherical silver nanoparticles with an average size of 19 nm was performed utilizing *Piper chaba* aqueous stem extract. The prepared silver nanoparticles efficiently catalyzed the degradation of MB and reduction of 4-nitrpphenol [241]. In 2020, Akintelu, Sunday Adewale, et al. tested the anti-microbial commotion of *Garcinia kola*-based silver nanoparticles against *E. faecalis* (ZOI = 2 mm), *B. cereus* (ZOI = 4 mm), *C. sporogenes* (ZOI = 6 mm), and *E. coli* (ZOI = 10 mm) [242]. In another report, Dawodu, Folasegun A., et al. explained a quicker, inexpensive process

for the preparation of silver nanoparticles with a mean size of ~25 nm by utilizing *Vigna unguiculata* aqueous stem extract [243].

Table 14. Synthesis of Silver nanoparticles using stem and stem bark extracts.

Sr. No	Reducing Agent	Part of Plant	Size	Shape	Biological Activities	Year of Publication	Ref.
1	*Grewia lasiocarpa*	Stem bark	diameter between 38.3 and 46.7 nm	Spherical	*S. aureus* (MIC = 15.67 ± 2.08 µg/mL). Exhibited cytotoxicity toward HeLa (IC_{50} = > 1 µg/mL).	2021	[238]
2	*Euphorbia nivulia*	Stem bark	20–90 nm	Spherical	*K. pneumoniae* (MIC = 23.5 ± o.5 µg/mL), *B. cereus* (MIC = 27 ± 1 µg/mL), *S. aureus* (MIC = 24.5 ± 1.5 µg/mL), *P. aeruginosa* (MIC = 30.5 ± 0.5 µg/mL), *B. subtilis* (MIC = 29 ± 1 µg/mL), and *C. albicans* (MIC = 26 ± 1 µg/mL)	2021	[239]
3	*Boswellia dalzielii*	Stem	2 nm to 101 nm	-	Anti-oxidant activity of prepared silver nanoparticles was tested using DPPH (TEAC = 300.91)	2020	[240]
4	*Piper chaba*	Stem	19 nm	Spherical	Degradation of MB and reduction of 4-nitrppheno	2020	[241]
5	*Garcinia kola*	Stem	-	-	*E. faecalis* (ZOI = 2 mm), *B. cereus* (ZOI = 4 mm), *C. sporogenes* (ZOI = 6 mm), and *E. coli* (ZOI = 10 mm)	2020	[242]
6	*Vigna unguiculata*	Stem	~25 nm	-	-	2019	[243]

6.3.5. Synthesis of Silver Nanoparticles Using Seed Extracts: (2019–2021)

The seed extract of the different plants has been widely used as a reducing and capping agent for the biosynthesis of silver nanoparticles, as shown in Table 15. In 2021, Awad, Manal A., et al. explained a green approach of biosynthesis of silver nanoparticles utilizing *Trigonella foenum-graecum* and tested it against *B. cereus* (ZOI = 10,0.9 mm), *E. coli* (ZOI = 14 ± 2.0 mm), and *S. aureus* (ZOI = 5.0 ± 2.0 mm) [244]. *Morinda citrifolia* was utilized to prepare spherical silver nanoparticles with an average size of 3 nm and used to evaluate bacterial activity toward *S. aureus* (ZOI = 9.81 mm) and *E. coli* (ZOI = 10.63 mm) [245]. In another work, round silver nanoparticles were derived from *Mangifera indica* aqueous seed extract and tested against *B. cereus* (ATCC11778), *K. pneumonia* (NMCIM2719), *S. aureus* (ATCC29737), *P. aeruginosa* (ATCC9027), *C. rubrum* (ATCC14898), *E. coli* (NCIM2931), *S. typhimurium* (ATCC23564), *C. neoformans* (ATCC34664), *C. albicans* (ATCC2091), and *C. glabrata* (NCIM3438) [246]. The formation of spherical nanoparticles with an average of 22 nm utilizing *Annona squamosa* L. was reported by Jose, Vimala, et al. The biosynthesized silver nanoparticles showed excellent catalytic activity against degradation of Coomassie brilliant blue dye [247]. Saygi, Kadriye Ozlem, et al. reported *Rosa canina* aqueous seed extract-inspired biosynthesis of spherical and rod shape silver nanoparticles with a mean size of 150 nm [248]. In another study, an advanced approach for the synthesis of silver nanoparticles utilizing *Nigella sativa* aqueous seed extract was reported by Chand, Kishore, et al. The prepared silver nanoparticles showed good photocatalytic activity on the degradation of Congo red [249]. Perveen, Rehana, et al., described a facile and green process for the preparation of silver nanoparticles by utilizing *Moringa oleifera* seed polysaccharide. The conclusion drawn from the above study was that prepared silver nanoparticles were spherically shaped. *Moringa oleifera*-mediated silver nanoparticles can enhance wound contraction and tissue growth wall [250]. Khan, Ibrahim, et al., reported the eco-friendly, facile, and rapid biosynthesis of silver nanoparticles utilizing *Bunium persicum* alcohol/methanol seed extract with a mean size range of 35 to 70 nm. *Bunium persicum*-mediated silver nanoparticles inhibited Urease and tyrosinase [251]. de Carvalho Bernardo, Wagner Luís, et al. reported a facile and rapid preparation of silver nanoparticles utilizing *Syzygium cumini* ethanol seed extract and tested against *F. nucleatum* (MIC =

NO), A. naeslundii (MIC = 125 µg/mL), S. aureus (MIC = 125 µg/mL), S. mutans (MIC = 250 µg/mL), S. epidermidis (MIC = 31.2 µg/mL), V. dispar (MIC = 62.5 µg/mL), *and S. oralis (*MIC = 31.2 µg/mL) [252]. Encapsulated silver nanoparticles were bio-synthesized by biogenic synthesis utilizing *Vitis vinifera* with a size range of 10–50 nm [253].

Table 15. Synthesis of Silver nanoparticles using seed extracts.

Sr. No	Reducing Agent	Part of Plant	Size	Shape	Biological Activities	Year of Publication	Ref.
1	*Trigonella foenum-graecum*	Seed	-	-	B. cereus (ZOI = 10 mm), E. coli (ZOI = 14 mm), and S. aureus (ZOI = 5.0 mm)	2021	[244]
2	*Morinda citrifolia*	Seed	3 nm	Spherical	*S. aureus* (ZOI = 9.81 mm) and *E. coli* (ZOI = 10.63 mm)	2021	[245]
3	*Mangifera indica*	Seed	-	-	*B. cereus* (ATCC11778) (*K. pneumonia* (NMCIM2719), *S. aureus (*ATCC29737), *P. aeruginosa* (ATCC9027), *C. rubrum* (ATCC14898), *E. coli* (NCIM2931), *S. typhimurium* (ATCC23564), *C. neoformans* (ATCC34664), *C. albicans* (ATCC2091), and *C. glabrata (*NCIM3438)	2021	[246]
4	*Annona squamosa* L.	Seed	22 nm	Spherical	Showed excellent catalytic activity against degradation of Coomassie brilliant blue dye	2021	[247]
5	*Rosa canina*	Seed	150 nm	Rod and Spherical	-	2021	[248]
6	*Nigella sativa*	Seed	-	-	Showed good photocatalytic activity on degradation of Congo red (Degraded 96%, 97%, and 98.5%, at 0.2, 0.15, and 1.3 min, respectively).	2021	[249]
7	*Moringa oleifera*	Seed	-	Spherical	*Enhanced wound contraction and tissue growth wall*	2021	[250]
8	*Bunium persicum*	Seed	35 to 70 nm	-	Inhibited Urease and tyrosinase	2021	[251]
9	*Syzygium cumini*	Seed	-	-	*F. nucleatum* (MIC = NO), *A. naeslundii* (MIC = 125 µg/mL), *S. aureus* (MIC = 125 µg/mL), *S. mutans* (MIC = 250 µg/mL), *S. epidermidis* (MIC = 31.2 µg/mL), *V. dispar* (MIC = 62.5 µg/mL), *and S. oralis* (MIC = 31.2 µg/mL)	2021	[252]
10	*Vitis vinifera*	Seed	10–50 nm	-	-	2021	[253]
11	*Ginger*and *Nigella sativa*	Seed	~12–8 nm	-	*P. Aeruginosa* and *E. coli*	2020	[254]
12	*Cuminum cyminum L.*	Seed	~100 nm	Spherical	Effective against human breast cancer cells (IC50 = 1.25 µg/mL)	2020	[255]
13	*Punica granatum*	Seed	10 to 35 nm	Spherical	-	2020	[256]
14	*Salvia hispanicaL.*	Seed	7 nm	Spherical	*S. aureus* (ZOI = 14.9 mm) and *E. coli* (ZOI = 18.5 mm)	2019	[257]
15	*Avicennia marina*	Seed	5–10 nm	-	*pneumoniae* ATCC 700,603 (ZOI = 12.5 ± 0.01 mm), *E. faecalis* ATCC 5129 (ZOI = No), *S. aureus* ATCC 43,300 (ZOI = 3.25 ± 0.02 mm), *P. aeruginosa* ATCC 27,853 (ZOI = 12.5 ± 0.05 mm), and *E. coli* ATCC 35,218 (ZOI = 6.25 ± 0.05 mm)	2019	[258]
16	*Tectona grandis*	Seed	10–30 nm	-	*B. cereus* (ZOI = 12 mm), *E. coli* (ZOI = 17 mm), and *S. aureus* (ZOI = 16 mm)	2019	[259]

From 2020 to 2019, several publications were reported in which silver nanoparticles were synthesized using seed extract of various plants such as *Ginger and Nigella sativa* [254],

Cuminum cyminum L. [255], *Punica granatum* [256], *Salvia hispanica L* [257], *Avicennia marina* [258], and *Tectona grandis* [259].

6.3.6. Synthesis of Silver Nanoparticles Using Flower Extracts:(2021)

Flowers were also used in the biosynthesis of silver nanoparticles, as shown in Table 16. In 2021, biosynthesis of silver nanoparticles with a mean size of 7.6 nm was conducted utilizing *Avera lanata*. The DPPH radical scavenging analysis showed the antioxidant activity of prepared silver nanoparticles [260]. A rapid, facile, sustainable, and controlled process was reported for the synthesis of silver nanoparticles by utilizing *Fraxinus excelsior* aqueous and ethanolic flower extract. The prepared silver nanoparticles can be used as an environmentally friendly material for the coloration of woven glass fabrics [261]. Aravind, M., et al. derived silver nanoparticles with an average size of 40 nm utilizing jasmine aqueous extract (flower) and tested them against *S. aureus* and *E. coli*. The abovementioned prepared silver nanoparticles degraded the MB [262].

Table 16. Synthesis of Silver nanoparticles using flower extracts.

Sr. No	Reducing Agent	Part of Plant	Size	Shape	Biological Activities	Year of Publication	Ref.
1	*Avera lanata*	Flower	7.6 nm	-	DPPH radical scavenging analysis showed antioxidant activity of prepared silver nanoparticles (IC50 = 50.08 ± 3.34)	2021	[260]
2	*Fraxinus excelsior*	Flower	-	-	Used as environmentally friendly material for the coloration of woven glass fabrics	2021	[261]
3	Jasmine	Flower	40 nm	-	Prepared silver nanoparticles degraded the MB (78% after 120 min).	2021	[262]

6.4. Titanium Oxide Nanoparticles

Titania (existing as TiO_2 nanoparticles) constitutes specific thermal, magnetic, optical, and electric properties. Normally, Titanium oxide existed in three forms e.g., brookite crystalline polymorphs' form, anatase form, and rutile form. The most important applications of TiO_2 are photocatalytic degradation and splitting [263], electronic and electrochromic [264], sensing instruments [265], and photovoltaic cells [266]. Among all other metal nanoparticles' oxide, titanium oxide nanoparticles showed distinctive morphologies (size, shape, and texture) and surface chemistry. It is utilized in the preparation of papers, foodstuff, tints, cosmetics, and medicine [267]. Colloidal titanium oxide nanoparticles are utilized in the degradation of hazardous chemicals in water [268,269]. Conventionally, titanium oxide nanoparticles are prepared using chemical and physical techniques, e.g., chemical precipitation, chemical vapor deposition, sol-gel, and hydrothermal [270]. All these conventional approaches require high pressure, temperature, and toxic chemicals [271]. However, environmentally friendly, rapid, and inexpensive methods are required to prepare nanoparticles on a larger scale with lesser toxicity [272]. This could be only possible by utilizing biological extract (plants, bacteria, algae, and fungi) through green chemistry.

Synthesis of Titanium Oxide Nanoparticles from Leaves, Roots, Flowers, Seeds, and Fruit Peel Extracts: (2019–2021)

Among the biological extracts, plants are considered as one of the most favorable agents for the preparation of titanium oxide nanoparticles, as shown in Table 17. Various types of phytochemicals (phenol, amino acid, carbohydrate, and flavonoid) in plants regulate the biosynthesis of titanium oxide nanoparticles through stabilization and reduction processes [273]. The reaction starts strenuously when a titanium salt (precursor) is mixed with plant extract and color change (light-green to dark) shows the first sign of biosynthesis

of titanium oxide, as shown in Figure 7 [274]. Synthesis of titanium oxide nanoparticles using various parts of plant is shown in Table 18.

Table 17. Synthesis of Titanium Oxide nanoparticles from leaves, roots, flowers, seeds, and fruit peel extracts.

Sr. No	Reducing Agent	Part of Plant	Size	Shape	Biological Activities	Year of Publication	Ref.
1	*Mentha arvensis*	Leaf	20–70 nm	Spherical	At 10 (µg/mL) Concen of AgNPs *P. Vulgaris* (ZOI = 25 mm), *E. coli* (ZOI = 20 mm), *S. aureus* (ZOI = 21 mm), *A. niger* (ZOI = No), *A. fumigates* (ZOI = 6 mm), and *A. cuboid* (ZOI = No)	2021	[275]
2	*Pouteria campechiana*	Leaf	-	Spherical	Exhibited larvicidal activity toward *Aedes aegypti*	2021	[276]
3	*Coleus aromaticus*	Leaf	12–33 nm	Hexagonal	*S. boydii* (ZOI = 30 mm) *and E. faecalis* (ZOI = 33 mm) Larvicidal activity toward fourth stages of instars' larvae of *Aedes aegypti.* Cytotoxic activity toward HeLa cell line	2021	[277]
4	*Ochradenusarabicusis*	Leaf	20–40 nm	-	*S. aureus* (MIC = 31.25 µg/mL) and *P. aeruginosa* (MIC = 128 µg/mL)	2021	[278]
5	*Aegle marmelos*	Leaf	150 nm	Spherical	Removed ornidazole from wastewater.	2020	[279]
6	*Azadirachta indica*	Leaf	25–87 nm	Spherical	*B. subtilis* (MIC = 25 µg/mL), *E. coli* (MIC = 10.42 µg/mL), *K. pneumoniae* (MIC = 16.66 µg/mL), and *S. typhi* (MIC = 10.42 µg/mL).	2019	[280]
7	*Carica papaya*	Leaf	20 nm	Spherical	Photocatalytic activity (91.19%) against degradation of RO-4 dye	2019	[281]
8	*Aloe barbadensis*	Leaf	~20 nm	Spherical	Anti-biofilm activity toward *P. aeruginosa* (ZOI = 30.69 ± 3.78 mm)	2019	[282]
9	*Glycyrrhiza glabra*	Root	69 nm	Spherical	Cytotoxicity toward HEP2 and vero cell line	2019	[283]
10	Jasmine	Flower	31–42 nm	Spherical	Exhibited excellent degradation toward methylene blue dye (92% after 120 min).	2021	[284]
11	*Myristica fragrans*	Seed	-	-	Showed degradation against Congo red (99% after 45 min) and methylene blue (97% after 60 min).	2021	[285]
12	*Cuminum cyminum*	Seed	15.17 nm	-	-	2021	[286]
13	*Trachyspermum ammi*	Seed	16.63 nm	Spherical and spheroidal	-	2021	[287]
14	*Bixa orellana*	Seed	13 ± 2 nm	Spherical	-	2019	[288]
15	*Nephelium lappaceumL.*	Fruit peel	70–90 nm	-	Cytotoxicity was tested against MDA-MB-231 (death rate of cell = 73.65 µg/mL)	2019	[288]

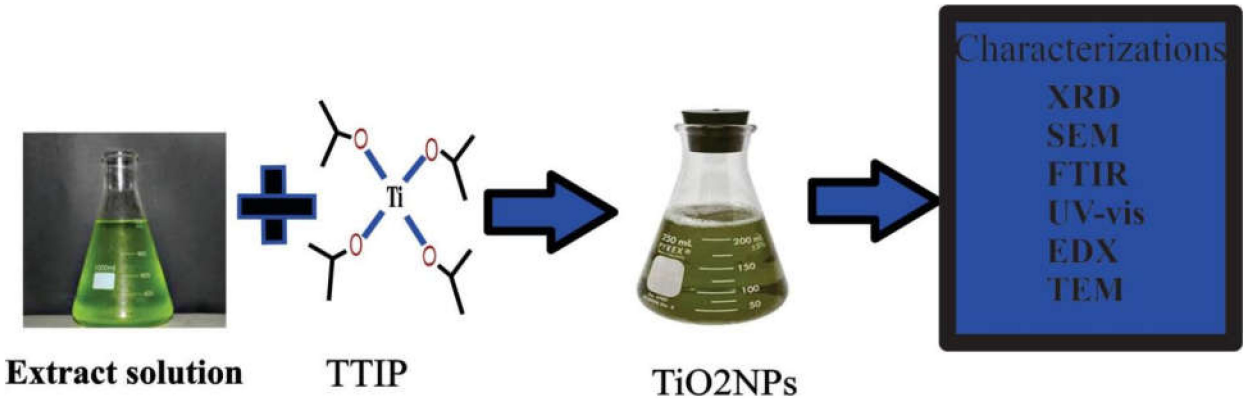

Figure 7. Schematic of green synthesis of TiO_2 nanoparticles using plants. XRD (X-Ray Diffraction Analysis), SEM (Scanning Electron Microscope), FTIR (Fourier transform infrared), UV-Vis (Ultraviolet-visible spectroscopy), EDX (Energy Dispersive X-Ray Analysis), TEM (transmission electron microscopy).

6.5. Copper and Copper Oxide Nanoparticles

Among all metal or metal oxide nanoparticles, copper oxide nanoparticles get more interest due to their multiple applications [289]. Copper oxide is a p-type semiconductor having a narrow bandgap of 1.7 eV. [290]. Biomedical applications of copper oxide nanoparticles involved antifouling, antioxidant, anti-microbial targeted drug delivery, and antibiotics. Copper oxide nanoparticles also have applications in other fields of science such as gas sensors, environmental remediation, nanocomposites' synthesis, magneto-resistant material, textiles, high-temperature superconductor, and conducting material [291–294]. Various physiochemical methods have been extensively used to prepare copper oxide nanoparticles [295]. However, these methods have some flaws, e.g., releasing different hazardous chemicals, time consuming, and high cost. Thus, there is a need for a simple, quicker, eco-friendly, and inexpensive method to prepare nanoparticles with phase selectivity, purity, and homogeneity in morphology [296]. Biological synthesized copper oxide nanoparticles exhibited excellent anti-microbial activity [297]. Green approaches have led to developing a simple, cost-effective, and environmentally friendly process for the biosynthesis of nanoparticles [298].

Synthesis of Copper and Copper Oxide Nanoparticles Using Leaves, Seeds, Flower, and Fruit Peel Extracts: (2019–2021)

Plants create various secondary metabolites and consist of phytochemicals, which are excellent bioresources for the fabrication of copper and copper oxide nanoparticles (Table 18). The most favorable phytochemicals in plants are flavonoids and phenols, present in various parts of the plant, i.e., stems, leaves, fruits, seeds, and flowers. These phenolic phytochemicals have ketone and hydroxyl groups, taking part in the iron chelation and subsequently describing an excellent antioxidant activity [299]. Nanoparticles synthesized through this green approach increase instability, fend off the deformation and agglomeration of nanoparticles, and increase the phenomena of adsorption of phytochemicals on the nanoparticles' surface, which increase the reaction rate of nanoparticles [300]. One of the common approaches in preparing copper and copper oxide nanoparticles is mixing a stoichiometric concentration of plant extract to a stoichiometric concentration of copper salt, heating the nano solution to a suitable temperature, with contentious stirring (shown in Figure 8). The mechanism of formation of copper oxide nanoparticles is shown in Figure 9.

Table 18. Synthesis of copper and copper oxide nanoparticles using leaves, seeds, flowers, and fruit peel extracts.

Sr. No	Reducing Agent	Part of Plant	Size	Cu/CuO NPs	Shape	Biological Activities	Year of Publication	Ref.
1	*Terminalia chebula*	Leaf	100 nm	CuO	Rod-like shape	Applications on diesel engine.	2021	[301]
2	*Cedrus deodara*	Leaf	100 nm	CuO	Spherical	*S. aureus* (MIC = 25 lg/mL) and *E. coli* (MIC = 150 lg/mL)	2021	[302]
3	*Psidium guajava*	Leaf	40–150 nm	CuO	Oval	*epidermis* (ZOI = 1.8 mm), *E. coli* (ZOI = 2 mm), *S. pneumoniae* (ZOI = 1.4 mm), and *P. aeruginosa* (ZOI = 3 mm)	2021	[303]
4	*Sesbania aculeata*	Leaf	-	Cu	-	*C. lunata* (ZOI = 22 mm) and *Phoma destructiva* (ZOI = 23 mm)		[304]
5	*Celastrus paniculatus*	Leaf	2–10 nm	CuO	Spherical	F. Oxysporum (maximum mycelial inhibition = 76.29 mm)	2020	[305]
6	*Catha edulis*	Leaf	-	CuO	Spherical	*K. Pneumonia* (ZOI = 29 ± 0.03 mm), *E. coli* (ZOI = 32 ± 0.02 mm), *S. aureus* (ZOI = 22 ± 0.01 mm), and *S. pyogenes* (ZOI = 24 ± 0.02 mm)	2020	[306]
7	*Ageratum houstonianumMill*	Leaf	~80 nm	Cu	Cubic, rectangular, hexagonal	*E. coli* (ZOI = 12.43 ± 0.233 mm). Photocatalytic property of prepared particles was tested toward an azo dye Congo red (40%).	2020	[307]
8	*Jatropha curcas*	Leaf	10 ± 1 and 12 ± 1 nm	Cu	-	Photocatalytic activity toward methylene blue (70%)	2020	[308]
9	*Citrofortunella microcarpa*	Leaf	-	CuO	-	Photocatalytic activity against Rhodamin B (98%)	2020	[309]
10	*Enicostemma axillare*	Leaf	330 nm	CuO	-	-	2019	[310]
11	*Camelia sinensis*	Leaf	60 ± 6 nm	CU	Spherical	Photocatalytic degradation (83.7%) of prepared copper nanoparticles was tested by utilizing bromophenol blue	2019	[311]
12	*Annona squamosa*	Seed	-	CuO	Spherical	*Microbacterium testaceum* (ZOI = 17 mm) and *E. coli* (ZOI = 21 mm)	2021	[312]
13	*Azadirachta indica*	Seed	41 ± 21 nm	CuO	-	Positive effect on nutrition, growth, and enhanced seed germination	2020	[313]
14	*Elettaria cardamom*	Seed	1–100 nm	CuO	-	-	2020	[314]
15	Wheat	Seed	22 ± 1.5 nm	CuO	Spherical	Described catalytic activity toward 4-nitrophenol removal (97.6% after 5 days)	2019	[315]
16	*Ocimum tenuiflorum*	Flower	5–10 nm	Cu	Spherical	Amino acid detection	2019	[316]
17	*Stachys Lavandulifolia*	Flower	20–25 nm	CuO	Spherical	-	2021	[317]
18	*Punica granatum*	Fruit peel	38.50 nm	CuO	-	-	2020	[318]

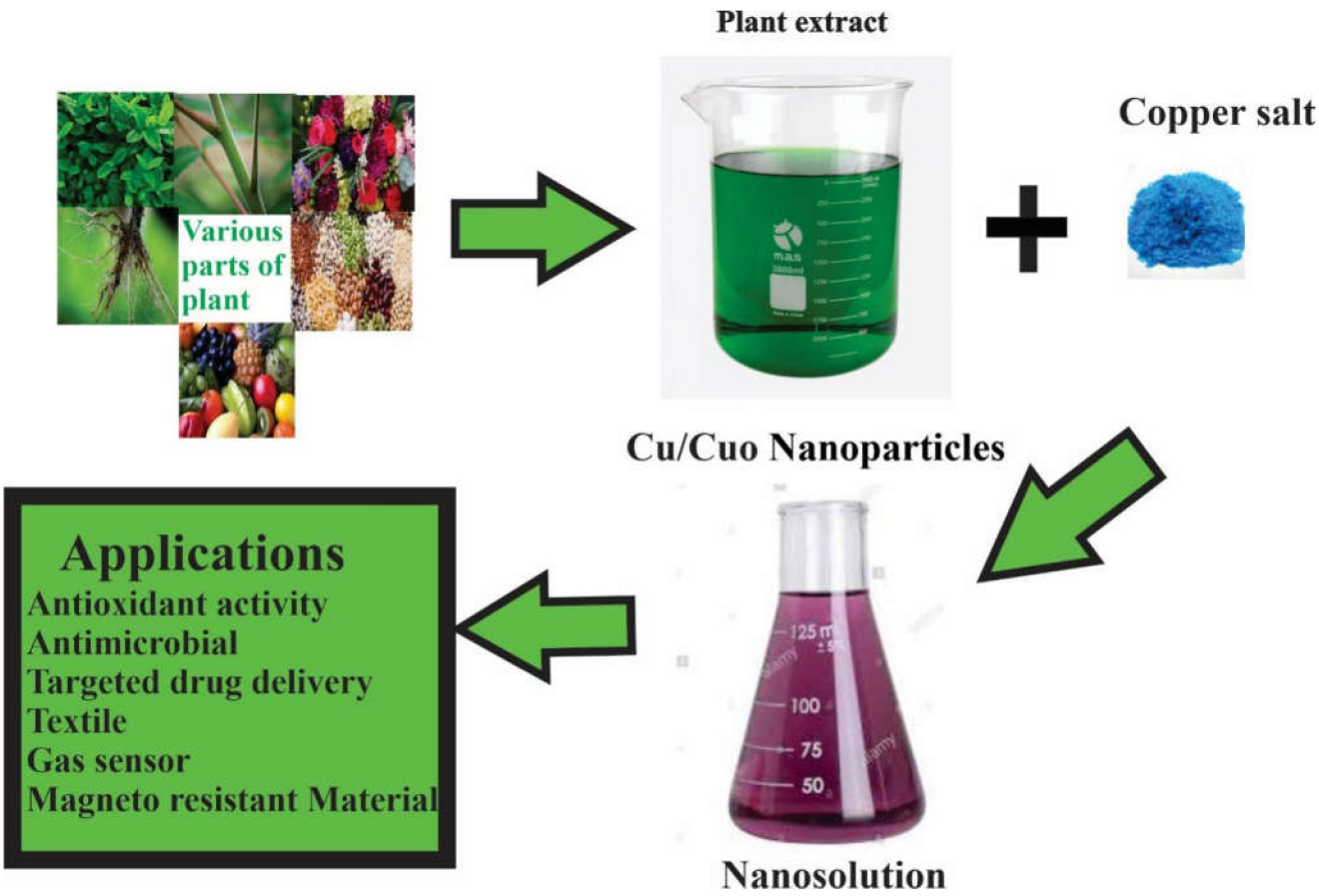

Figure 8. Schematic of green synthesis of Cu/CuO nanoparticles using plants.

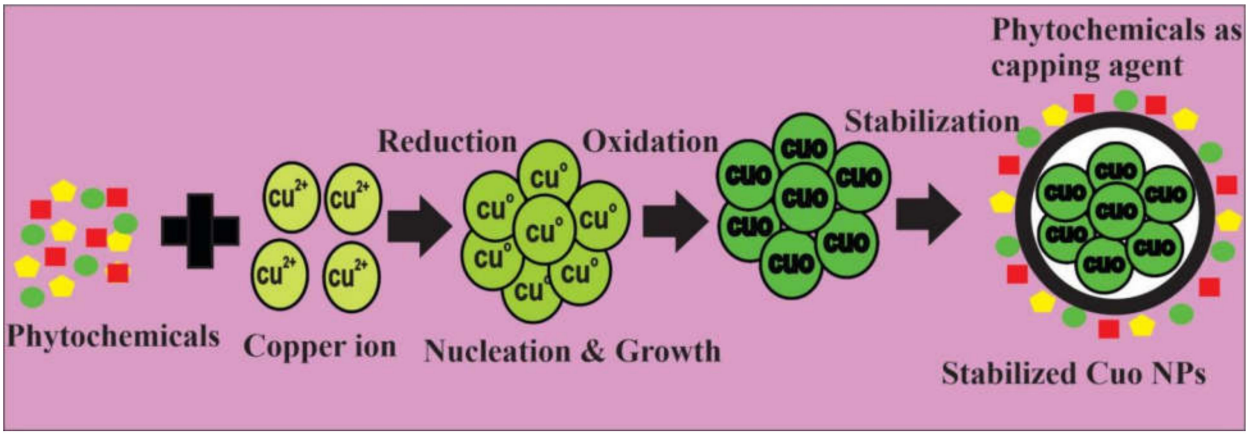

Figure 9. Mechanism of formation of copper oxide nanoparticles.

6.6. Iron or Iron Oxide Nanoparticles

The structure of nanoparticles contains the magnetic core and their combinations, which have magnetic features in the presence of a textan erior magnetic field. Various types of iron oxide nanoparticles, each with its peculiar properties, magnetic behavior, formulas, and applications. The magnetic behavior is because of the motion of electrons [319]. Depending on the response to an external magnetic field, there are six types of material: super magnetic, ferromagnetic, diamagnetic, paramagnetic, antiferromagnetic, and ferrimagnetic. Due to the presence of one electron in the third sub-shell of intermediate metals, e.g., cobalt, iron, and nickel, which is in the absence of an external magnetic field, ferromagnetism

behavior is produced [320]. Magnetic property is also exhibited by Ferromagnetic material. Paramagnetic and magnetic phenomena are also reported among magnetic materials. Because of the superparamagnetic feature of the magnetic nanocatalyst, these nanoparticles have been utilized in various fields. These nanoparticles consist of gadolinium, nickel, cobalt, iron metal, and metal oxide, e.g., Fe_2O_3 [321]. Among different types of metal and metal oxide nanoparticles, iron and iron oxide nanoparticles have exhibited high efficiency in various biomedical and industrial applications. There are eight types of iron oxide nanoparticles, among which magnetite, hematite, and maghemite have very useful applicants. Each of these three oxides has specific catalytic, magnetic, and biochemical properties. Hematite is extensively utilized in pigments, catalysts, and catalysis. It is also a reagent for the preparation of magnetite and maghemite, which have been kept in sight for various applications.

Synthesis of Iron and Iron Oxide Nanoparticles from Leaf, Flower, Seed, and Fruit Extracts: (2019–2021)

Different and cost-efficient synthesis processes have been used by utilizing plants, as shown in Table 19. Synthesis of iron or iron oxides nanoparticles using plants are showed in Figure 10. Arjaghi, Shayan Khalili, et al. synthesized the spherical iron oxide nanoparticles with a size range of 20–70 nm by utilizing *Ramalina sinensis* [322]. In another report, *Chlorophytum comosum* aqueous leaf extract was utilized for the biosynthesis of iron nanoparticles with a size of 100 nm and tested against *P. aeruginosa*, *E. faecalis*, *E. coli,* and *S. aureus.* The prepared iron nanoparticles showed Methyl orange degradation (77% after 7 h) [323]. Jamzad, Mina, et al. carried out an experiment to derive spherical and hexagonal iron oxide nanoparticles utilizing *Laurus nobilis* and tested them against *E. coli* (ZOI = No), *L. monocytogenes* (ZOI = 12 mm), *S. aureus* (ZOI = No), *P. spinulosum* (ZOI = 14 mm), and *A. aspergillus* (ZOI = 13 mm) [324]. In 2020, Bhuiyan, Md Shakhawat Hossen, et al. reported the biosynthesis of iron oxide nanoparticles by utilizing *Carica papaya* aqueous leaf extract and tested them against *S. aureus (*ZOI = 14 mm), *Klebsiella spp (*ZOI = 9 mm), and *E. coli (*ZOI = 9 mm). The prepared iron oxide nanoparticles were tested against BHK-21 and Hela cell lines [325]. Vitta, Yosmery, et al. achieved iron nanoparticles from *Eucalyptus robusta* aqueous leaf extract and tested their antimicrobial commotion against *S. aureus* (ZOI = 1.15 $\pm$ 0.05 mm), *B. subtilis* (ZOI = 3.60 $\pm$ 0.40 mm), *P. aeruginosa* (ZOI = 29 $\pm$ 0.03 mm), and *E. coli* (ZOI = 1.10 $\pm$ 0.10 mm) [326]. In 2019, iron oxide nanoparticles with an average size of 52.78 nm were synthesized utilizing *Ruellia tuberosa* aqueous leaf extract and tested against *K. pneumoniae* (ZOI = 12 mm) and *E. coli* (ZOI = 17 mm) [327]. In 2021, *Avicennia marine* aqueous flower extract was utilized to synthesize iron oxide nanoparticles with an average size of 30–100 nm [328]. Semi-spherical Iron oxide nanoparticles with a size range of 25 to 55 nm were prepared through a green process utilizing *Punica granatum* seed. The prepared iron oxide nanoparticles exhibited efficient degradation toward reactive blue (95.08% after 56 min) [329]. An eco-friendly biosynthesis of iron oxide nanoparticles utilizing B*orassus flabellifer* ethanol seed coat extract was reported by Sandhya et al. and was tested against *B. subtilis, E. coli, S. aureus, C. albicans, and A. niger* [330]. Aziz, Wisam J., et al. reported the biosynthesis of iron oxide nanoparticles by utilizing Iraqi grapes' aqueous extract and tested against *E. coli* (ZOI = 19 mm) and *S. aureus* (ZOI = 18 mm) [331]. Rostamizadeh, Elham, et al. fabricated the iron oxide nanoparticles by utilizing *Cornelian cherry* aqueous extract [332].

Table 19. Synthesis of Iron and Iron oxide nanoparticles from Leaf, flower, seed, and fruit extracts.

Sr. No	Reducing Agent	Part of Plant	Size	Iron/Iron Oxide NPs	Shape	Biological Activities	Year of Publication	Ref.
1	*Romalina sinensis*	Leaf	20–70 nm	Iron Oxide	Spherical	-	2021	[322]
2	*Chlorophytum comosum*	Leaf	100 nm	Iron	-	*P. aeruginosa*, *E. faecalis*, *E. coli*, *and S. aureus.* The prepared iron nanoparticles showed Methyl orange degradation (77% after 7 h)	2021	[323]
3	*Laurus nobilis*	Leaf	8.03 ± 8.99 nm	Iron Oxide	Spherical and hexagonal	*E. coli* (ZOI = No), *L. monocytogenes* (ZOI = 12 mm), *S. aureus* (ZOI = No), *P. spinulosum* (ZOI = 14 mm), and *A. aspergillus* (ZOI = 13 mm)	2020	[324]
4	*Carica papaya*	Leaf	-	Iron Oxide	-	*S. aureus* (ZOI = 14 mm), *Klebsiella spp* (ZOI = 9 mm), and *E. coli* (ZOI = 9 mm). Exhibited against BHK-21 and Hela cell lines	2020	[325]
5	*Eucalyptus robusta*	Leaf	-	Iron	-	*S. aureus* (ZOI = 1.15 ± 0.05 mm), *B. subtilis* (ZOI = 3.60 ± 0.40 mm), *P. aeruginosa* (ZOI = 29 ± 0.03 mm), and *E. coli* (ZOI = 1.10 ± 0.10 mm)	2020	[326]
6	*Ruellia tuberosa*	Leaf	52.78 nm	Iron Oxide	-	*K. pneumonia* (ZOI = 12 mm) and *E. coli* (ZOI = 17 mm)	2019	[327]
7	*Avicennia marine*	Flower	30–100 nm	Iron oxide	Honeycomb	-	2021	[328]
8	*Punica granatum*	Seed	25–55nm	Iron oxide	Semi spherical	Exhibited efficient degradation toward reactive blue (95.08% after 56 min)	2019	[329]
9	*Borassusflabellifer*	Seed	10–40 nm	Iron oxide	Hexagonal	At 50 (μg/mL) Concen of Fe_2O_3NPs *B. subtilis* (ZOI = 18 mm), *E. coli* (ZOI = 14 mm), *S. aureus* (ZOI = 11 mm), *C. albicans* (ZOI = 9 mm), and *A. niger* (ZOI = 9 mm) At 100 (μg/mL) Concen of Fe_2O_3NPs *C. subtilis* (ZOI = 24 mm), *E. coli* (ZOI = 14 mm), *S. aureus* (ZOI = 18 mm), *C. albicans* (ZOI = 10 mm), and *A. niger* (ZOI = 11 mm) At 500 (μg/mL) Concen of Fe_2O_3NPs *B. subtilis* (ZOI = 26 mm), *E. coli* (ZOI = 23 mm), *S. aureus* (ZOI = 20 mm), *C. albicans* (ZOI = 13 mm), and *A. niger* (ZOI = 15 mm)	2020	[330]
10	*Iraqi grapes*	Fruit	29–37 nm	Iron oxide	-	*E. coli* (ZOI = 19 mm) and *S. aureus* (ZOI = 18 mm)	2020	[331]
11	*Cornelian cherry*	Fruit	20–40 nm	Iron oxide	Spherical	-	2020	[333]

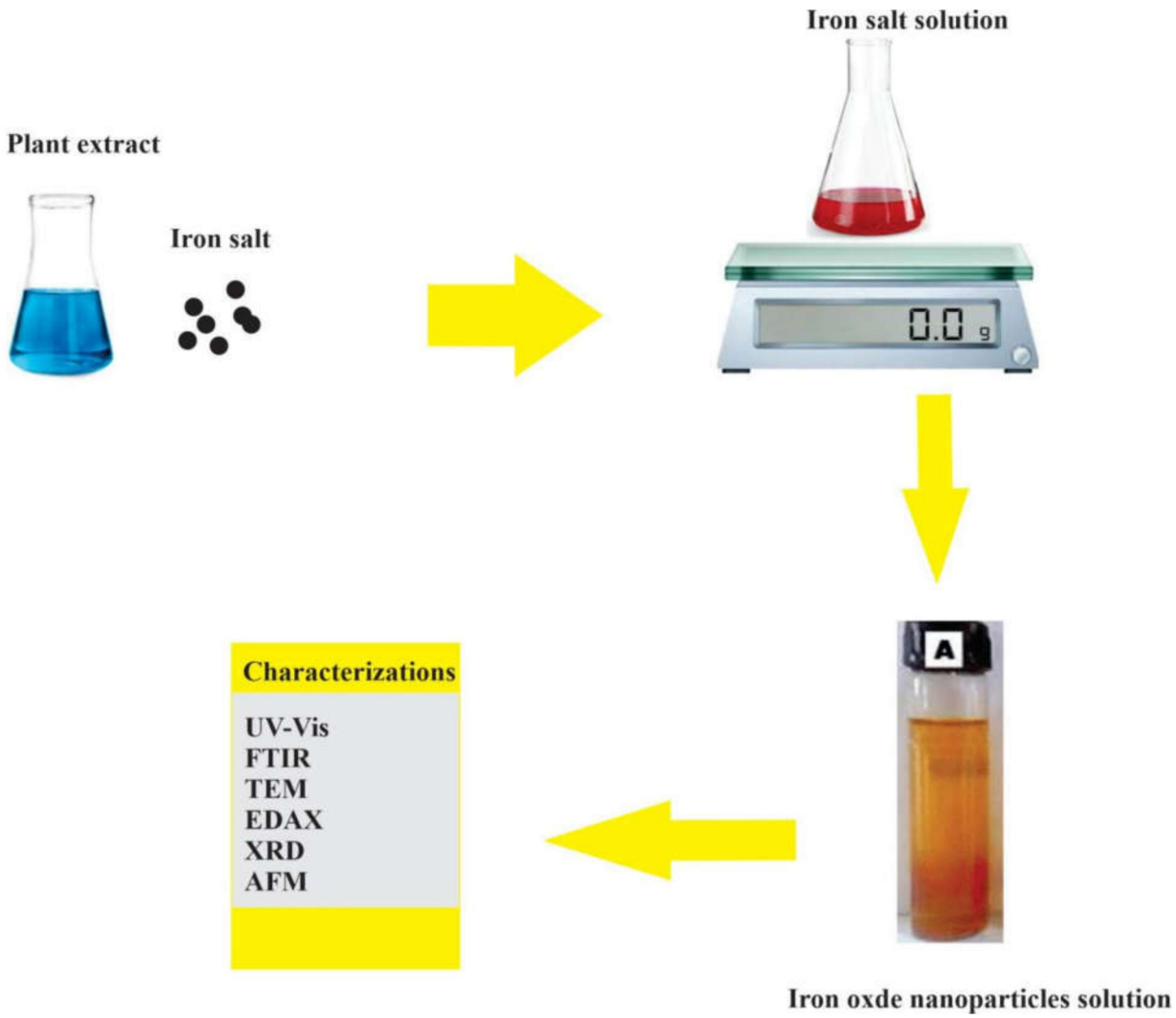

Figure 10. Schematic of green synthesis of Fe and Fe_2O_3 nanoparticles using plants. UV-Vis (Ultraviolet-visible spectroscopy), FTIR (Fourier transform infrared), TEM (transmission electron microscopy), EDAX (Energy Dispersive X-Ray Analysis), XRD (X-Ray Diffraction Analysis), and AFM (Atomic Force Microscopy).

6.7. Cobalt and Cobalt Oxide Nanoparticles

Cobalt is a transition (d-block) metal that has useful effects on human health [333,334]. It is an essential part of Cobalamin (Vitamin B12), which is helpful in the cure of anemia as it excites the production of red blood cells [334]. Cobalt has unique catalytic, electrical, and optical properties that make it favorable for a vast range of applications involving catalysts, nano-electronic devices, and nano-sensors [335]. Cobalt can show variable oxidation states, e.g., CO^{4+}, CO^{3+}, and CO^{2+}, that make it favorable to be utilized in various fields [336]. Now, cobalt nanoparticles have attracted remarkable interest because they are cheaper than other metal or metal oxide nanoparticles and exhibit various properties, e.g., magnetic and electrical, because of their huge surface area [337,338].

Synthesis of Cobalt or Cobalt Oxide Nanoparticles Using Plants

Synthesis of cobalt and cobalt oxide nanoparticles by a green approach utilizing plants, in general, includes washing or drying the plants' part (leaves, root, stem, flower, seed, and fruit), as shown in Table 20. The plant materials (fresh or powder) are boiled with water and the resultant extract is filtered. Phytochemical properties are because of the presence of biomolecules in plant extracts, e.g., vitamin, phenol, protein, carbohydrate, flavonoid, and

more. Adding cobalt salt to plant extract reduces and stabilizes the cobalt ion to prepare cobalt and cobalt oxide nanoparticles [339].

Table 20. Synthesis of cobalt or cobalt oxide nanoparticles using plants.

Sr. No	Reducing Agent	Part of Plant	Size	Cobalt/Cobalt Oxide NPs	Shape	Biological Activities	Year of Publication	Ref.
1	*Hibiscus rosa sinensis*	Leaf	-	Co_3O_4	-	*P. aeruginosa* (ZOI = 20 ± 1.47 mm), *E. coli* (ZOI = 16 ± 1.61 mm), and *Proteus vulgaris* (ZOI = 21 ± 1.32 mm)	2021	[340]
2	*Conocarpus erectus L*	Leaf	4.9 nm	Co	Spherical	-	2021	[341]
3	*Citrus medica*	Leaf	100 nm	Co_3O_4	-	Degradation of methyl orange (90% after 1 h)	2021	[342]
4	*Foenum-graceum L.*	Leaf	13.2 nm	Co_3O_4	Quasi-spherical	-	2020	[343]
5	*Populus ciliata*	Leaf	-	Co_3O_4	-	At 2(mg/mL) Concen of CoNPs *B. Lichenifermis* (ZOI = 14.1 ± 0.4 mm), *E. coli* (ZOI = 1.10 ± 0.5 mm), *B. subtilis* (ZOI = 19.7 ± 0.4 mm), and *K. pneumonia* (ZOI = 12.8 ± 0.2 mm) At 4(mg/mL) Concen of CoNPs *B. Lichenifermis* (ZOI = 19.2 ± 1.2 mm), *E. coli* (ZOI = 15.1 ± 0.6 mm), *B. subtilis* (ZOI = 21.2 ± 0.5 mm), and *K. pneumonia* (ZOI = 17.8 ± 0.9 mm) At 2(mg/mL) Concen of CoNPs *B. Lichenifermis* (ZOI = 22.5 ± 0.9 mm), *E. coli* (ZOI = 16.0 ± 0.8 mm), *B. subtilis* ZOI = 24.5 ± 1.3 mm), and *K. pneumonia* (ZOI = 20.4 ± 0.7 mm)	2020	[344]
6	*Selinum wallichianum*	Leaf	-	Co	-	-	2019	[345]

7. Antibacterial Activities of Metal and Metal Oxide Nanoparticles

Research is going on and a vast amount of literature exists on the antimicrobial activity of metal and metal oxide nanoparticles. The silver nanoparticles excellently discompose the polymer sub-units of the cell membrane in micro-organisms. The plant-mediated silver nanoparticles consequently rupture the cell membrane, destroying the protein synthesis mechanism in the bacteria [346]. The higher concentration of silver nanoparticles has rapid membrane permeability, as compared to a lower concentration, and subsequently breaks the cell wall of bacteria, as shown in Figure 11 [347]. The highest conductivity was seen in *Rhizophora apiculate*-reduced silver nanoparticles, which exhibited a lower number of a bacterial colony in the experimental plate than the silver nitrate-treated cells, which may be because of a larger surface area and smaller size of nanoparticles. These two factors increase the permeability across the cell membrane and cell destruction [348]. The green-synthesized silver nanoparticles were prepared using Citrus sinensis peel extract and evaluated for antibacterial activity toward *S. aureus*, *P. aeruginosa*, and *E. coli* [349].

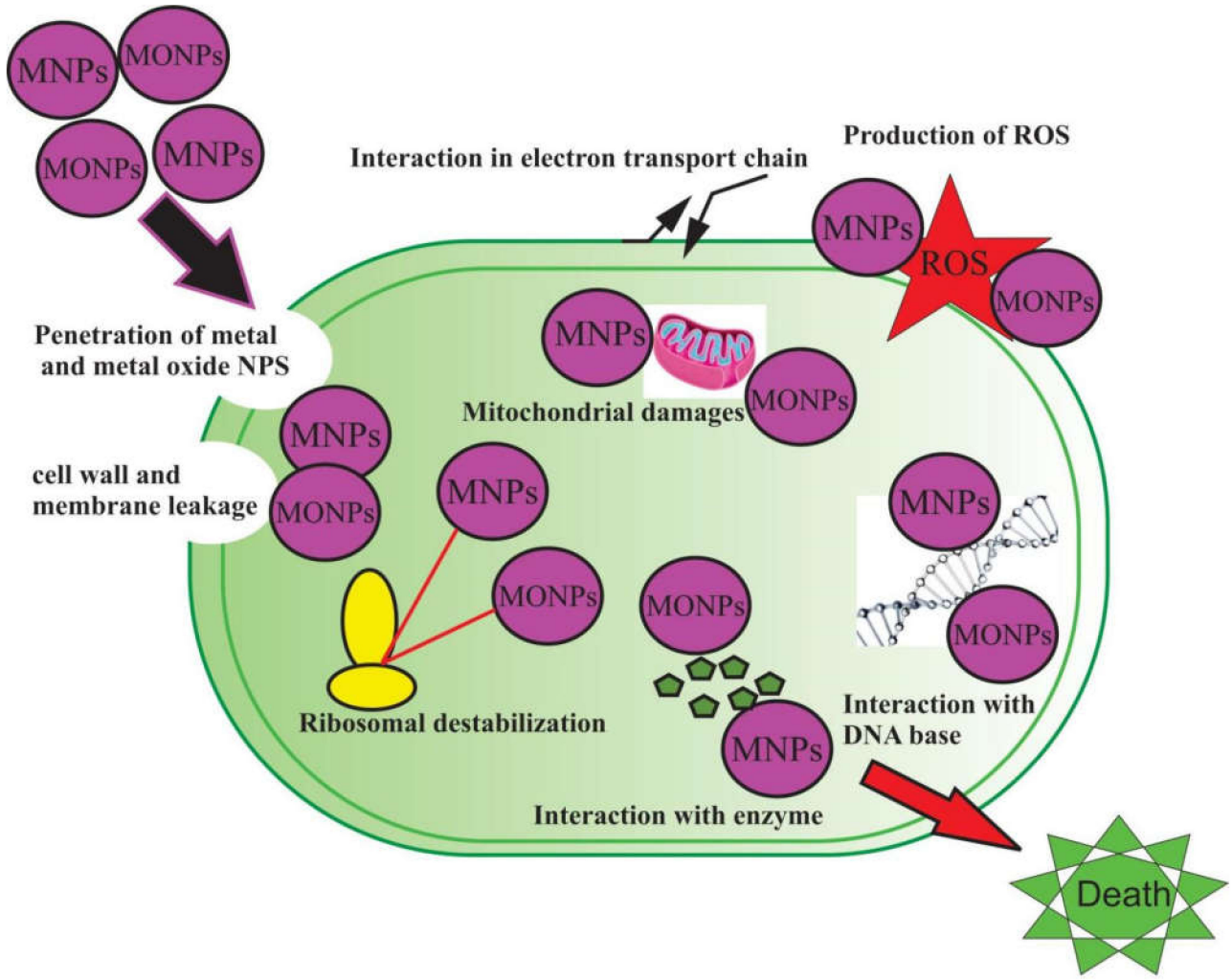

Figure 11. Mechanism of antibacterial activity of metal or metal oxide nanoparticles. MNPs means metal nanoparticles, MONPs means metal oxide nanoparticles, and ROS means Reactive oxygen species.

8. Antifungal Activity

The fungicidal mechanism of plant-mediated metal and metal oxide nanoparticles has greater potential as compared to commercial antibiotics, e.g., amphotericin. The plant-mediated silver nanoparticles have clearly exhibited the membrane breakage in Candida sp. and damage in fungal components (intercellular) and, consequently, cell function was destroyed [350]. Most commercial drugs have limited clinical applications and have more adverse effects. Consequently, the commercial antifungal agents induce side effects, e.g., liver damage and renal failure and nausea, diarrhea, and body temperature increased after utilizing the drugs. The cell wall of fungi is made up of protein and fatty acid. The plant-mediated silver nanoparticles have promising activity toward spore-producing fungus and efficiently damage the fungal growth. In the fungal cell membrane composition and structure, significant changes were seen by interacting it with metal and metal oxide nanoparticles [351].

9. Anticancer Activity

Cancer is an uncontrollable cell proliferation, having extensive changes of enzymatic parameters and bio-chemicals, which is the universal behavior of cancer cells. The over-exposure of cellular growth will be triggered, and the cell cycle mechanism in cancerous cells will be arrested by utilizing plant-based nanoparticles [352]. The plant-based metal or metal oxide nanoparticles have excellent effects on different cancer cell lines, e.g., Hela,

Hep 2, and HCT 116 cell lines. To date, various works reported that plant-mediated nanoparticles have the ability to control cancer cell growth. The bettered cytotoxic effect is because of secondary metabolites and some other non-metal composition in the prepared medium [353,354]. The bio-synthesized silver nanoparticles triggered the cell cycle and enzymes in the bloodstream [355]. Furthermore, the plant-derived nanoparticles control the formation of free radicals from the cell. Free radicals normally are the cause of cell proliferation and harm normal cell function. The moderate quantity of gold nanoparticles is the cause of the apoptosis mechanism in tumor cells (malignant cells) [356]. The metal and metal oxide nanoparticles have proven their application in medical science to diagnose and cure different types of cancer cells. The plant-mediated nanoparticles are advanced and revolutionized to cure the malignant deposits without disturbing the normal cell line.

10. Challenge and Future Perspectives of Plant-Mediated Metal and Metal Oxide Nanoparticles

To date, various plants' extracts have been investigated for the preparation of metal or metal oxide nanoparticles and have been excellently used in a wide range of applications due to their huge abundance in nature. Recently, plant extracts have been investigated for their effectiveness in the formation of nanoparticles, which are based on the compositions of diverse phytochemicals and plant sources. However, the specific phytochemicals causing the reduction, capping, and stabilization of nanoparticles in the green synthesis mechanism are still not completely understood. Thus, further studies are required to understand these details. A suggested approach that might be able to describe the responsible phytochemicals serving as stabilizing and reducing candidates involves isolation protocols of the pure compound to identify specific phytochemicals. Additionally, the composition of phytochemicals in plant extract can be determined through various analytical techniques, e.g., ICP-AES (Inductively coupled plasma—atomic emission spectroscopy), HPLC (High Pressure Liquid Chromatography), NMR (Nuclear magnetic resonance), and GC-MS (gas chromatography-Mass spectroscopy) and various quantitative and qualitative chemical processes can be utilized to know the variety of phytochemicals through Coomassie blue assays, phenol-sulfuric acid assays, and colorimetric assays. The main challenge may be in knowing the basic profile of bio-molecules needed for serving as reducing agents of metal ions. Despite the various benefits of plant extracts, there are many other hindrances that should be accounted for before they can be applied practically, e.g., structure, control of shape, size, monodispersity, and crystallinity of plant-mediated nanoparticles. This template morphology is also connected to the phytochemicals that exist in the plant extract. Additionally, some other factors affect the morphology of nanoparticles such as metal ion concentration, reaction temperature, plant extract concentration, and pH. Furthermore, as described, the capability to attain a high yield of nanoparticles is also influenced, as is the reduction power of the plant.

The stability of plant-mediated nanoparticles is another important parameter to consider. It is very necessary to ensure that plant-mediated nanoparticles can remain stable for a long time without any changes in morphology. Another condition that should be discussed is an estimation of toxicity and biocompatibility of plant-mediated nanoparticles to human health and the ecosystem, which are still not described efficiently and are frequently reported.

More integrated, detailed, and systematic research work is still needed to fully define the human and ecological toxicity profile of plant-mediated nanoparticles to develop a stable system for the preparation of nanoparticles with well-defined size, morphology, and efficient homogeneity.

11. Conclusions

Biosynthesis of metal and metal oxide nanoparticles has been advanced and is a highly attractive research field of science over the last decades. Thus, knowledge of green chemistry and the use of green routes for the synthesis of nanoparticles is increasing day by day in order to get an environmentally friendly process. Various types of natural extracts (such

as plants, fungi, algae, and bacteria) have been utilized for the preparation of nanoparticles. Among all the above mentioned sources, plants have been considered to possess remarkable efficiency as capping, reducing, and stabilizing agents for the preparation of nanoparticles with desired morphology due to the presence of Phytomolecules. This review delivers an excellent platform to researchers or the scientific community to gain diverse information related to detailing green synthesis of metal or metal oxide nanoparticles using multiple plant parts. Fundamentally, the greener production of metal or metal oxide nanoparticles using plant extracts has different biological applications such as anticancer, anti-microbial, and antifungal activity.

Author Contributions: Conceptualization, I.I. and A.B.; methodology, E.G. and A.N.; software, S.H.; validation, R.S., S.S.A. and R.A.; formal analysis, H.Z. and R.S.; investigation, S.S.A.; resources, E.G. and R.A.; data curation, I.I.; writing—original draft preparation, I.I. and A.B.; writing—review and editing, H.Z. and A.N.; visualization, S.H.; supervision, Y.N.; project administration, Y.N.; funding acquisition, I.I. All authors have read and agreed to the published version of the manuscript.

Funding: The author from King Khalid University is thankful for support of Deanship Scientific grant under the project No. RGP.2/156/42.

Institutional Review Board Statement: Not applicable.

Informed Consent Statement: Not applicable.

Data Availability Statement: Data sharing is not applicable for this article.

Acknowledgments: All authors acknowledge the School of Chemistry, Minhaj University Lahore for providing platform for this work.

Conflicts of Interest: The authors declare that they have no known competing financial interest or personal relationships that could have appeared to influence the work reported in this paper.

Abbreviation

S. aureus	*Staphylococcus aureus*
E. coli	*Escherichia coli*
B. Subtilis	*Bacillus subtilis*
P. aeruginosa	*Pseudomonas aeruginosa*
C. Albicans	*Candida albicans*
E. faecalis	*Enterococcus faecalis*
B. cereus	*Bacillus cereus*
K. Pneumoniae	*Klebsiella pneumoniae*
S. typhi	*Salmonella typhi*
P. mirabilis	*Proteus mirabilis*

References

1. Auffan, M.; Rose, J.; Bottero, J.-Y.; Lowry, G.V.; Jolivet, J.-P.; Wiesner, M.R. Towards a definition of inorganic nanoparticles from an environmental, health and safety perspective. *Nat. Nanotechnol.* **2009**, *4*, 634–641. [CrossRef] [PubMed]
2. Narayanan, K.B.; Sakthivel, N. Biological synthesis of metal nanoparticles by microbes. *Adv. Colloid Interface Sci.* **2010**, *156*, 1–13. [CrossRef] [PubMed]
3. Surendra, T.V.; Roopan, S.M.; Khan, M.R. Biogenic approach to synthesize rod shaped Gd2O3 nanoparticles and its optimization using response surface methodology-Box–Behnken design model. *Biotechnol. Prog.* **2019**, *35*, e2823. [CrossRef]
4. Sabir, S.; Arshad, M.; Chaudhari, S.K. Zinc Oxide Nanoparticles for Revolutionizing Agriculture: Synthesis and Applications. *Sci. World J.* **2014**, *2014*, 1–8. [CrossRef]
5. Ditta, A.; Arshad, M.; Ibrahim, M. Nanoparticles in Sustainable Agricultural Crop Production: Applications and Perspectives. In *Nanotechnology and Plant Sciences*; Springer: Cham, Switzerland, 2015; pp. 55–75. [CrossRef]
6. Sukumaran, P.; Poulose, E.K. Silver nanoparticles: Mechanism of antimicrobial action, synthesis, medical applications, and toxicity effects. *Int. Nano Lett.* **2012**, *2*, 1–10.
7. Lee, Y.; Choi, J.-R.; Lee, K.J.; E Stott, N.; Kim, D. Large-scale synthesis of copper nanoparticles by chemically controlled reduction for applications of inkjet-printed electronics. *Nanotechnology* **2008**, *19*, 415604. [CrossRef] [PubMed]
8. Naoki, T.; Yonezawa, T. Bimetallic nanoparticles—novel materials for chemical and physical applications. *New J. Chem.* **1998**, *22*, 1179–1201.
9. Reddy, L.H.; Arias, J.L.; Nicolas, J.; Couvreur, P. Magnetic Nanoparticles: Design and Characterization, Toxicity and Biocompatibility, Pharmaceutical and Biomedical Applications. *Chem. Rev.* **2012**, *112*, 5818–5878. [CrossRef] [PubMed]

10. Antonyraj, C.A.; Jeong, J.; Kim, B.; Shin, S.; Kim, S.; Lee, K.-Y.; Cho, J.K. Selective oxidation of HMF to DFF using Ru/γ-alumina catalyst in moderate boiling solvents toward industrial production. *J. Ind. Eng. Chem.* **2012**, *19*, 1056–1059. [CrossRef]
11. Neville, F.; A Pchelintsev, N.; Broderick, M.J.F.; Gibson, T.; A Millner, P. Novel one-pot synthesis and characterization of bioactive thiol-silicate nanoparticles for biocatalytic and biosensor applications. *Nanotechnology* **2009**, *20*, 055612. [CrossRef]
12. Staniland, S.S. Magnetosomes: Bacterial biosynthesis of magnetic nanoparticles and potential biomedical applications. *Nanotechnol. Life Sci. Online* **2007**, *2011*.
13. Luo, X.; Luo, X.; Morrin, A.; Killard, A.J.; Smyth, M.R. Application of nanoparticles in electrochemical sensors and biosensors. *Electroanal. Int. J. Devoted Fundam. Pract. Asp. Electroanal.* **2006**, *18*, 319–326. [CrossRef]
14. Murthy, S.K. Nanoparticles in modern medicine: State of the art and future challenges. *Int. J. Nanomed.* **2007**, *2*, 129–141.
15. Wen, Z.-Q.; Li, G.; Ren, D. Detection of Trace Melamine in Raw Materials Used for Protein Pharmaceutical Manufacturing Using Surface-Enhanced Raman Spectroscopy (SERS) with Gold Nanoparticles. *Appl. Spectrosc.* **2011**, *65*, 514–521. [CrossRef]
16. Xia, Y.; Yang, H.; Campbell, C.T. Nanoparticles for catalysis. *Acc. Chem. Res.* **2013**, *46*, 1671–1672. [CrossRef]
17. Cao, G.; Wang, Y. *Nanostructures and Nanomaterials: Synthesis, Properties Applications*; Imperial College Press: London, UK, 2004.
18. Fazal-ur-Rehman, M.; Qayyum, I.; Ibrahim, M.S. Nanotechnology: An innovation in scientific research and technology. *Curr. Sci.* **2019**, *5*, 48–59.
19. Tshoko, S. Spectroelectrochemical Graphene-Silver/Zinc Oxide Nanoparticulate Phenotype Biosensors for Ethambutol and Pyrazinamide. Master's Thesis, University of the Western Cape, Cape Town, South Africa, 2019.
20. El Shafey, A.M. Green synthesis of metal and metal oxide nanoparticles from plant leaf extracts and their applications: A review. *Green Process. Synth.* **2020**, *9*, 304–339. [CrossRef]
21. Clark, J.H.; Macquarrie, D.J. *Handbook of Green Chemistry and Technology*; Wiley: Hoboken, NJ, USA, 2008.
22. Robert, K.W.; Parris, T.M.; Leiserowitz, A.A. What is sustainable development? Goals, indicators, values, and practice. *Environ. Sci. Policy Sustain. Dev.* **2005**, *47*, 8–21. [CrossRef]
23. Omer, A.M. Energy, environment and sustainable development. *Renew. Sustain. Energy Rev.* **2008**, *12*, 2265–2300. [CrossRef]
24. Wilson, M.P.; Schwarzman, M.R. Toward a new US chemicals policy: Rebuilding the foundation to advance new science, green chemistry, and environmental health. *Environ. Health Perspect.* **2009**, *117*, 1202–1209. [CrossRef]
25. Crowl, D.A.; Louvar, J.F. *Chemical Process Safety: Fundamentals with Applications*; Pearson Education: London, UK, 2001.
26. Anastas, P.; Eghbali, N. Green chemistry: Principles and practice. *Chem. Soc. Rev.* **2010**, *39*, 301–312. [CrossRef]
27. Centi, G.; Perathoner, S. From green to sustainable industrial chemistry. In *Sustainable Industrial Chemistry*; Cavani, F., Centi, G., Perathoner, S., Trifiró, F., Eds.; Wiley: Hoboken, NJ, USA, 2009.
28. Al Ansari, M.S. A review of optimal designs in relation to supply chains and sustainable chemical processes. *Mod. Appl. Sci.* **2012**, *6*, 74. [CrossRef]
29. Pal, G.; Rai, P.; Pandey, A. Green synthesis of nanoparticles: A greener approach for a cleaner future. In *Green Synthesis, Characterization and Applications of Nanoparticles*; Elsevier: Amsterdam, The Netherlands, 2019; pp. 1–26.
30. Mohanpuria, P.; Rana, N.K.; Yadav, S.K. Biosynthesis of nanoparticles: Technological concepts and future applications. *J. Nanoparticle Res.* **2007**, *10*, 507–517. [CrossRef]
31. Hulkoti Nasreen, I.; Taranath, T.C. Biosynthesis of nanoparticles using microbes—a review. *Colloids Surf. B Biointerfaces* **2014**, *121*, 474–483. [CrossRef]
32. Iravani, S. Green synthesis of metal nanoparticles using plants. *Green Chem.* **2011**, *13*, 2638–2650. [CrossRef]
33. Gittins, D.I.; Bethell, D.; Schiffrin, D.J.; Nichols, R. A nanometre-scale electronic switch consisting of a metal cluster and redox-addressable groups. *Nature* **2000**, *408*, 67–69. [CrossRef] [PubMed]
34. Sumera; Anwar, A.; Ovais, M.; Khan, A.; Raza, A. Docetaxel-loaded solid lipid nanoparticles: A novel drug delivery system. *IET Nanobiotechnology* **2017**, *11*, 621–629. [CrossRef]
35. Awan, U.A.; Ali, S.; Rehman, M.; Zia, N.; Naz, S.S.; Ovais, M.; Raza, A. Stable and reproducible synthesis of gold nanorods for biomedical applications: A comprehensive study. *Iet Nanobiotechnology* **2018**, *12*, 182–190. [CrossRef]
36. Emmanuel, R.; Saravanan, M.; Ovais, M.; Padmavathy, S.; Shinwari, Z.K.; Prakash, P. Antimicrobial efficacy of drug blended biosynthesized colloidal gold nanoparticles from Justicia glauca against oral pathogens: A nanoantibiotic approach. *Microb. Pathog.* **2017**, *113*, 295–302. [CrossRef]
37. Khalil, A.T.; Ovais, M.; Ullah, I.; Ali, M.; Shinwari, Z.K.; Khamlich, S.; Maaza, M. Sageretia thea (Osbeck.) mediated synthesis of zinc oxide nanoparticles and its biological applications. *Nanomedicine* **2017**, *12*, 1767–1789. [CrossRef]
38. Mashwani, Z.-U.; Khan, M.A.; Khan, T.; Nadhman, A. Applications of plant terpenoids in the synthesis of colloidal silver nanoparticles. *Adv. Colloid Interface Sci.* **2016**, *234*, 132–141. [CrossRef]
39. Mukherjee, S.; Sushma, V.; Patra, S.; Barui, A.K.; Bhadra, M.P.; Sreedhar, B.; Patra, C.R. Green chemistry approach for the synthesis and stabilization of biocompatible gold nanoparticles and their potential applications in cancer therapy. *Nanotechnology* **2012**, *23*, 455103. [CrossRef] [PubMed]
40. Mukherjee, S.; Vinothkumar, B.; Prashanthi, S.; Bangal, P.R.; Sreedhar, B.; Patra, C.R. Potential therapeutic and diagnostic applications of one-step in situ biosynthesized gold nanoconjugates (2-in-1 system) in cancer treatment. *RSC Adv.* **2012**, *3*, 2318–2329. [CrossRef]
41. Mukherjee, S.; Debabrata, C.; Rajesh, K.; Sujata, P. Potential theranostics application of bio-synthesized silver nanoparticles (4-in-1 system). *Theranostics* **2014**, *4*, 316. [CrossRef] [PubMed]

42. Mukherjee, S.; Dasari, M.; Priyamvada, S.; Kotcherlakota, R.; Bollu, V.S.; Patra, C.R. A green chemistry approach for the synthesis of gold nanoconjugates that induce the inhibition of cancer cell proliferation through induction of oxidative stress and their in vivo toxicity study. *J. Mater. Chem. B* **2015**, *3*, 3820–3830. [CrossRef]
43. Mukherjee, S.; Sau, S.; Madhuri, D.; Bollu, V.S.; Madhusudana, K.; Sreedhar, B.; Banerjee, R.; Patra, C.R. Green synthesis and characterization of monodispersed gold nanoparticles: Toxicity study, delivery of doxorubicin and its bio-distribution in mouse model. *J. Biomed. Nanotechnol.* **2016**, *12*, 165–181. [CrossRef] [PubMed]
44. Zohra, T.; Ovais, M.; Khalil, A.T.; Qasim, M.; Ayaz, M.; Shinwari, Z.K. Extraction optimization, total phenolic, flavonoid contents, HPLC-DAD analysis and diverse pharmacological evaluations of Dysphania ambrosioides (L.) Mosyakin & Clemants. *Nat. Prod. Res.* **2018**, *33*, 136–142. [CrossRef]
45. Maruyama, T.; Fujimoto, Y.; Maekawa, T. Synthesis of gold nanoparticles using various amino acids. *J. Colloid Interface Sci.* **2015**, *447*, 254–257. [CrossRef]
46. Polavarapu, L.; Xu, Q.H. A single-step synthesis of gold nanochains using an amino acid as a capping agent and characterization of their optical properties. *Nanotechnology* **2008**, *19*, 075601. [CrossRef]
47. Ramani, M.; Ponnusamy, S.; Muthamizhchelvan, C.; Marsili, E. Amino acid-mediated synthesis of zinc oxide nanostructures and evaluation of their facet-dependent antimicrobial activity. *Colloids Surfaces B: Biointerfaces* **2014**, *117*, 233–239. [CrossRef]
48. Li, S.; Shen, Y.; Xie, A.; Yu, X.; Qiu, L.; Zhang, L.; Zhang, Q. Green synthesis of silver nanoparticles using Capsicum annuum L. extract. *Green Chem.* **2007**, *9*, 852–858. [CrossRef]
49. Ashraf, S.; Abbasi, A.Z.; Pfeiffer, C.; Hussain, S.Z.; Khalid, Z.M.; Gil, P.R.; Parak, W.J.; Hussain, I. Protein-mediated synthesis, pH-induced reversible agglomeration, toxicity and cellular interaction of silver nanoparticles. *Colloids Surfaces B Biointerfaces* **2013**, *102*, 511–518. [CrossRef] [PubMed]
50. Parveen, R.; Shamsi, T.N.; Fatima, S. Nanoparticles-protein interaction: Role in protein aggregation and clinical implications. *Int. J. Biol. Macromol.* **2016**, *94*, 386–395. [CrossRef] [PubMed]
51. Shukla, R.; Nune, S.K.; Chanda, N.; Katti, K.; Mekapothula, S.; Kulkarni, R.R.; Welshons, W.V.; Kannan, R.; Katti, K.V. Soybeans as a phytochemical reservoir for the production and stabilization of biocompatible gold nanoparticles. *Small* **2008**, *4*, 1425–1436. [CrossRef]
52. Raveendran, P.; Fu, J.; Wallen, S.L. Completely "green" synthesis and stabilization of metal nanoparticles. *J. Am. Chem. Soc.* **2003**, *125*, 13940–13941. [CrossRef]
53. Zhao, X.; Xia, Y.; Li, Q.; Ma, X.; Quan, F.; Geng, C.; Han, Z. Microwave-assisted synthesis of silver nanoparticles using sodium alginate and their antibacterial activity. *Colloids Surfaces A: Physicochem. Eng. Asp.* **2014**, *444*, 180–188. [CrossRef]
54. Akhlaghi, S.P.; Peng, B.; Yao, Z.; Tam, K.C. Sustainable nanomaterials derived from polysaccharides and amphiphilic compounds. *Soft Matter* **2013**, *9*, 7905–7918. [CrossRef]
55. Duan, H.; Wang, D.; Li, Y. Green chemistry for nanoparticle synthesis. *Chem. Soc. Rev.* **2015**, *44*, 5778–5792. [CrossRef] [PubMed]
56. Boury, B.; Plumejeau, S. Metal oxides and polysaccharides: An efficient hybrid association for materials chemistry. *Green Chem.* **2014**, *17*, 72–88. [CrossRef]
57. Philip, D. Biosynthesis of Au, Ag and Au–Ag nanoparticles using edible mushroom extract. *Spectrochim. Acta Part A: Mol. Biomol. Spectrosc.* **2009**, *73*, 374–381. [CrossRef]
58. Ali, M.; Khan, T.; Fatima, K.; Ali, Q.U.A.; Ovais, M.; Khalil, A.T.; Ullah, I.; Raza, A.; Shinwari, Z.K.; Idrees, M. Selected hepatoprotective herbal medicines: Evidence from ethnomedicinal applications, animal models, and possible mechanism of actions. *Phytother. Res.* **2018**, *32*, 199–215. [CrossRef]
59. Edison, T.J.I.; Sethuraman, M.G. Instant green synthesis of silver nanoparticles using Terminalia chebula fruit extract and evaluation of their catalytic activity on reduction of methylene blue. *Process. Biochem.* **2012**, *47*, 1351–1357. [CrossRef]
60. Kumar, K.M.; Mandal, B.K.; Sinha, M.; Krishnakumar, V. Terminalia chebula mediated green and rapid synthesis of gold nanoparticles. *Spectrochim. Acta Part A Mol. Biomol. Spectrosc.* **2012**, *86*, 490–494. [CrossRef]
61. Winkel-Shirley, B. Flavonoid biosynthesis. A colorful model for genetics, biochemistry, cell biology, and biotechnology. *Plant Physiol.* **2001**, *126*, 485–493. [CrossRef] [PubMed]
62. Zhou, Y.; Lin, W.; Huang, J.; Wang, W.; Gao, Y.; Lin, L.; Li, Q.; Lin, L.; Du, M. Biosynthesis of Gold Nanoparticles by Foliar Broths: Roles of Biocompounds and Other Attributes of the Extracts. *Nanoscale Res. Lett.* **2010**, *5*, 1351–1359. [CrossRef]
63. Lee, J.; Kim, H.Y.; Zhou, H.; Hwang, S.; Koh, K.; Han, D.-W.; Lee, J. Green synthesis of phytochemical-stabilized Au nanoparticles under ambient conditions and their biocompatibility and antioxidative activity. *J. Mater. Chem.* **2011**, *21*, 13316–13326. [CrossRef]
64. Mittal, A.K.; Kumar, S.; Banerjee, U.C. Quercetin and gallic acid mediated synthesis of bimetallic (silver and selenium) nanoparticles and their antitumor and antimicrobial potential. *J. Colloid Interface Sci.* **2014**, *431*, 194–199. [CrossRef] [PubMed]
65. Moulton, M.C.; Braydich-Stolle, L.K.; Nadagouda, M.N.; Kunzelman, S.; Hussain, S.M.; Varma, R.S. Synthesis, characterization and biocompatibility of green" synthesized silver nanoparticles using tea polyphenols. *Nanoscale* **2010**, *2*, 763–770. [CrossRef]
66. Raghunandan, D.; Basavaraja, S.; Mahesh, B.; Balaji, S.; Manjunath, S.Y.; Venkataraman, A. Biosynthesis of Stable Polyshaped Gold Nanoparticles from Microwave-Exposed Aqueous Extracellular Anti-malignant Guava (Psidium guajava) Leaf Extract. *NanoBiotechnology* **2009**, *5*, 34–41. [CrossRef]
67. Ahmad, N.; Sharma, S.; Alam, K.; Singh, V.; Shamsi, S.; Mehta, B.; Fatma, A. Rapid synthesis of silver nanoparticles using dried medicinal plant of basil. *Colloids Surfaces B Biointerfaces* **2010**, *81*, 81–86. [CrossRef]

68. Ghoreishi, S.M.; Behpour, M.; Khayatkashani, M. Green synthesis of silver and gold nanoparticles using Rosa damascena and its primary application in electrochemistry. *Phys. E Low Dimens. Syst. Nanostructures* **2011**, *44*, 97–104. [CrossRef]
69. Singh, J.; Dutta, T.; Kim, K.H.; Rawat, M.; Samddar, P.; Kumar, P. 'Green'synthesis of metals and their oxide nanoparticles: Applications for environmental remediation. *J. Nanobiotechnol.* **2018**, *16*, 1–24. [CrossRef]
70. Vilas, V.; Philip, D.; Mathew, J. Catalytically and biologically active silver nanoparticles synthesized using essential oil. *Spectrochim. Acta Part A Mol. Biomol. Spectrosc.* **2014**, *132*, 743–750. [CrossRef]
71. Song, J.Y.; Kim, B.S. Rapid biological synthesis of silver nanoparticles using plant leaf extracts. *Bioprocess Biosyst. Eng.* **2009**, *32*, 79–84. [CrossRef]
72. Kumari, M.M.; Philip, D. Facile one-pot synthesis of gold and silver nanocatalysts using edible coconut oil. *Spectrochim. Acta Part A Mol. Biomol. Spectrosc.* **2013**, *111*, 154–160. [CrossRef] [PubMed]
73. González-Rivera, J.; Duce, C.; Ierardi, V.; Longo, I.; Spepi, A.; Tiné, M.R.; Ferrari, C. Fast and Eco-friendly Microwave-Assisted Synthesis of Silver Nanoparticles using Rosemary Essential Oil as Renewable Reducing Agent. *ChemistrySelect* **2017**, *2*, 2131–2138. [CrossRef]
74. Da Silva, E.C.; Da Silva, M.G.A.; Meneghetti, S.M.P.; Machado, G.; Alencar, M.A.R.C.; Hickmann, J.M.; Meneghetti, M.R. Synthesis of colloids based on g.old nanoparticles dispersed in castor oil. *J. Nanoparticle Res.* **2008**, *10*, 201–208. [CrossRef]
75. Sheny, D.; Mathew, J.; Philip, D. Synthesis characterization and catalytic action of hexagonal gold nanoparticles using essential oils extracted from Anacardium occidentale. *Spectrochim. Acta Part A: Mol. Biomol. Spectrosc.* **2012**, *97*, 306–310. [CrossRef]
76. Jiang, J.; Pi, J.; Cai, J. The Advancing of Zinc Oxide Nanoparticles for Biomedical Applications. *Bioinorg. Chem. Appl.* **2018**, *2018*, 1–18. [CrossRef] [PubMed]
77. Rajeshkumar, S.; Kumar, S.V.; Ramaiah, A.; Agarwal, H.; Lakshmi, T.; Roopan, S.M. Biosynthesis of zinc oxide nanoparticles using Mangifera indica leaves and evaluation of their antioxidant and cytotoxic properties in lung cancer (A549) cells. *Enzym. Microb. Technol.* **2018**, *117*, 91–95. [CrossRef] [PubMed]
78. Madhumitha, G.; Elango, G.; Roopan, S.M. Biotechnological aspects of ZnO nanoparticles: Overview on synthesis and its applications. *Appl. Microbiol. Biotechnol.* **2015**, *100*, 571–581. [CrossRef]
79. Saemi, R.; Taghavi, E.; Jafarizadeh-Malmiri, H.; Anarjan, N. Fabrication of green ZnO nanoparticles using walnut leaf extract to develop an antibacterial film based on polyethylene–starch–ZnO NPs. *Green Process. Synth.* **2021**, *10*, 112–124. [CrossRef]
80. Demissie, M.G.; Sabir, F.K.; Edossa, G.D.; Gonfa, B.A. Synthesis of zinc oxide nanoparticles using leaf extract of lippiaadoensis (koseret) and evaluation of its antibacterial activity. *J. Chem.* **2020**, *2020*, 7459042. [CrossRef]
81. Jayachandran, A.; Aswathy, T.R.; Nair, A.S. Green synthesis and characterization of zinc oxide nanoparticles using Cayratiapedata leaf extract. *Biochem. Biophys. Rep.* **2021**, *26*, 100995.
82. Thi Tran, Q.M.; Thi Nguyen, H.A.; Doan, V.D.; Tran, Q.H.; Nguyen, V.C. Biosynthesis of Zinc Oxide Nanoparticles Using Aqueous Piper betle Leaf Extract and Its Application in Surgical Sutures. *J. Nanomater.* **2021**, *2021*, 8833864. [CrossRef]
83. Hagos, K.M. Synthesis and characterization of ZnO nanoparticles using aqueous extract of Becium grandiflorum for antimicrobial activity and adsorption of methylene blue. *Appl. Water Sci.* **2021**, *11*, 1–12.
84. Saeed, S.; Nawaz, S.; Nisar, A.; Mehmood, T.; Tayyab, M.; Nawaz, M.; Firyal, S.; Bilal, M.; Mohyuddin, A.; Ullah, A. Effective fabrication of zinc-oxide (ZnO) nanoparticles using Achyranthes aspera leaf extract and their potent biological activities against the bacterial poultry pathogens. *Mater. Res. Express* **2021**, *8*, 035004. [CrossRef]
85. El-Belely, E.F.; Farag, M.; Said, H.A.; Amin, A.S.; Azab, E.; Gobouri, A.A.; Fouda, A. Green synthesis of zinc oxide nanoparticles (ZnO-NPs) using Arthrospira platensis (Class: Cyanophyceae) and evaluation of their biomedical activities. *Nanomaterials* **2021**, *11*, 95. [CrossRef] [PubMed]
86. Alamdari, S.; Ghamsari, M.S.; Lee, C.; Han, W.; Park, H.-H.; Tafreshi, M.J.; Afarideh, H.; Ara, M.H.M. Preparation and Characterization of Zinc Oxide Nanoparticles Using Leaf Extract of Sambucus ebulus. *Appl. Sci.* **2020**, *10*, 3620. [CrossRef]
87. Droepenu, E.K.; Asare, E.A.; Wee, B.S.; Wahi, R.B.; Ayertey, F.; Kyene, M.O. Biosynthesis, characterization, and antibacterial activity of ZnO nanoaggregates using aqueous extract from Anacardium occidentale leaf: Comparative study of different precursors. *Beni Suef Univ. J. Basic Appl. Sci.* **2021**, *10*, 1–10. [CrossRef]
88. Barzinjy, A.A.; Azeez, H.H. Green synthesis and characterization of zinc oxide nanoparticles using Eucalyptus globulus Labill. leaf extract and zinc nitrate hexahydrate salt. *SN Appl. Sci.* **2020**, *2*, 1–14. [CrossRef]
89. Naseer, M.; Aslam, U.; Khalid, B.; Chen, B. Green route to synthesize Zinc Oxide Nanoparticles using leaf extracts of Cassia fistula and Melia azadarach and their antibacterial potential. *Sci. Rep.* **2020**, *10*, 1–10. [CrossRef] [PubMed]
90. Ahmad, W.; Kalra, D. Green synthesis, characterization and anti microbial activities of ZnO nanoparticles using Euphorbia hirta leaf extract. *J. King Saud Univ. Sci.* **2020**, *32*, 2358–2364. [CrossRef]
91. Rahaiee, S.; Ranjbar, M.; Azizi, H.; Govahi, M.; Zare, M. Green synthesis, characterization, and biological activities of saffron leaf extract-mediated zinc oxide nanoparticles: A sustainable approach to reuse an agricultural waste. *Appl. Organomet. Chem.* **2020**, *34*, e5705. [CrossRef]
92. Rahaiee, S.; Ranjbar, M.; Azizi, H.; Govahi, M.; Zare, M. Synthesis of ZnO nanoparticles by two different methods comparison of their structural, antibacterial, photocatalytic and optical properties. *Nano Express* **2020**, *1*, 010007.
93. Jan, H.; Shah, M.; Usman, H.; Khan, A.; Muhammad, Z.; Hano, C.; Abbasi, B.H. Biogenic synthesis and characterization of antimicrobial and anti-parasitic zinc oxide (ZnO) nanoparticles using aqueous extracts of the Himalayan columbine (Aquilegia pubiflora). *Front. Mater.* **2020**, *7*, 249. [CrossRef]

94. Osuntokun, J.; Onwudiwe, D.C.; Ebenso, E.E. Green synthesis of ZnO nanoparticles using aqueous Brassica oleracea L. var. italica and the photocatalytic activity. *Green Chem. Lett. Rev.* **2019**, *12*, 444–457. [CrossRef]
95. Vinotha, V.; Iswarya, A.; Thaya, R.; Govindarajan, M.; Alharbi, N.S.; Kadaikunnan, S.; Khaled, J.M.; Al-Anbr, M.N.; Vaseeharan, B. Synthesis of ZnO nanoparticles using insulin-rich leaf extract: Anti-diabetic, antibiofilm and anti-oxidant properties. *J. Photochem. Photobiol. B Biol.* **2019**, *197*, 111541. [CrossRef]
96. Hussain, A.; Oves, M.; Alajmi, M.F.; Hussain, I.; Amir, S.; Ahmed, J.; Rehman, T.; El-Seedi, H.R.; Ali, I. Biogenesis of ZnO nanoparticles using Pandanus odorifer leaf extract: Anticancer and antimicrobial activities. *RSC Adv.* **2019**, *9*, 15357–15369. [CrossRef]
97. Ezealisiji, K.M.; Siwe-Noundou, X.; Maduelosi, B.; Nwachukwu, N.; Krause, R.W.M. Green synthesis of zinc oxide nanoparticles using Solanum torvum (L) leaf extract and evaluation of the toxicological profile of the ZnO nanoparticles–hydrogel composite in Wistar albino rats. *Int. Nano Lett.* **2019**, *9*, 99–107. [CrossRef]
98. Rajendran, N.; George, B.; Houreld, N.; Abrahamse, H. Synthesis of Zinc Oxide Nanoparticles Using *Rubus fairholmianus* Root Extract and Their Activity against Pathogenic Bacteria. *Molecules* **2021**, *26*, 3029. [CrossRef]
99. Naser, R.; Abu-Huwaij, R.; Al-Khateeb, I.; Abbas, M.M.; Atoom, A.M. Green synthesis of zinc oxide nanoparticles using the root hair extract of Phoenix dactylifera: Antimicrobial and anticancer activity. *Appl. Nanosci.* **2021**, *11*, 1747–1757. [CrossRef]
100. Liu, D.; Liu, L.; Yao, L.; Peng, X.; Li, Y.; Jiang, T.; Kuang, H. Synthesis of ZnO nanoparticles using radish root extract for effective wound dressing agents for diabetic foot ulcers in nursing care. *J. Drug Deliv. Sci. Technol.* **2019**, *55*, 101364. [CrossRef]
101. Shaik, A.M.; David Raju, M.; Rama Sekhara Reddy, D. Green synthesis of zinc oxide nanoparticles using aqueous root extract of Sphagneticolatrilobata Lin and investigate its role in toxic metal removal, sowing germination and fostering of plant growth. *Inorg. Nano Met. Chem.* **2020**, *50*, 569–579. [CrossRef]
102. Espenti, C.S.; Krishna, A.G.R.; Reddy, Y.V.R. Green biosynthesis of ZnO nanomaterials and their anti-bacterial activity by using Moringa Oleifera root aqueous extract. *SN Appl. Sci.* **2020**, *2*, 1–11. [CrossRef]
103. Jobie, F.N.; Ranjbar, M.; Moghaddam, A.H.; Kiani, M. Green synthesis of zinc oxide nanoparticles using Amygdalus scoparia Spach stem bark extract and their applications as an alternative antimicrobial, anticancer, and anti-diabetic agent. *Adv. Powder Technol.* **2021**, *32*, 2043–2052. [CrossRef]
104. Ansari, M.A.; Murali, M.; Prasad, D.; Alzohairy, M.A.; Almatroudi, A.; Alomary, M.N.; Udayashankar, A.C.; Singh, S.B.; Asiri, S.M.M.; Ashwini, B.S.; et al. Cinnamomum verum Bark Extract Mediated Green Synthesis of ZnO Nanoparticles and Their Antibacterial Potentiality. *Biomolecules* **2020**, *10*, 336. [CrossRef] [PubMed]
105. Jayappa, M.D.; Ramaiah, C.K.; Kumar, M.A.P.; Suresh, D.; Prabhu, A.; Devasya, R.P.; Sheikh, S. Green synthesis of zinc oxide nanoparticles from the leaf, stem and in vitro grown callus of Mussaendafrondosa L.: Characterization and their applications. *Appl. Nanosci.* **2020**, *10*, 3057–3074. [CrossRef]
106. Umar, H.; Kavaz, D.; Rizaner, N. Biosynthesis of zinc oxide nanoparticles using Albizia lebbeck stem bark, and evaluation of its antimicrobial, antioxidant, and cytotoxic activities on human breast cancer cell lines. *Int. J. Nanomed.* **2019**, *14*, 87. [CrossRef] [PubMed]
107. Seshadri, V.D. Zinc oxide nanoparticles from Cassia auriculata flowers showed the potent antimicrobial and in vitro anticancer activity against the osteosarcoma MG-63 cells. *Saudi J. Biol. Sci.* **2021**, *28*, 4046–4054. [CrossRef]
108. Ifeanyichukwu, U.L.; Fayemi, O.E.; Ateba, C.N. Green Synthesis of Zinc Oxide Nanoparticles from Pomegranate (*Punica granatum*) Extracts and Characterization of Their Antibacterial Activity. *Molecules* **2020**, *25*, 4521. [CrossRef]
109. Ngom, I.; Ngom, B.; Sackey, J.; Khamlich, S. Biosynthesis of zinc oxide nanoparticles using extracts of Moringa Oleifera: Structural & optical properties. *Mater. Today Proc.* **2020**, *36*, 526–533.
110. Ogunyemi, S.O.; Abdallah, Y.; Zhang, M.; Fouad, H.; Hong, X.; Ibrahim, E.; Masum, M.M.I.; Hossain, A.; Mo, J.; Li, B. Green synthesis of zinc oxide nanoparticles using different plant extracts and their antibacterial activity against Xanthomonas oryzaepv. oryzae. *Artif. Cells Nanomed. Biotechnol.* **2019**, *47*, 341–352. [CrossRef] [PubMed]
111. Lakshmeesha, T.R.; Kalagatur, N.K.; Mudili, V.; Mohan, C.D.; Rangappa, S.; Prasad, B.D.; Ashwini, B.S.; Hashem, A.; Alqarawi, A.A.; Malik, J.A.; et al. Biofabrication of zinc oxide nanoparticles with Syzygiumaromaticum flower buds extract and finding its novel application in controlling the growth and mycotoxins of Fusarium graminearum. *Front. Microbiol.* **2019**, *10*, 1244. [CrossRef] [PubMed]
112. Umavathi, S.; Mahboob, S.; Govindarajan, M.; Al-Ghanim, K.A.; Ahmed, Z.; Virik, P.; Al-Mulhm, N.; Subash, M.; Gopinath, K.; Kavitha, C. Green synthesis of ZnO nanoparticles for antimicrobial and vegetative growth applications: A novel approach for advancing efficient high quality health care to human wellbeing. *Saudi J. Biol. Sci.* **2020**, *28*, 1808–1815. [CrossRef] [PubMed]
113. Rawashdeh, R.Y.; Harb, A.M.; AlHasan, A.M. Biological interaction levels of zinc oxide nanoparticles; lettuce seeds as case study. *Heliyon* **2020**, *6*, e03983. [CrossRef]
114. Shabaani, M.; Rahaiee, S.; Zare, M.; Jafari, S.M. Green synthesis of ZnO nanoparticles using loquat seed extract; Biological functions and photocatalytic degradation properties. *LWT* **2020**, *134*, 110133. [CrossRef]
115. Chankaew, C.; Tapala, W.; Grudpan, K.; Rujiwatra, A. Microwave synthesis of ZnO nanoparticles using longan seeds biowaste and their efficiencies in photocatalytic decolorization of organic dyes. *Environ. Sci. Pollut. Res.* **2019**, *26*, 17548–17554. [CrossRef]
116. Alshehri, A.A.; Malik, M.A. Biogenic fabrication of ZnO nanoparticles using Trigonella foenum-graecum (Fenugreek) for proficient photocatalytic degradation of methylene blue under UV irradiation. *J. Mater. Sci. Mater. Electron.* **2019**, *30*, 16156–16173. [CrossRef]

117. Khan, M.; Ware, P.; Shimpi, N. Synthesis of ZnO nanoparticles using peels of Passiflora foetida and study of its activity as an efficient catalyst for the degradation of hazardous organic dye. *SN Appl. Sci.* **2021**, *3*, 1–17. [CrossRef]
118. Faisal, S.; Jan, H.; Shah, S.A.; Shah, S.; Khan, A.; Akbar, M.T.; Rizwan, M.; Jan, F.; Wajidullah; Akhtar, N.; et al. Green Synthesis of Zinc Oxide (ZnO) Nanoparticles Using Aqueous Fruit Extracts of Myristica fragrans: Their Characterizations and Biological and Environmental Applications. *ACS Omega* **2021**, *6*, 9709–9722. [CrossRef]
119. Gao, Y.; Xu, D.; Ren, D.; Zeng, K.; Wu, X. Green synthesis of zinc oxide nanoparticles using Citrus sinensis peel extract and application to strawberry preservation: A comparison study. *LWT* **2020**, *126*, 109297. [CrossRef]
120. Thi, T.U.D.; Nguyen, T.T.; Thi, Y.D.; Thi, K.H.T.; Phan, B.T.; Pham, K.N. Green synthesis of ZnO nanoparticles using orange fruit peel extract for antibacterial activities. *RSC Adv.* **2020**, *10*, 23899–23907. [CrossRef]
121. Awwad, A.M.; Amer, M.W.; Salem, N.M.; Abdeen, A.O. Green synthesis of zinc oxide nanoparticles (ZnO-NPs) using Ailanthus altissima fruit extracts and antibacterial activity. *Chem. Int.* **2020**, *6*, 151–159.
122. Grace, A.N.; Pandian, K. Antibacterial efficacy of aminoglycosidic antibiotics protected gold nanoparticles—A brief study. *Colloids Surf. A Physicochem. Eng. Asp.* **2007**, *297*, 63–70. [CrossRef]
123. Drechsler, U.; Erdogan, B.; Rotello, V.M. Nanoparticles: Scaffolds for Molecular Recognition. *Chem. A Eur. J.* **2004**, *10*, 5570–5579. [CrossRef]
124. Lee, J.-S. Recent progress in gold nanoparticle-based non-volatile memory devices. *Gold Bull.* **2010**, *43*, 189–199. [CrossRef]
125. van der Molen, S.J.; Liao, J.; Kudernac, T.; Agustsson, J.S.; Bernard, L.; Calame, M.; van Wees, B.J.; Feringa, B.L.; Schoönenberger, C. Light-controlled conductance switching of ordered metal-molecule-metal devices. *Nano Lett.* **2009**, *9*, 76–80. [CrossRef]
126. Mackowski, S. Hybrid nanostructures for efficient light harvesting. *J. Physics Condens. Matter* **2010**, *22*, 193102. [CrossRef]
127. Khan, A.; Rashid, R.; Murtaza, G.; Zahra, A. Gold Nanoparticles: Synthesis and Applications in Drug Delivery. *Trop. J. Pharm. Res.* **2014**, *13*, 1169. [CrossRef]
128. Rocha-Rocha, O.; Cortez-Valadez, M.; Calderón-Ayala, G.; Martínez-Nuñez, C.; Pedroza-Montero, M.; Flores-Acosta, M. Confined clustering of AuCu nanoparticles under ambient conditions. *Phys. Lett. A* **2019**, *383*, 125985. [CrossRef]
129. Aminabad, N.S.; Farshbaf, M.; Akbarzadeh, A. Recent Advances of Gold Nanoparticles in Biomedical Applications: State of the Art. *Cell Biophys.* **2018**, *77*, 123–137. [CrossRef]
130. Hu, X.; Zhang, Y.; Ding, T.; Liu, J.; Zhao, H. Multifunctional Gold Nanoparticles: A Novel Nanomaterial for Various Medical Applications and Biological Activities. *Front. Bioeng. Biotechnol.* **2020**, *8*, 990. [CrossRef] [PubMed]
131. Jiang, P.; Wang, Y.; Zhao, L.; Ji, C.; Chen, D.; Nie, L. Applications of Gold Nanoparticles in Non-Optical Biosensors. *Nanomaterials* **2018**, *8*, 977. [CrossRef] [PubMed]
132. Madkour, L.H. Applications of gold nanoparticles in medicine and therapy. *Pharm. Pharmacol. Int. J.* **2018**, *6*, 1. [CrossRef]
133. Nadeem, M.; Abbasi, B.H.; Younas, M.; Ahmad, W.; Khan, T. A review of the green syntheses and anti-microbial applications of gold nanoparticles. *Green Chem. Lett. Rev.* **2017**, *10*, 216–227. [CrossRef]
134. Guliani, A.; Kumari, A.; Acharya, A. Green synthesis of gold nanoparticles using aqueous leaf extract of Populus alba: Characterization, antibacterial and dye degradation activity. *Int. J. Environ. Sci. Technol.* **2021**, *6*, 1–12.
135. Le, V.T.; Ngu, N.N.Q.; Chau, T.P.; Nguyen, T.D.; Nguyen, V.T.; Nguyen, T.L.H.; Cao, X.T.; Doan, V.D. Silver and Gold Nanoparticles from Limnophila rugosa Leaves: Biosynthesis, Characterization, and Catalytic Activity in Reduction of Nitrophenols. *J. Nanomater.* **2021**, *2021*, 5571663. [CrossRef]
136. Olajire, A.; Mohammed, A. Bio-directed synthesis of gold nanoparticles using Ananas comosus aqueous leaf extract and their photocatalytic activity for LDPE degradation. *Adv. Powder Technol.* **2021**, *32*, 600–610. [CrossRef]
137. El-Borady, O.M.; Fawzy, M.; Hosny, M. Antioxidant, anticancer and enhanced photocatalytic potentials of gold nanoparticles biosynthesized by common reed leaf extract. *Appl. Nanosci.* **2021**, *3*, 1–12.
138. Li, S.; Al-Misned, F.A.; El-Serehy, H.A.; Yang, L. Green synthesis of gold nanoparticles using aqueous extract of Mentha Longifolia leaf and investigation of its anti-human breast carcinoma properties in the in vitro condition. *Arab. J. Chem.* **2020**, *14*, 102931. [CrossRef]
139. Shah, S.; Shah, S.A.; Faisal, S.; Khan, A.; Ullah, R.; Ali, N.; Bilal, M. Engineering novel gold nanoparticles using Sageretiathea leaf extract and evaluation of their biological activities. *J. Nanostruct. Chem.* **2021**, 1–12.
140. Jiao, Y.; Wang, X.; Chen, J.-H. Biofabrication of AuNPs using Coriandrum sativum leaf extract and their antioxidant, analgesic activity. *Sci. Total. Environ.* **2021**, *767*, 144914. [CrossRef]
141. Hosny, M.; Fawzy, M. Instantaneous phytosynthesis of gold nanoparticles via Persicaria salicifolia leaf extract, and their medical applications. *Adv. Powder Technol.* **2021**, *8*, 2891–2904. [CrossRef]
142. Chen, J.; Li, Y.; Fang, G.; Cao, Z.; Shang, Y.; Alfarraj, S.; Alharbi, S.A.; Li, J.; Yang, S.; Duan, X. Green synthesis, characterization, cytotoxicity, antioxidant, and anti-human ovarian cancer activities of Curcumae kwangsiensis leaf aqueous extract green-synthesized gold nanoparticles. *Arab. J. Chem.* **2021**, *14*, 103000. [CrossRef]
143. Abdoli, M.; Arkan, E.; Shekarbeygi, Z.; Khaledian, S. Green synthesis of gold nanoparticles using Centaurea behen leaf aqueous extract and investigating their antioxidant and cytotoxic effects on acute leukemia cancer cell line (THP-1). *Inorg. Chem. Commun.* **2021**, *129*, 108649. [CrossRef]
144. Padalia, H.; Chanda, S. Antioxidant and Anticancer Activities of Gold Nanoparticles Synthesized Using Aqueous Leaf Extract of Ziziphus nummularia. *BioNanoScience* **2021**, *11*, 281–294. [CrossRef]

145. Balasubramanian, S.; Kala, S.M.J.; Pushparaj, T.L. Biogenic synthesis of gold nanoparticles using Jasminum auriculatum leaf extract and their catalytic, antimicrobial and anticancer activities. *J. Drug Deliv. Sci. Technol.* **2020**, *57*, 101620. [CrossRef]
146. Sunayana, N.; Uzma, M.; Dhanwini, R.P.; Govindappa, M.; Prakash, H.S.; Raghavendra, B.V. Green Synthesis of Gold Nanoparticles from Vitex negundo Leaf Extract to Inhibit Lipopolysaccharide-Induced Inflammation Through In Vitro and In Vivo. *J. Clust. Sci.* **2019**, *31*, 463–477. [CrossRef]
147. Khatua, A.; Priyadarshini, E.; Rajamani, P.; Patel, A.; Kumar, J.; Naik, A.; Saravanan, M.; Barabadi, H.; Prasad, A.; Ghosh, L.; et al. Phytosynthesis, Characterization and Fungicidal Potential of Emerging Gold Nanoparticles Using Pongamia pinnata Leave Extract: A Novel Approach in Nanoparticle Synthesis. *J. Clust. Sci.* **2019**, *31*, 125–131. [CrossRef]
148. Vo, T.-T.; Dang, C.-H.; Doan, V.-D.; Dang, V.-S.; Nguyen, T.-D. Biogenic Synthesis of Silver and Gold Nanoparticles from Lactuca indica Leaf Extract and Their Application in Catalytic Degradation of Toxic Compounds. *J. Inorg. Organomet. Polym. Mater.* **2019**, *30*, 388–399. [CrossRef]
149. Kumar, P.V.; Kala, S.M.J.; Prakash, K. Green synthesis of gold nanoparticles using Croton Caudatus Geisel leaf extract and their biological studies. *Mater. Lett.* **2018**, *236*, 19–22. [CrossRef]
150. Kumar, I.; Mondal, M.; Meyappan, V.; Sakthivel, N. Green one-pot synthesis of gold nanoparticles using Sansevieria roxburghiana leaf extract for the catalytic degradation of toxic organic pollutants. *Mater. Res. Bull.* **2019**, *117*, 18–27. [CrossRef]
151. Thangamani, N.; Bhuvaneshwari, N. Green synthesis of gold nanoparticles using Simarouba glauca leaf extract and their biological activity of micro-organism. *Chem. Phys. Lett.* **2019**, *732*, 136587. [CrossRef]
152. Khoshnamvand, M.; Ashtiani, S.; Huo, C.; Saeb, S.P.; Liu, J. Use of Alcea rosea leaf extract for biomimetic synthesis of gold nanoparticles with innate free radical scavenging and catalytic activities. *J. Mol. Struct.* **2018**, *1179*, 749–755. [CrossRef]
153. Vijayan, R.; Joseph, S.; Mathew, B. Anticancer, antimicrobial, antioxidant, and catalytic activities of green-synthesized silver and gold nanoparticles using Bauhinia purpurea leaf extract. *Bioprocess Biosyst. Eng.* **2018**, *42*, 305–319. [CrossRef] [PubMed]
154. Boomi, P.; Ganesan, R.; Poorani, G.; Prabu, H.G.; Ravikumar, S.; Jeyakanthan, J. Biological synergy of greener gold nanoparticles by using Coleus aromaticus leaf extract. *Mater. Sci. Eng. C* **2019**, *99*, 202–210. [CrossRef] [PubMed]
155. Al-Radadi, N.S. Facile one-step green synthesis of gold nanoparticles (AuNp) using licorice root extract: Antimicrobial and anticancer study against HepG2 cell line. *Arab. J. Chem.* **2020**, *14*, 102956. [CrossRef]
156. Hosny, M.; Fawzy, M.; El-Borady, O.M.; Mahmoud, A.E.D. Comparative study between Phragmites australis root and rhizome extracts for mediating gold nanoparticles synthesis and their medical and environmental applications. *Adv. Powder Technol.* **2021**, *32*, 2268–2279. [CrossRef]
157. Doan, V.D.; Huynh, B.A.; Nguyen, T.D.; Cao, X.T.; Nguyen, V.C.; Nguyen, T.L.H.; Nguyen, H.T.; Le, V.T. Biosynthesis of silver and gold nanoparticles using aqueous extract of Codonopsispilosula roots for antibacterial and catalytic applications. *J. Nanomater.* **2020**, *2020*, 8492016. [CrossRef]
158. Zhang, T.; Dang, M.; Zhang, W.; Lin, X. Gold nanoparticles synthesized from Euphorbia fischeriana root by green route method alleviates the isoprenaline hydrochloride induced myocardial infarction in rats. *J. Photochem. Photobiol. B Biol.* **2019**, *202*, 111705. [CrossRef] [PubMed]
159. Xue, J.; Liu, T.; Liu, Y.; Jiang, Y.; Seshadri, V.; Mohan, S.K.; Ling, L. Neuroprotective effect of biosynthesised gold nanoparticles synthesised from root extract of Paeonia moutan against Parkinson disease—In vitro & In vivo model. *J. Photochem. Photobiol. B Biol.* **2019**, *200*, 111635. [CrossRef]
160. González-Ballesteros, N.; Vidal-González, J.; Rodríguez-Argüelles, M.C. Wealth from by-products: An attempt to synthesize valuable gold nanoparticles from Brassica oleracea var. acephala cv. Galega stems. *J. Nanostructure Chem.* **2021**, 1–10. [CrossRef]
161. Khoshnamvand, M.; Hao, Z.; Huo, C.; Liu, J. Photocatalytic degradation of 4-nitrophenol pollutant and in vitro antioxidant assay of gold nanoparticles synthesized from Apium graveolens leaf and stem extracts. *Int. J. Environ. Sci. Technol.* **2020**, *17*, 2433–2442. [CrossRef]
162. Chokkalingam, M.; Rupa, E.J.; Huo, Y.; Mathiyalagan, R.; Anandapadmanaban, G.; Ahn, J.C.; Park, J.K.; Lu, J.; Yang, D.C. Photocatalytic degradation of industrial dyes using Ag and Au nanoparticles synthesized from Angelica gigas ribbed stem extracts. *Optik* **2019**, *185*, 1213–1219. [CrossRef]
163. Alhumaydhi, F.A.; Khan, I.; Rauf, A.; Qureshi, M.N.; Aljohani, A.S.M.; Khan, S.A.; Khalil, A.A.; A El-Esawi, M.; Muhammad, N. Synthesis, characterization, biological activities, and catalytic applications of alcoholic extract of saffron (Crocus sativus) flower stigma-based gold nanoparticles. *Green Process. Synth.* **2021**, *10*, 230–245. [CrossRef]
164. Chan, J.Z.; Ali, R.R.; Shameli, K.; Salleh, M.S.N.; Lee, K.X.; Isa, E.M. Green Synthesis of Gold Nanoparticles using Aqueous Extract of ClitoriaTernatea Flower. In *IOP Conference Series: Materials Science and Engineering*; IOP Publishing: London, UK, 2020; Volume 808.
165. Valsalam, S.; Agastian, P.; Esmail, G.A.; Ghilan, A.-K.M.; Al-Dhabi, N.A.; Arasu, M.V. Biosynthesis of silver and gold nanoparticles using Musa acuminata colla flower and its pharmaceutical activity against bacteria and anticancer efficacy. *J. Photochem. Photobiol. B Biol.* **2019**, *201*, 111670. [CrossRef] [PubMed]
166. Rajan, A.; Rajan, A.R.; Philip, D. Elettaria cardamomum seed mediated rapid synthesis of gold nanoparticles and its biological activities. *OpenNano* **2017**, *2*, 1–8. [CrossRef]
167. Srinivas, M.; Venkata, R.C.; Kakarla, R.R.; Shetti, N.P.; Reddy, M.S.; Anjanapura, V.R. Novel Co and Ni metal nanostructures as efficient photocatalysts for photodegradation of organic dyes. *Mater. Res. Express* **2019**, *6*, 125502. [CrossRef]

168. Shan, G.; Surampalli, R.Y.; Tyagi, R.D.; Zhang, T.C. Nanomaterials for environmental burden reduction, waste treatment, and nonpoint source pollution control: A review. *Front. Environ. Sci. Eng. China* **2009**, *3*, 249–264. [CrossRef]
169. Savithramma, N.; Rao, M.L.; Rukmini, K.; Devi, P.S. Antimicrobial activity of silver nanoparticles synthesized by using medicinal plants. *Int. J. ChemTech Res.* **2011**, *3*, 1394–1402.
170. Pan, D.; Caruthers, S.D.; Hu, G.; Senpan, A.; Scott, M.J.; Gaffney, P.J.; Wickline, S.A.; Lanza, G.M. Ligand-Directed Nanobialys as Theranostic Agent for Drug Delivery and Manganese-Based Magnetic Resonance Imaging of Vascular Targets. *J. Am. Chem. Soc.* **2008**, *130*, 9186–9187. [CrossRef] [PubMed]
171. Hullmann, A. Measuring and assessing the development of nanotechnology. *Scientometrics* **2007**, *70*, 739–758. [CrossRef]
172. Maheshwari, P.V.; Gupta, N.V. Advances of nanotechnology in healthcare. *Int. J. Pharm Tech Res.* **2012**, *4*, 1221–1227.
173. Savage, N.; Diallo, M.S. Nanomaterials and water purification: Opportunities and challenges. *J. Nanoparticle Res.* **2005**, *7*, 331–342. [CrossRef]
174. Kamat, P.V. Photophysical, photochemical and photocatalytic aspects of metal nanoparticles. *J. Phys. Chem. B* **2002**, *106*, 7729–7744. [CrossRef]
175. Mirkin, C.A.; Letsinger, R.L.; Mucic, R.C.; Storhoff, J.J. A DNA-based method for rationally assembling nanoparticles into macroscopic materials. *Nature* **1996**, *382*, 607–609. [CrossRef]
176. Han, M.; Gao, X.; Su, J.Z.; Nie, S. Quantum-dot-tagged microbeads for multiplexed optical coding of biomolecules. *Nature Bio.* **2001**, *19*, 631–635. [CrossRef]
177. Boncheva, M.; Gracias, D.; Jacobs, H.O.; Whitesides, G.M. Biomimetic self-assembly of a functional asymmetrical electronic device. *Proc. Natl. Acad. Sci.* **2002**, *99*, 4937–4940. [CrossRef]
178. Mishra, A.; Mehta, A.; Basu, S.; Malode, S.J.; Shetti, N.P.; Shukla, S.S.; Nadagouda, M.N.; Aminabhavi, T.M. Electrode materials for lithium-ion batteries. *Mater. Sci. Energy Technol.* **2018**, *1*, 182–187. [CrossRef]
179. Cao, Y.; Jin, R.; Mirkin, C.A. DNA-modified core− shell Ag/Au nanoparticles. *J. Am. Chem. Soc.* **2001**, *123*, 7961–7962. [CrossRef]
180. Barillo, D.J.; Marx, D.E. Silver in medicine: A brief history BC 335 to present. *Burns* **2014**, *40*, S3–S8. [CrossRef]
181. Hong, X.; Wen, J.; Xiong, X.; Hu, Y. Shape effect on the antibacterial activity of silver nanoparticles synthesized via a microwave-assisted method. *Environ. Sci. Pollut. Res.* **2015**, *23*, 4489–4497. [CrossRef] [PubMed]
182. Akbarzadeh, A.; Kafshdooz, L.; Razban, Z.; Tbrizi, A.D.; Rasoulpour, S.; Khalilov, R.; Kavetskyy, T.; Saghfi, S.; Nasibova, A.N.; Kaamyabi, S.; et al. An overview application of silver nanoparticles in inhibition of herpes simplex virus. *Artif. Cells, Nanomedicine, Biotechnol.* **2017**, *46*, 263–267. [CrossRef]
183. Cohan, R.A.; Shoari, A.; Baghbani-Arani, F.; Shandiz, S.A.S.; Khosravy, M.S.; Janani, A.; Bigdeli, R.; Bashar, R.; Asgary, V. Green synthesis and evaluation of silver nanoparticles as adjuvant in rabies veterinary vaccine. *Int. J. Nanomed.* **2016**, *11*, 3597–3605. [CrossRef]
184. Saratale, G.D.; Saratale, R.G.; Benelli, G.; Kumar, G.; Pugazhendhi, A.; Kim, D.-S.; Shin, H.-S. Anti-diabetic Potential of Silver Nanoparticles Synthesized with Argyreia nervosa Leaf Extract High Synergistic Antibacterial Activity with Standard Antibiotics Against Foodborne Bacteria. *J. Clust. Sci.* **2017**, *28*, 1709–1727. [CrossRef]
185. Elsupikhe, R.F.; Shameli, K.; Ahmad, M.B. Sonochemical method for the synthesis of silver nanoparticles in κ-carrageenan from silver salt at different concentrations. *Res. Chem. Intermed.* **2015**, *41*, 8515–8525. [CrossRef]
186. Akter, S.; Lee, S.-Y.; Siddiqi, M.Z.; Balusamy, S.R.; Ashrafudoulla; Rupa, E.J.; Huq, A. Ecofriendly Synthesis of Silver Nanoparticles by *Terrabacter humi* sp. nov. and Their Antibacterial Application against Antibiotic-Resistant Pathogens. *Int. J. Mol. Sci.* **2020**, *21*, 9746. [CrossRef] [PubMed]
187. Bapat, R.A.; Chaubal, T.V.; Joshi, C.P.; Bapat, P.R.; Choudhury, H.; Pandey, M.; Gorain, B.; Kesharwani, P. An overview of application of silver nanoparticles for biomaterials in dentistry. *Mater. Sci. Eng. C* **2018**, *91*, 881–898. [CrossRef] [PubMed]
188. Chávez-Andrade, G.M.; Tanomaru-Filho, M.; Bernardi, M.I.B.; Leonardo, R.D.T.; Faria, G.; Guerreiro-Tanomaru, J.M. Antimicrobial and biofilm anti-adhesion activities of silver nanoparticles and farnesol against endodontic microorganisms for possible application in root canal treatment. *Arch. Oral Biol.* **2019**, *107*, 104481. [CrossRef] [PubMed]
189. Yamamoto, Y.S.; Ishikawa, M.; Ozaki, Y.; Itoh, T. Fundamental studies on enhancement and blinking mechanism of surface-enhanced Raman scattering (SERS) and basic applications of SERS biological sensing. *Front. Phys.* **2013**, *9*, 31–46. [CrossRef]
190. Abdolmohammad-Zadeh, H.; Azari, Z.; Pourbasheer, E. Fluorescence resonance energy transfer between carbon quantum dots and silver nanoparticles: Application to mercuric ion sensing. *Spectrochim. Acta Part A Mol. Biomol. Spectrosc.* **2020**, *245*, 118924. [CrossRef]
191. Affes, S.; Maalej, H.; Aranaz, I.; Kchaou, H.; Acosta, N.; Heras; Nasri, M. Controlled size green synthesis of bioactive silver nanoparticles assisted by chitosan and its derivatives and their application in biofilm preparation. *Carbohydr. Polym.* **2020**, *236*, 116063. [CrossRef] [PubMed]
192. Rauf, A.; Ahmad, T.; Khan, A.; Maryam; Uddin, G.; Ahmad, B.; Mabkhot, Y.N.; Bawazeer, S.; Riaz, N.; Malikovna, B.K.; et al. Green synthesis and biomedicinal applications of silver and gold nanoparticles functionalized with methanolic extract of Mentha longifolia. *Artif. Cells Nanomedicine, Biotechnol.* **2021**, *49*, 194–203. [CrossRef]
193. Manikandan, D.B.; Sridhar, A.; Sekar, R.K.; Perumalsamy, B.; Veeran, S.; Arumugam, M.; Karuppaiah, P.; Ramasamy, T. Green fabrication, characterization of silver nanoparticles using aqueous leaf extract of Ocimumamericanum (Hoary Basil) and investigation of its in vitro antibacterial, antioxidant, anticancer and photocatalytic reduction. *J. Environ. Chem. Eng.* **2021**, *9*, 104845. [CrossRef]

194. Khan, S.A.; Shahid, S.; Lee, C.S. Green synthesis of gold and silver nanoparticles using leaf extract of clerodendruminerme; characterization, antimicrobial, and antioxidant activities. *Biomolecules* **2020**, *10*, 835. [CrossRef]
195. Okaiyeto, K.; Hoppe, H.; Okoh, A. Plant-Based Synthesis of Silver Nanoparticles Using Aqueous Leaf Extract of Salvia officinalis: Characterization and its Antiplasmodial Activity. *J. Clust. Sci.* **2020**, *32*, 101–109. [CrossRef]
196. Esan, V.; Mahboob, S.; Al-Ghanim, K.A.; Elanchezhiyan, C.; Al-Misned, F.; Ahmed, Z.; Govindarajan, M. Novel biogenic synthesis of silver nanoparticles using Alstonia venenata leaf extract: An enhanced mosquito larvicidal agent with negligible impact on important eco-biological fish and insects. *J. Clust. Sci.* **2021**, *32*, 489–497. [CrossRef]
197. Sooraj, M.P.; Nair, A.S.; Vineetha, D. Sunlight-mediated green synthesis of silver nanoparticles using Sida retusa leaf extract and assessment of its antimicrobial and catalytic activities. *Chem. Pap.* **2020**, *75*, 351–363. [CrossRef]
198. Singh, S.P.; Mishra, A.; Shyanti, R.K.; Singh, R.P.; Acharya, A. Silver nanoparticles synthesized using Carica papaya leaf extract (AgNPs-PLE) causes cell cycle arrest and apoptosis in human prostate (DU145) cancer cells. *Biol. Trace Elem. Res.* **2021**, *199*, 1316–1331. [CrossRef]
199. Singh, R.; Hano, C.; Nath, G.; Sharma, B. Green Biosynthesis of Silver Nanoparticles Using Leaf Extract of Carissa carandas L. and Their Antioxidant and Antimicrobial Activity against Human Pathogenic Bacteria. *Biomolecules* **2021**, *11*, 299. [CrossRef]
200. Al-Otibi, F.; Perveen, K.; Al-Saif, N.A.; Alharbi, R.I.; Bokhari, N.A.; Albasher, G.; Al-Otaibi, R.M.; Al-Mosa, M.A. Biosynthesis of silver nanoparticles using Malva parviflora and their antifungal activity. *Saudi J. Biol. Sci.* **2021**, *28*, 2229–2235. [CrossRef]
201. Padalia, H.; Chanda, S. Synthesis of silver nanoparticles using Ziziphus nummularia leaf extract and evaluation of their antimicrobial, antioxidant, cytotoxic and genotoxic potential (4-in-1 system). *Artif. Cells Nanomed. Biotechnol.* **2021**, *49*, 354–366. [CrossRef] [PubMed]
202. Sharifi-Rad, M.; Pohl, P.; Epifano, F. Phytofabrication of Silver Nanoparticles (AgNPs) with Pharmaceutical Capabilities Using Otostegia persica (Burm.) Boiss. Leaf Extract. *Nanomaterials* **2021**, *11*, 1045. [CrossRef]
203. Abdallah, B.M.; Ali, E.M. Green Synthesis of Silver Nanoparticles Using the Lotus lalambensis Aqueous Leaf Extract and Their Anti-Candidal Activity against Oral Candidiasis. *ACS Omega* **2021**, *6*, 8151–8162. [CrossRef]
204. Panda, M.K.; Dhal, N.K.; Kumar, M.; Mishra, P.M.; Behera, R.K. Green synthesis of silver nanoparticles and its potential effect on phytopathogens. *Mater. Today Proc.* **2020**, *35*, 233–238. [CrossRef]
205. Anju, T.R.; Parvathy, S.; Veettil, M.V.; Rosemary, J.; Ansalna, T.H.; Shahzabanu, M.M.; Devika, S. Green synthesis of silver nanoparticles from Aloe vera leaf extract and its antimicrobial activity. *Mater. Today Proc.* **2021**, *43*, 3956–3960. [CrossRef]
206. Seerangaraj, V.; Sathiyavimal, S.; Shankar, S.N.; Nandagopal, J.G.T.; Balashanmugam, P.; Al-Misned, F.A.; Shanmugavel, M.; Senthilkumar, P.; Pugazhendhi, A. Cytotoxic effects of silver nanoparticles on Ruellia tuberosa: Photocatalytic degradation properties against crystal violet and coomassie brilliant blue. *J. Environ. Chem. Eng.* **2021**, *9*, 105088. [CrossRef]
207. Sharma, Y.; Kawatra, A.; Sharma, V.; Dhull, D.; Kaushik, S.; Yadav, J.P.; Kaushik, S. In-vitro and in-silico evaluation of the anti-chikungunya potential of Psidium guajava leaf extract and their synthesized silver nanoparticles. *VirusDisease* **2021**, *32*, 260–265. [CrossRef]
208. Ekennia, A.C.; Uduagwu, D.N.; Nwaji, N.N.; Olowu, O.J.; Nwanji, O.L.; Ejimofor, M.; Sonde, C.U.; Oje, O.O.; Igwe, D.O. Green synthesis of silver nanoparticles using leaf extract of Euphorbia sanguine: An in vitro study of its photocatalytic and melanogenesis inhibition activity. *Inorg. Nano Met. Chem.* **2021**, *9*, 1–9. [CrossRef]
209. Hazaa, M.; Alm-Eldin, M.; Ibrahim, A.E.; Elbarky, N.; Salama, M.; Sayed, R.; Sayed, W. Biosynthesis of Silver Nanoparticles using Borago officinslis leaf extract, characterization and larvicidal activity against cotton leaf worm, Spodoptera littoralis (Bosid). *Int. J. Trop. Insect Sci.* **2021**, *41*, 145–156. [CrossRef]
210. Seifipour, R.; Nozari, M.; Pishkar, L. Green Synthesis of Silver Nanoparticles using Tragopogon Collinus Leaf Extract and Study of Their Antibacterial Effects. *J. Inorg. Organomet. Polym. Mater.* **2020**, *30*, 2926–2936. [CrossRef]
211. Jebris, S.; Jenana, R.K.B.; Dridi, C. Green synthesis of silver nanoparticles using Melia azedarach leaf extract and their antifungal activities: In vitro and in vivo. *Mater. Chem. Phys.* **2020**, *248*, 122898. [CrossRef]
212. Nouri, A.; Yaraki, M.T.; Lajevardi, A.; Rezaei, Z.; Ghorbanpour, M.; Tanzifi, M. Ultrasonic-assisted green synthesis of silver nanoparticles using Mentha aquatica leaf extract for enhanced antibacterial properties and catalytic activity. *Colloid Interface Sci. Commun.* **2020**, *35*, 100252. [CrossRef]
213. Guimarães, M.L.; da Silva, F.A.G.; da Costa, M.M.; de Oliveira, H.P. Green synthesis of silver nanoparticles using Ziziphus joazeiro leaf extract for production of antibacterial agents. *Appl. Nanosci.* **2020**, *10*, 1073–1081. [CrossRef]
214. Rangayasami, A.; Kannan, K.; Joshi, S.; Subban, M. Bioengineered silver nanoparticles using Elytraria acaulis (L.f.) Lindau leaf extract and its biological applications. *Biocatal. Agric. Biotechnol.* **2020**, *27*, 101690. [CrossRef]
215. Lateef, A.; Oladejo, S.M.; Akinola, P.O.; Aina, D.A.; Beukes, L.S.; Folarin, B.I.; Gueguim-Kana, E.B. Facile synthesis of silver nanoparticles using leaf extract of Hyptissuaveolens (L.) Poit for environmental and biomedical applications. In *IOP Conference Series: Materials Science and Engineering*; IOP Publishing: London, UK, 2020; Volume 805.
216. Moteriya, P.; Chanda, S. Green synthesis of silver nanoparticles from Caesalpinia pulcherrima leaf extract and evaluation of their antimicrobial, cytotoxic and genotoxic potential (3-in-1 system). *J. Inorg. Organomet. Polym. Mater.* **2020**, *30*, 3920–3932. [CrossRef]
217. Tamilarasi, P.; Meena, P. Green synthesis of silver nanoparticles (Ag NPs) using Gomphrena globosa (Globe amaranth) leaf extract and their characterization. *Mater. Today: Proc.* **2020**, *33*, 2209–2216. [CrossRef]

218. Govindan, L.; Anbazhagan, S.; Altemimi, A.B.; Lakshminarayanan, K.; Kuppan, S.; Pratap-Singh, A.; Kandasamy, M. Efficacy of Antimicrobial and Larvicidal Activities of Green Synthesized Silver Nanoparticles Using Leaf Extract of *Plumbago auriculata* Lam. *Plants* **2020**, *9*, 1577. [CrossRef] [PubMed]
219. Hemlata; Meena, P.R.; Singh, A.P.; Tejavath, K.K. Biosynthesis of silver nanoparticles using cucumisprophetarum aqueous leaf extract and their antibacterial and antiproliferative activity against cancer cell lines. *ACS Omega* **2020**, *5*, 5520–5528. [CrossRef] [PubMed]
220. Rawat, V.; Sharma, A.; Bhatt, V.P.; Singh, R.P.; Maurya, I.K. Sunlight mediated green synthesis of silver nanoparticles using Polygonatum graminifolium leaf extract and their antibacterial activity. *Mater. Today: Proc.* **2020**, *29*, 911–916. [CrossRef]
221. Uddin, A.K.M.R.; Siddique, A.B.; Rahman, F.; Ullah, A.K.M.A.; Khan, R. Cocos nucifera Leaf Extract Mediated Green Synthesis of Silver Nanoparticles for Enhanced Antibacterial Activity. *J. Inorg. Organomet. Polym. Mater.* **2020**, *30*, 3305–3316. [CrossRef]
222. Pilaquinga, F.; Amaguaña, D.; Morey, J.; Moncada-Basualto, M.; Pozo-Martínez, J.; Olea-Azar, C.; Fernández, L.; Espinoza-Montero, P.; Jara-Negrete, E.; Meneses, L.; et al. Synthesis of Silver Nanoparticles Using Aqueous Leaf Extract of Mimosa albida (Mimosoideae): Characterization and Antioxidant Activity. *Materials* **2020**, *13*, 503. [CrossRef] [PubMed]
223. Nilavukkarasi, M.; Vijayakumar, S.; Kumar, S.P. Biological synthesis and characterization of silver nanoparticles with Capparis zeylanica L. leaf extract for potent antimicrobial and anti proliferation efficiency. *Mater. Sci. Energy Technol.* **2020**, *3*, 371–376. [CrossRef]
224. Kumar, V.; Singh, S.; Srivastava, B.; Bhadouria, R.; Singh, R. Green synthesis of silver nanoparticles using leaf extract of Holoptelea integrifolia and preliminary investigation of its antioxidant, anti-inflammatory, antidiabetic and antibacterial activities. *J. Environ. Chem. Eng.* **2019**, *7*, 103094. [CrossRef]
225. Parthiban, E.; Manivannan, N.; Ramanibai, R.; Mathivanan, N. Green synthesis of silver-nanoparticles from Annona reticulata leaves aqueous extract and its mosquito larvicidal and anti-microbial activity on human pathogens. *Biotechnol. Rep.* **2018**, *21*, e00297. [CrossRef]
226. Jemilugba, O.T.; Sakho, E.H.M.; Parani, S.; Mavumengwana, V.; Oluwafemi, O.S. Green synthesis of silver nanoparticles using Combretum erythrophyllum leaves and its antibacterial activities. *Colloid Interface Sci. Commun.* **2019**, *31*, 100191. [CrossRef]
227. Behravan, M.; Panahi, A.H.; NaghiZadeh, A.; Ziaee, M.; Mahdavi, R.; Mirzapour, A. Facile green synthesis of silver nanoparticles using Berberis vulgaris leaf and root aqueous extract and its antibacterial activity. *Int. J. Biol. Macromol.* **2018**, *124*, 148–154. [CrossRef]
228. Ahmad, S.; Tauseef, I.; Haleem, K.S.; Khan, K.; Shahzad, M.; Ali, M.; Sultan, F. Synthesis of silver nanoparticles using leaves of Catharanthus roseus and their antimicrobial activity. *Appl. Nanosci.* **2019**, *10*, 4459–4464. [CrossRef]
229. Doan, V.D.; Nguyen, T.D.; Nguyen, T.L.H.; Nguyen, H.T. Green synthesis of silver nanoparticles using aganonerionpolymorphum leaves extract and evaluation of their antibacterial and catalytic activity. *Mater. Res. Express* **2019**, *6*, 1150g1. [CrossRef]
230. Singh, C.; Kumar, J.; Kumar, P.; Chauhan, B.S.; Tiwari, K.N.; Mishra, S.K.; Doan, V.D.; Nguyen, T.D.; Nguyen, T.L.H.; Nguyen, H.T.; et al. Green synthesis of silver nanoparticles using aqueous leaf extract of Premna integrifolia (L.) rich in polyphenols and evaluation of their antioxidant, antibacterial and cytotoxic activity. *Biotechnol. Biotechnol. Equip.* **2019**, *33*, 359–371. [CrossRef]
231. Khan, S.; Singh, S.; Gaikwad, S.; Nawani, N.; Junnarkar, M.; Pawar, S.V. Optimization of process parameters for the synthesis of silver nanoparticles from Piper betle leaf aqueous extract, and evaluation of their antiphytofungal activity. *Environ. Sci. Pollut. Res.* **2019**, *27*, 27221–27233. [CrossRef] [PubMed]
232. Gul, A.; Fozia; Shaheen, A.; Ahmad, I.; Khattak, B.; Ahmad, M.; Ullah, R.; Bari, A.; Ali, S.S.; Alobaid, A.; et al. Green Synthesis, Characterization, Enzyme Inhibition, Antimicrobial Potential, and Cytotoxic Activity of Plant Mediated Silver Nanoparticle Using Ricinus communis Leaf and Root Extracts. *Biomolecules* **2021**, *11*, 206. [CrossRef] [PubMed]
233. Ilahi, I.; Khuda, F.; Sahibzada, M.U.K.; Alghamdi, S.; Ullah, R.; Zakiullah; Dablool, A.S.; Alam, M.; Khan, A.; Khalil, A.A.K. Synthesis of silver nanoparticles using root extract of Duchesnea indica and assessment of its biological activities. *Arab. J. Chem.* **2021**, *14*, 103110. [CrossRef]
234. Arshad, H.; Sami, M.A.; Sadaf, S.; Hassan, U. Salvadora persica mediated synthesis of silver nanoparticles and their antimicrobial efficacy. *Sci. Rep.* **2021**, *11*, 1–11. [CrossRef] [PubMed]
235. Tripathi, D.; Modi, A.; Smita, S.S.; Narayan, G.; Pandey-Rai, S. Biomedical potential of green synthesized silver nanoparticles from root extract of Asparagus officinalis. *J. Plant Biochem. Biotechnol.* **2021**, 1–6. [CrossRef]
236. Sharifi-Rad, M.; Pohl, P.; Epifano, F.; Álvarez-Suarez, J.M. Green synthesis of silver nanoparticles using Astragalus tribuloides delile. root extract: Characterization, antioxidant, antibacterial, and anti-inflammatory activities. *Nanomaterials* **2020**, *10*, 2383. [CrossRef]
237. Dangi, S.; Gupta, A.; Gupta, D.K.; Singh, S.; Parajuli, N. Green synthesis of silver nanoparticles using aqueous root extract of Berberis asiatica and evaluation of their antibacterial activity. *Chem. Data Collect.* **2020**, *28*, 100411. [CrossRef]
238. Akwu, N.A.; Naidoo, Y.; Singh, M.; Nundkumar, N.; Daniels, A.; Lin, J. Two Temperatures Biogenic Synthesis of Silver Nanoparticles from Grewia lasiocarpa E. Mey. ex Harv. Leaf and Stem Bark Extracts: Characterization and Applications. *BioNanoScience* **2021**, *11*, 142–158. [CrossRef]
239. Devi, N.S.; Padma, Y.; Raju, R.R.V. Green synthesis of silver nanoparticles through reduction with Euphorbia nivulia Buch.-Ham., stem bark extract: Characterization and antimicrobial activity. *J. Pharmacogn. Phytother.* **2021**, *13*, 60–67.

240. Adebayo, I.A.; Usman, A.I.; Shittu, F.B.; Ismail, N.Z.; Arsad, H.; Muftaudeen, T.K.; Samian, M.R. Boswellia dalzielii-mediated silver nanoparticles inhibited acute myeloid leukemia (AML) Kasumi-1 cells by inducing cell cycle arrest. *Bioinorg. Chem. Appl.* **2020**, *2020*, 8898360. [CrossRef]
241. Mahiuddin; Saha, P.; Ochiai, B. Green Synthesis and Catalytic Activity of Silver Nanoparticles Based on *Piper chaba* Stem Extracts. *Nanomaterials* **2020**, *10*, 1777. [CrossRef] [PubMed]
242. Akintelu, S.A.; Olugbeko, S.C.; Folorunso, F.A.; Oyebamiji, A.K.; Folorunso, A.S. Characterization and Pharmacological Efficacy of Silver Nanoparticles Biosynthesized Using the Bark Extract of Garcinia Kola. *J. Chem.* **2020**, *2020*, 1–7. [CrossRef]
243. Dawodu, F.A.; Onuh, C.U.; Akpomie, K.G.; Unuabonah, E.I. Synthesis of silver nanoparticle from Vigna unguiculata stem as adsorbent for malachite green in a batch system. *SN Appl. Sci.* **2019**, *1*, 346. [CrossRef]
244. Awad, M.A.; Hendi, A.A.; Ortashi, K.M.; Alzahrani, B.; Soliman, D.; Alanazi, A.; Alenazi, W.; Taha, R.M.; Ramadan, R.; El-Tohamy, M.; et al. Biogenic synthesis of silver nanoparticles using Trigonella foenum-graecum seed extract: Characterization, photocatalytic and antibacterial activities. *Sens. Actuators A Phys.* **2021**, *323*, 112670. [CrossRef]
245. Morales-Lozoya, V.; Espinoza-Gómez, H.; Flores-López, L.Z.; Sotelo-Barrera, E.L.; Núñez-Rivera, A.; Cadena-Nava, R.D.; Alonso-Nuñez, G.; Rivero, I.A. Study of the effect of the different parts of Morinda citrifolia L. (noni) on the green synthesis of silver nanoparticles and their antibacterial activity. *Appl. Surf. Sci.* **2020**, *537*, 147855. [CrossRef]
246. Donga, S.; Chanda, S. Facile green synthesis of silver nanoparticles using Mangifera indica seed aqueous extract and its antimicrobial, antioxidant and cytotoxic potential (3-in-1 system). *Artif. Cells Nanomed. Biotechnol.* **2021**, *49*, 292–302. [CrossRef]
247. Jose, V.; Raphel, L.; Aiswariya, K.S.; Mathew, P. Green synthesis of silver nanoparticles using Annona squamosa L. seed extract: Characterization, photocatalytic and biological activity assay. *Bioprocess Biosyst. Eng.* **2021**, *44*, 1819–1829. [CrossRef] [PubMed]
248. Saygi, K.O.; Usta, C. Rosa canina waste seed extract-mediated synthesis of silver nanoparticles and the evaluation of its antimutagenic action in Salmonella typhimurium. *Mater. Chem. Phys.* **2021**, *266*, 124537. [CrossRef]
249. Chand, K.; Jiao, C.; Lakhan, M.N.; Shah, A.H.; Kumar, V.; Fouad, D.E.; Chandio, M.B.; Maitlo, A.A.; Ahmed, M.; Cao, D. Green synthesis, characterization and photocatalytic activity of silver nanoparticles synthesized with Nigella Sativa seed extract. *Chem. Phys. Lett.* **2020**, *763*, 138218. [CrossRef]
250. Mehwish, H.M.; Liu, G.; Rajoka, M.S.R.; Cai, H.; Zhong, J.; Song, X.; Xia, L.; Wang, M.; Aadil, R.M.; Inam-Ur-Raheem, M.; et al. Therapeutic potential of Moringa oleifera seed polysaccharide embedded silver nanoparticles in wound healing. *Int. J. Biol. Macromol.* **2021**, *184*, 144–158. [CrossRef] [PubMed]
251. Khan, I.; Bawazeer, S.; Rauf, A.; Qureshi, M.N.; Muhammad, N.; Al-Awthan, Y.S.; Bahattab, O.; Maalik, A.; Rengasamy, K.R. Synthesis, biological investigation and catalytic application using the alcoholic extract of Black Cumin (BuniumPersicum) seeds-based silver nanoparticles. *J. Nanostruct. Chem.* **2021**, 1–19.
252. de Carvalho Bernardo, W.L.; Boriollo, M.F.G.; Tonon, C.C.; da Silva, J.J.; Cruz, F.M.; Martins, A.L.; Höfling, J.F.; Spolidorio, D.M.P. Antimicrobial effects of silver nanoparticles and extracts of Syzygiumcumini flowers and seeds: Periodontal, cariogenic and opportunistic pathogens. *Arch. Oral Biol.* **2021**, *125*, 105101. [CrossRef]
253. Kara, Z.; Sabır, A.; Koç, F.; Sabır, F.K.; Avcı, A.; Koplay, M.; Doğan, O. Silver Nanoparticles Synthesis by Grape Seeds (Vitis vinifera L.) Extract and Rooting Effect on Grape Cuttings. *Erwerbs-Obstbau* **2021**, 1–8. [CrossRef]
254. Alkhathlan, A.H.; AL-Abdulkarim, H.A.; Khan, M.; Khan, M.; AlDobiy, A.; Alkholief, M.; Alshamsan, A.; Alkhathlan, H.Z.; Siddiqui, M.R.H. Ecofriendly Synthesis of Silver Nanoparticles Using Aqueous Extracts of Zingiber officinale (Ginger) and Nigella sativa L. Seeds (Black Cumin) and Comparison of Their Antibacterial Potential. *Sustainability* **2020**, *12*, 10523. [CrossRef]
255. Dinparvar, S.; Bagirova, M.; Allahverdiyev, A.M.; Abamor, E.S.; Safarov, T.; Aydogdu, M.; Aktaş, D. A nanotechnology-based new approach in the treatment of breast cancer: Biosynthesized silver nanoparticles using Cuminum cyminum L. seed extract. *J. Photochem. Photobiol. B Biol.* **2020**, *208*, 111902. [CrossRef]
256. Muthu, K.; Rajeswari, S.; Akilandaeaswari, B.; Nagasundari, S.M.; Rangasamy, R. Synthesis, characterisation and photocatalytic activity of silver nanoparticles stabilised by Punica granatum seeds extract. *Mater. Technol.* **2020**, *36*, 684–693. [CrossRef]
257. Hernández-Morales, L.; Espinoza-Gómez, H.; Flores-López, L.Z.; Sotelo-Barrera, E.L.; Núñez-Rivera, A.; Cadena-Nava, R.D.; Alonso-Núñez, G.; Espinoza, K.A. Study of the green synthesis of silver nanoparticles using a natural extract of dark or white Salvia hispanica L. seeds and their antibacterial application. *Appl. Surf. Sci.* **2019**, *489*, 952–961. [CrossRef]
258. Naidu, K.S.B.; Murugan, N.; Adam, J.K. Biogenic synthesis of silver nanoparticles from avicennia marina seed extract and its antibacterial potential. *Bionanoscience* **2019**, *9*, 266–273. [CrossRef]
259. Rautela, A.; Rani, J.; Das, M.D. Green synthesis of silver nanoparticles from Tectona grandis seeds extract: Characterization and mechanism of antimicrobial action on different microorganisms. *J. Anal. Sci. Technol.* **2019**, *10*, 5. [CrossRef]
260. Palithya, S.; Gaddam, S.A.; Kotakadi, V.S.; Penchalaneni, J.; Golla, N.; Krishna, S.B.N.; Naidu, C.V. Green synthesis of silver nanoparticles using flower extracts of Aervalanata and their biomedical applications. *Part. Sci. Technol.* **2021**, *10*, 1–13. [CrossRef]
261. Hasan, K.F.; Horváth, P.G.; Horváth, A.; Alpár, T. Coloration of woven glass fabric using biosynthesized silver nanoparticles from Fraxinus excelsior tree flower. *Inorg. Chem. Commun.* **2021**, *126*, 108477. [CrossRef]
262. Aravind, M.; Ahmad, A.; Ahmad, I.; Amalanathan, M.; Naseem, K.; Mary, S.M.M.; Parvathiraja, C.; Hussain, S.; Algarni, T.S.; Pervaiz, M.; et al. Critical green routing synthesis of silver NPs using jasmine flower extract for biological activities and photocatalytical degradation of methylene blue. *J. Environ. Chem. Eng.* **2020**, *9*, 104877. [CrossRef]
263. Narkevica, I.; Stradina, L.; Stipniece, L.; Jakobsons, E.; Ozolins, J. Electrophoretic deposition of nanocrystalline TiO 2 particles on porous TiO 2-x ceramic scaffolds for biomedical applications. *J. Eur. Ceram. Soc.* **2017**, *37*, 3185–3193. [CrossRef]

264. Pant, B.; Park, M.; Park, S.-J. TiO2 NPs Assembled into a Carbon Nanofiber Composite Electrode by a One-Step Electrospinning Process for Supercapacitor Applications. *Polymers* **2019**, *11*, 899. [CrossRef] [PubMed]
265. Irshad, M.A.; Nawaz, R.; Rehman, M.Z.U.; Imran, M.; Ahmad, J.; Ahmad, S.; Inam, A.; Razzaq, A.; Rizwan, M.; Ali, S. Synthesis and characterization of titanium dioxide nanoparticles by chemical and green methods and their antifungal activities against wheat rust. *Chemosphere* **2020**, *258*, 127352. [CrossRef]
266. Mollavali, M.; Falamaki, C.; Rohani, S. Efficient light harvesting by NiS/CdS/ZnS NPs incorporated in C, N-co-doped-TiO2 nanotube arrays as visible-light sensitive multilayer photoanode for solar applications. *Int. J. Hydrog. Energy* **2018**, *43*, 9259–9278. [CrossRef]
267. Julkapli, N.M.; Bagheri, S.; Hamid, S.B.A. Recent Advances in Heterogeneous Photocatalytic Decolorization of Synthetic Dyes. *Sci. World J.* **2014**, *2014*, 1–25. [CrossRef]
268. Ziental, D.; Czarczynska-Goslinska, B.; Mlynarczyk, D.T.; Glowacka-Sobotta, A.; Stanisz, B.; Goslinski, T.; Sobotta, L. Titanium Dioxide Nanoparticles: Prospects and Applications in Medicine. *Nanomaterials* **2020**, *10*, 387. [CrossRef] [PubMed]
269. Pirkanniemi, K.; Sillanpää, M. Heterogeneous water phase catalysis as an environmental application: A review. *Chemosphere* **2002**, *48*, 1047–1060. [CrossRef]
270. Valencia, S.; Vargas, X.; Rios, L.; Restrepo, G.; Marín, J.M. Sol–gel and low-temperature solvothermal synthesis of photoactive nano-titanium dioxide. *J. Photochem. Photobiol. A Chem.* **2012**, *251*, 175–181. [CrossRef]
271. Chen, Y.-F.; Tsai, H.-Y.; Wu, T.-S. Anti-Inflammatory and Analgesic Activities from Roots ofAngelica pubescens. *Planta Medica* **1995**, *61*, 2–8. [CrossRef] [PubMed]
272. Jayaseelan, C.; Rahuman, A.A.; Roopan, S.M.; Kirthi, A.V.; Venkatesan, J.; Kim, S.K.; Iyappan, M.; Siva, C. Biological approach to synthesize TiO2 nanoparticles using Aeromonas hydrophila and its antibacterial activity. *Spectrochim. Acta Part A Mol. Biomol. Spectrosc.* **2013**, *107*, 82–89. [CrossRef] [PubMed]
273. Mittal, A.K.; Bhaumik, J.; Kumar, S.; Banerjee, U.C. Biosynthesis of silver nanoparticles: Elucidation of prospective mechanism and therapeutic potential. *J. Colloid Interface Sci.* **2014**, *415*, 39–47. [CrossRef]
274. Khan, M. Preparation, Characterization and Applications of Polyaniline Impregnated Silica Gel for the Identification and Separation of Some Important Organics. Ph.D. Dissertation, Aligarh Muslim University, Aligarh, India, 2018.
275. Ahmad, W.; Jaiswal, K.K.; Soni, S. Green synthesis of titanium dioxide (TiO2) nanoparticles by using Mentha arvensis leaves extract and its antimicrobial properties. *Inorg. Nano Metal Chem.* **2020**, *50*, 1032–1038. [CrossRef]
276. Narayanan, M.; Devi, P.G.; Natarajan, D.; Kandasamy, S.; Devarayan, K.; Alsehli, M.; Elfasakhany, A.; Pugazhendhi, A. Green synthesis and characterization of titanium dioxide nanoparticles using leaf extract of Pouteria campechiana and larvicidal and pupicidal activity on Aedes aegypti. *Environ. Res.* **2021**, *200*, 111333. [CrossRef] [PubMed]
277. Narayanan, M.; Vigneshwari, P.; Natarajan, D.; Kandasamy, S.; Alsehli, M.; Elfasakhany, A.; Pugazhendhi, A. Synthesis and characterization of TiO2 NPs by aqueous leaf extract of Coleus aromaticus and assess their antibacterial, larvicidal, and anticancer potential. *Environ. Res.* **2021**, *200*, 111335. [CrossRef] [PubMed]
278. Zubair, M.; Husain, F.M.; Qais, F.A.; Alam, P.; Ahmad, I.; Albalawi, T.; Ahmad, N.; Alam, M.; Baig, M.H.; Dong, J.J.; et al. Bio-fabrication of titanium oxide nanoparticles from Ochradenusarabicus to obliterate biofilms of drug-resistant Staphylococcus aureus and Pseudomonas aeruginosa isolated from diabetic foot infections. *Appl. Nanosci.* **2021**, *11*, 375–387. [CrossRef]
279. Ahmad, W.; Singh, A.; Jaiswal, K.K.; Gupta, P. Green Synthesis of Photocatalytic TiO2 Nanoparticles for Potential Application in Photochemical Degradation of Ornidazole. *J. Inorg. Organomet. Polym. Mater.* **2020**, *31*, 614–623. [CrossRef]
280. Thakur, B.; Kumar, A.; Kumar, D. Green synthesis of titanium dioxide nanoparticles using Azadirachta indica leaf extract and evaluation of their antibacterial activity. *South Afr. J. Bot.* **2019**, *124*, 223–227. [CrossRef]
281. Kaur, H.; Kaur, S.; Singh, J.; Rawat, M.; Kumar, S. Expanding horizon: Green synthesis of TiO2 nanoparticles using Carica papaya leaves for photocatalysis application. *Mater. Res. Express* **2019**, *6*, 095034. [CrossRef]
282. Rajkumari, J.; Magdalane, C.M.; Siddhardha, B.; Madhavan, J.; Ramalingam, G.; Al-Dhabi, N.A.; Arasu, M.V.; Ghilan, A.; Duraipandiayan, V.; Kaviyarasu, K. Synthesis of titanium oxide nanoparticles using Aloe barbadensis mill and evaluation of its antibiofilm potential against Pseudomonas aeruginosa PAO1. *J. Photochem. Photobiol. B Biol.* **2019**, *201*, 111667. [CrossRef]
283. Bavanilatha, M.; Yoshitha, L.; Nivedhitha, S.; Sahithya, S. Bioactive studies of TiO2 nanoparticles synthesized using Glycyrrhiza glabra. *Biocatal. Agric. Biotechnol.* **2019**, *19*. [CrossRef]
284. Aravind, M.; Amalanathan, M.; Mary, M.S.M. Synthesis of TiO2 nanoparticles by chemical and green synthesis methods and their multifaceted properties. *SN Appl. Sci.* **2021**, *3*, 1–10. [CrossRef]
285. Sagadevan, S.; Lett, J.A.; Vennila, S.; Prasath, P.V.; Kaliaraj, G.S.; Fatimah, I.; Léonard, E.; Mohammad, F.; Al-Lohedan, H.A.; Alshahateet, S.F.; et al. Photocatalytic activity and antibacterial efficacy of titanium dioxide nanoparticles mediated by Myristica fragrans seed extract. *Chem. Phys. Lett.* **2021**, *771*, 138527. [CrossRef]
286. Mathew, S.S.; Sunny, N.E.; Shanmugam, V. Green synthesis of anatase titanium dioxide nanoparticles using Cuminum cyminum seed extract; effect on Mung bean (Vigna radiata) seed germination. *Inorg. Chem. Commun.* **2021**, *126*, 108485. [CrossRef]
287. Perveen, K.; Husain, F.M.; Qais, F.A.; Khan, A.; Razak, S.; Afsar, T.; Alam, P.; Almajwal, A.M.; Abulmeaty, M. Microwave-Assisted Rapid Green Synthesis of Gold Nanoparticles Using Seed Extract of Trachyspermumammi: ROS Mediated Biofilm Inhibition and Anticancer Activity. *Biomolecules* **2021**, *11*, 197. [CrossRef] [PubMed]

288. Isacfranklin, M.; Yuvakkumar, R.; Ravi, G.; Kumar, P.; Saravanakumar, B.; Velauthapillai, D.; Alahmadi, T.A.; Alharbi, S.A. Biomedical application of single anatase phase TiO2 nanoparticles with addition of Rambutan (Nephelium lappaceum L.) fruit peel extract. *Appl. Nanosci.* **2020**, *11*, 699–708. [CrossRef]
289. Krishnan, B.; Mahalingam, S. Improved surface morphology of silver/copper oxide/bentonite nanocomposite using aliphatic ammonium based ionic liquid for enhanced biological activities. *J. Mol. Liq.* **2017**, *241*, 1044–1058. [CrossRef]
290. Rafea, M.A.; Roushdy, N. Determination of the optical band gap for amorphous and nanocrystalline copper oxide thin films prepared by SILAR technique. *J. Phys. D Appl. Phys.* **2008**, *42*, 015413. [CrossRef]
291. Ren, G.; Hu, D.; Cheng, E.W.; Vargas-Reus, M.A.; Reip, P.; Allaker, R.P. Characterisation of copper oxide nanoparticles for antimicrobial applications. *Int. J. Antimicrob. Agents* **2009**, *33*, 587–590. [CrossRef]
292. Verma, N.; Kumar, N. Synthesis and biomedical applications of copper oxide nanoparticles: An expanding horizon. *ACS Biomater. Sci. Eng.* **2019**, *5*, 1170–1188. [CrossRef]
293. Chang, M.-H.; Liu, H.-S.; Tai, C.Y. Preparation of copper oxide nanoparticles and its application in nanofluid. *Powder Technol.* **2011**, *207*, 378–386. [CrossRef]
294. Devi, H.S.; Singh, T.D. Synthesis of copper oxide nanoparticles by a novel method and its application in the degradation of methyl orange. *Adv. Electron. Electr. Eng.* **2014**, *4*, 83–88.
295. Vasantharaj, S.; Sathiyavimal, S.; Saravanan, M.; Senthilkumar, P.; Gnanasekaran, K.; Shanmugavel, M.; Manikandan, E.; Pugazhendhi, A. Synthesis of ecofriendly copper oxide nanoparticles for fabrication over textile fabrics: Characterization of antibacterial activity and dye degradation potential. *J. Photochem. Photobiol. B: Biol.* **2018**, *191*, 143–149. [CrossRef]
296. Rehana, D.; Mahendiran, D.; Kumar, R.S.; Rahiman, A.K. Evaluation of antioxidant and anticancer activity of copper oxide nanoparticles synthesized using medicinally important plant extracts. *Biomed. Pharmacother.* **2017**, *89*, 1067–1077. [CrossRef] [PubMed]
297. Obaid, M.A.; Harbi, K.H.; Abd, A.N. Study the effect of antibacterial on the chemically prepared copper oxide. *Mater. Today: Proc.* **2021**, *47*, 6006–6010.
298. Singh, A.; Singh, N.; Hussain, I.; Singh, H. Effect of biologically synthesized copper oxide nanoparticles on metabolism and antioxidant activity to the crop plants Solanum lycopersicum and Brassica oleracea var. botrytis. *J. Biotechnol.* **2017**, *262*, 11–27. [CrossRef] [PubMed]
299. Singh, S.; Kumar, N.; Kumar, M.; Jyoti; Agarwal, A.; Mizaikoff, B. Electrochemical sensing and remediation of 4-nitrophenol using bio-synthesized copper oxide nanoparticles. *Chem. Eng. J.* **2017**, *313*, 283–292. [CrossRef]
300. Nasrollahzadeh, M.; Sajadi, S.M.; Rostami-Vartooni, A.; Hussin, S.M. Green synthesis of CuO nanoparticles using aqueous extract of Thymus vulgaris L. leaves and their catalytic performance for N-arylation of indoles and amines. *J. Colloid Interface Sci.* **2016**, *466*, 113–119. [CrossRef] [PubMed]
301. Yatish, K.; Prakash, R.M.; Ningaraju, C.; Sakar, M.; GeethaBalakrishna, R.; Lalithamba, H. Terminalia chebula as a novel green source for the synthesis of copper oxide nanoparticles and as feedstock for biodiesel production and its application on diesel engine. *Energy* **2020**, *215*, 119165. [CrossRef]
302. Ramzan, M.; Obodo, R.; Mukhtar, S.; Ilyas, S.; Aziz, F.; Thovhogi, N. Green synthesis of copper oxide nanoparticles using Cedrus deodara aqueous extract for antibacterial activity. *Mater. Today: Proc.* **2020**, *36*, 576–581. [CrossRef]
303. Sathiyavimal, S.; Vasantharaj, S.; Veeramani, V.; Saravanan, M.; Rajalakshmi, G.; Kaliannan, T.; Al-Misned, F.A.; Pugazhendhi, A. Green chemistry route of biosynthesized copper oxide nanoparticles using Psidium guajava leaf extract and their antibacterial activity and effective removal of industrial dyes. *J. Environ. Chem. Eng.* **2021**, *9*, 105033. [CrossRef]
304. Elakkiya, V.T.; Meenakshi, R.V.; Kumar, P.S.; Karthik, V.; Shankar, K.R.; Sureshkumar, P.; Hanan, A. Green synthesis of copper nanoparticles using Sesbania aculeata to enhance the plant growth and antimicrobial activities. *Int. J. Environ. Sci. Technol.* **2021**, 1–10. [CrossRef]
305. Mali, S.C.; Dhaka, A.; Githala, C.K.; Trivedi, R. Green synthesis of copper nanoparticles using CelastruspaniculatusWilld. leaf extract and their photocatalytic and antifungal properties. *Biotechnol. Rep.* **2020**, *27*, e00518. [CrossRef]
306. Andualem, W.W.; Sabir, F.K.; Mohammed, E.T.; Belay, H.H.; Gonfa, B.A. Synthesis of Copper Oxide Nanoparticles Using Plant Leaf Extract of Catha edulis and Its Antibacterial Activity. *J. Nanotechnol.* **2020**, *2020*, 1–10. [CrossRef]
307. Chandraker, S.K.; Lal, M.; Ghosh, M.K.; Tiwari, V.; Ghorai, T.K.; Shukla, R. Green synthesis of copper nanoparticles using leaf extract of Ageratum houstonianum Mill. and study of their photocatalytic and antibacterial activities. *Nano Express* **2020**, *1*, 010033. [CrossRef]
308. Ghosh, M.K.; Sahu, S.; Gupta, I.; Ghorai, T.K. Green synthesis of copper nanoparticles from an extract of Jatropha curcas leaves: Characterization, optical properties, CT-DNA binding and photocatalytic activity. *RSC Adv.* **2020**, *10*, 22027–22035. [CrossRef]
309. Rafique, M.; Shafiq, F.; Gillani, S.S.A.; Shakil, M.; Tahir, M.B.; Sadaf, I. Eco-friendly green and biosynthesis of copper oxide nanoparticles using Citrofortunella microcarpa leaves extract for efficient photocatalytic degradation of Rhodamin B dye form textile wastewater. *Optik* **2020**, *208*, 164053. [CrossRef]
310. Mali, S.C.; Raj, S.; Trivedi, R. Biosynthesis of copper oxide nanoparticles using Enicostemmaaxillare (Lam.) leaf extract. *Biochem. Biophys. Rep.* **2019**, *20*, 100699.
311. Ahmed, A.; Usman, M.; Liu, Q.-Y.; Shen, Y.-Q.; Yu, B.; Cong, H.-L. Plant mediated synthesis of copper nanoparticles by using Camelia sinensis leaves extract and their applications in dye degradation. *Ferroelectrics* **2019**, *549*, 61–69. [CrossRef]

312. Singh, P.; Singh, K.R.; Singh, J.; Das, S.N.; Singh, R.P. Tunable electrochemistry and efficient antibacterial activity of plant-mediated copper oxide nanoparticles synthesized by Annona squamosa seed extract for agricultural utility. *RSC Adv.* **2021**, *11*, 18050–18060. [CrossRef]
313. Jahagirdar, A.S.; Shende, S.; Gade, A.; Rai, M. Bioinspired Synthesis of Copper Nanoparticles and its Efficacy on Seed Viability and Seedling Growth in Mungbean (Vigna radiata L.). *Curr. Nanosci.* **2020**, *16*, 246–252. [CrossRef]
314. Venkatramanan, A.; Ilangovan, A.; Thangarajan, P.; Saravanan, A.; Mani, B. Green Synthesis of Copper Oxide Nanoparticles (CuO NPs) From Aqueous Extract of Seeds of Eletteria Cardamomum and Its Antimicrobial Activity against Pathogens. *Curr. Biotechnol.* **2021**, *9*, 304–311. [CrossRef]
315. Buazar, F.; Sweidi, S.; Badri, M.; Kroushawi, F. Biofabrication of highly pure copper oxide nanoparticles using wheat seed extract and their catalytic activity: A mechanistic approach. *Green Process. Synth.* **2019**, *8*, 691–702. [CrossRef]
316. Roy, K.; Ghosh, C.K.; Sarkar, C.K. Selective amino acid detection by green synthesized copper nanoparticles prepared using basil (Ocimumtenuiflorum) flower extract. *Microsyst. Technol.* **2021**, *27*, 353–357. [CrossRef]
317. Veisi, H.; Karmakar, B.; Tamoradi, T.; Hemmati, S.; Hekmati, M.; Hamelian, M. Biosynthesis of CuO nanoparticles using aqueous extract of herbal tea (Stachys Lavandulifolia) flowers and evaluation of its catalytic activity. *Sci. Rep.* **2021**, *11*, 1–13. [CrossRef]
318. Siddiqui, V.U.; Ansari, A.; Chauhan, R.; Siddiqi, W.A. Green synthesis of copper oxide (CuO) nanoparticles by Punica granatum peel extract. *Mater. Today: Proc.* **2020**, *36*, 751–755. [CrossRef]
319. Ramimoghadam, D.; Bagheri, S.; Hamid, S.B.A. Progress in electrochemical synthesis of magnetic iron oxide nanoparticles. *J. Magn. Magn. Mater.* **2014**, *368*, 207–229. [CrossRef]
320. Teja, A.S.; Koh, P.Y. Synthesis, properties, and applications of magnetic iron oxide nanoparticles. *Prog. Cryst. Growth Charact. Mater.* **2009**, *2*, 22–45. [CrossRef]
321. Faraji, M.; Yamini, Y.; Rezaee, M. Magnetic nanoparticles: Synthesis, stabilization, functionalization, characterization, and applications. *J. Iran. Chem. Soc.* **2010**, *7*, 1–37. [CrossRef]
322. Arjaghi, S.K.; Alasl, M.K.; Sajjadi, N.; Fataei, E.; Rajaei, G.E. Green Synthesis of Iron Oxide Nanoparticles by RS Lichen Extract and its Application in Removing Heavy Metals of Lead and Cadmium. *Biol. Trace Elem. Res.* **2021**, *199*, 763–768. [CrossRef] [PubMed]
323. Ardakani, L.S.; Alimardani, V.; Tamaddon, A.M.; Amani, A.M.; Taghizadeh, S. Green synthesis of iron-based nanoparticles using Chlorophytum comosum leaf extract: Methyl orange dye degradation and antimicrobial properties. *Heliyon* **2021**, *7*, e06159. [CrossRef] [PubMed]
324. Jamzad, M.; Bidkorpeh, M.K. Green synthesis of iron oxide nanoparticles by the aqueous extract of Laurus nobilis L. leaves and evaluation of the antimicrobial activity. *J. Nanostructure Chem.* **2020**, *10*, 193–201. [CrossRef]
325. Bhuiyan, S.H.; Miah, M.Y.; Paul, S.C.; Das Aka, T.; Saha, O.; Rahaman, M.; Sharif, J.I.; Habiba, O. Ashaduzzaman Green synthesis of iron oxide nanoparticle using Carica papaya leaf extract: Application for photocatalytic degradation of remazol yellow RR dye and antibacterial activity. *Heliyon* **2020**, *6*, e04603. [CrossRef] [PubMed]
326. Vitta, Y.; Figueroa, M.; Calderon, M.; Ciangherotti, C. Synthesis of iron nanoparticles from aqueous extract of Eucalyptus robustaSm and evaluation of antioxidant and antimicrobial activity. *Mater. Sci. Energy Technol.* **2020**, *3*, 97–103.
327. Vasantharaj, S.; Sathiyavimal, S.; Senthilkumar, P.; LewisOscar, F.; Pugazhendhi, A. Biosynthesis of iron oxide nanoparticles using leaf extract of Ruellia tuberosa: Antimicrobial properties and their applications in photocatalytic degradation. *J. Photochem. Photobiol. B Biol.* **2019**, *192*, 74–82. [CrossRef]
328. Lohrasbi, S.; Kouhbanani, M.A.J.; Beheshtkhoo, N.; Ghasemi, Y.; Amani, A.M.; Taghizadeh, S. Green Synthesis of Iron Nanoparticles Using Plantago major Leaf Extract and Their Application as a Catalyst for the Decolorization of Azo Dye. *BioNanoScience* **2019**, *9*, 317–322. [CrossRef]
329. Karpagavinayagam, P.; Vedhi, C. Green synthesis of iron oxide nanoparticles using Avicennia marina flower extract. *Vacuum* **2018**, *160*, 286–292. [CrossRef]
330. Bibi, I.; Nazar, N.; Ata, S.; Sultan, M.; Ali, A.; Abbas, A.; Jilani, K.; Kamal, S.; Sarim, F.M.; Khan, M.I.; et al. Green synthesis of iron oxide nanoparticles using pomegranate seeds extract and photocatalytic activity evaluation for the degradation of textile dye. *J. Mater. Res. Technol.* **2019**, *8*, 6115–6124. [CrossRef]
331. Sandhya, J.; Kalaiselvam, S. Biogenic synthesis of magnetic iron oxide nanoparticles using inedible borassus flabellifer seed coat: Characterization, antimicrobial, antioxidant activity and in vitro cytotoxicity analysis. *Mater. Res. Express* **2019**, *7*, 015045. [CrossRef]
332. Aziz, W.J.; Abid, M.A.; Kadhim, D.A.; Mejbel, M.K. Synthesis of iron oxide (β-fe2o3) nanoparticles from Iraqi grapes extract and its biomedical application. In *IOP Conference Series: Materials Science and Engineering*; IOP Publishing: London, UK, 2020; Volume 881.
333. Rostamizadeh, E.; Iranbakhsh, A.; Majd, A.; Arbabian, S.; Mehregan, I. Green synthesis of Fe2O3 nanoparticles using fruit extract of Cornus mas L. and its growth-promoting roles in Barley. *J. Nanostructure Chem.* **2020**, *10*, 125–131. [CrossRef]
334. Iravani, S.; Varma, R.S. Sustainable synthesis of cobalt and cobalt oxide nanoparticles and their catalytic and biomedical applications. *Green Chem.* **2020**, *22*, 2643–2661. [CrossRef]
335. Yu, Y.; Mendoza-Garcia, A.; Ning, B.; Sun, S. Cobalt-substituted magnetite nanoparticles and their assembly into ferrimagnetic nanoparticle arrays. *Adv. Mater.* **2013**, *25*, 3090–3094. [CrossRef] [PubMed]

336. Raveau, B.; Seikh, M.M. Charge ordering in cobalt oxides: Impact on structure, magnetic and transport properties. *Z. Anorg. Allg. Chem.* **2015**, *9*, 1385–1394. [CrossRef]
337. Liu, J.; Wang, Z.; Yan, X.; Jian, P. Metallic cobalt nanoparticles imbedded into ordered mesoporous carbon: A non-precious metal catalyst with excellent hydrogenation performance. *J. Colloid Interface Sci.* **2017**, *505*, 789–795. [CrossRef] [PubMed]
338. Su, Y.; Zhu, Y.; Jiang, H.; Shen, J.; Yang, X.; Zou, W.; Chen, J.; Li, C. Cobalt nanoparticles embedded in N-doped carbon as an efficient bifunctional electrocatalyst for oxygen reduction and evolution reactions. *Nanoscale* **2014**, *6*, 15080–15089. [CrossRef]
339. Diallo, A.; Beye, A.; Doyle, T.; Park, E.; Maaza, M. Green synthesis of Co3O4nanoparticles viaAspalathus linearis: Physical properties. *Green Chem. Lett. Rev.* **2015**, *8*, 30–36. [CrossRef]
340. Memon, S.A.; Hassan, D.; Buledi, J.A.; Solangi, A.R.; Memon, S.Q.; Palabiyik, I.M. Plant material protected cobalt oxide nanoparticles: Sensitive electro-catalyst for tramadol detection. *Microchem. J.* **2020**, *159*, 105480. [CrossRef]
341. Khan, M.A.; Ali, F.; Faisal, S.; Rizwan, M.; Hussain, Z.; Zaman, N.; Afsheen, Z.; Uddin, M.N.; Bibi, N. Exploring the therapeutic potential of Hibiscus rosa sinensis synthesized cobalt oxide (Co3O4-NPs) and magnesium oxide nanoparticles (MgO-NPs). *Saudi J. Biol. Sci.* **2021**, *28*, 5157–5167.
342. Khadhim, A.I.; Kadhim, R.E. Synthesis of Cobalt Nanoparticles Biologically by Conocarpus erectus L. Aqueous Leaves Extract. *Ann. Rom. Soc. Cell Biol.* **2021**, *25*, 5361–5372.
343. Raeisi, M.; Alijani, H.Q.; Peydayesh, M.; Khatami, M.; Baravati, F.B.; Borhani, F.; Šlouf, M.; Soltaninezhad, S. Magnetic cobalt oxide nanosheets: Green synthesis and in vitro cytotoxicity. *Bioprocess Biosyst. Eng.* **2021**, *44*, 1423–1432. [CrossRef]
344. Akhlaghi, N.; Najafpour-Darzi, G.; Younesi, H. Facile and green synthesis of cobalt oxide nanoparticles using ethanolic extract of Trigonella foenumgraceum (Fenugreek) leaves. *Adv. Powder Technol.* **2020**, *31*, 3562–3569. [CrossRef]
345. Hafeez, M.; Shaheen, R.; Akram, B.; Abdin, Z.U.; Haq, S.; Mahsud, S.; Ali, S.; Khan, R.T. Green synthesis of cobalt oxide nanoparticles for potential biological applications. *Mater. Res. Express* **2020**, *7*, 025019. [CrossRef]
346. Iqbal, J.; Abbasi, B.A.; Batool, R.; Khalil, A.T.; Hameed, S.; Kanwal, S.; Ullah, I.; Mahmood, T. Biogenic synthesis of green and cost effective cobalt oxide nanoparticles using Geranium wallichianum leaves extract and evaluation of in vitro antioxidant, antimicrobial, cytotoxic and enzyme inhibition properties. *Mater. Res. Express* **2019**, *6*, 115407. [CrossRef]
347. Sondi, I.; Salopek-Sondi, B. Silver nanoparticles as antimicrobial agent: A case study on E. coli as a model for Gram-negative bacteria. *J. Colloid Interface Sci.* **2004**, *275*, 177–182. [CrossRef]
348. Kasthuri, J.; Kathiravan, K.; Rajendiran, N. Phyllanthin-assisted biosynthesis of silver and gold nanoparticles: A novel biological approach. *J. Nanoparticle Res.* **2008**, *11*, 1075–1085. [CrossRef]
349. Ansari, M.A.; Khan, H.M.; Khan, A.A. Evaluation of antibacterial activity of silver nanoparticles against MSSA and MSRA on isolates from skin infections. *Biol. Med.* **2011**, *3*, 141–146.
350. Kaviya, S.; Santhanalakshmi, J.; Viswanathan, B.; Muthumary, J.; Srinivasan, K. Biosynthesis of silver nanoparticles using citrus sinensis peel extract and its antibacterial activity. *Spectrochim. Acta Part A: Mol. Biomol. Spectrosc.* **2011**, *79*, 594–598. [CrossRef]
351. Logeswari, P.; Silambarasan, S.; Abraham, J. Synthesis of silver nanoparticles using plants extract and analysis of their antimicrobial property. *J. Saudi Chem. Soc.* **2015**, *19*, 311–317. [CrossRef]
352. Gardea-Torresdey, J.L.; Parsons, J.G.; Gomez, E.; Peralta-Videa, J.; Troiani, H.E.; Santiago, P.; Yacaman, M.J. Formation and Growth of Au Nanoparticles inside Live Alfalfa Plants. *Nano Lett.* **2002**, *2*, 397–401. [CrossRef]
353. Akhtar, M.S.; Panwar, J.; Yun, Y.-S. Biogenic Synthesis of Metallic Nanoparticles by Plant Extracts. *ACS Sustain. Chem. Eng.* **2013**, *1*, 591–602. [CrossRef]
354. Raghunandan, D.; Ravishankar, B.; Sharanbasava, G.; Mahesh, D.B.; Harsoor, V.; Yalagatti, M.S.; Bhagawanraju, M.; Venkataraman, A. Anti-cancer studies of noble metal nanoparticles synthesized using different plant extracts. *Cancer Nanotechnol.* **2011**, *2*, 57–65. [CrossRef] [PubMed]
355. Das, S.; Das, J.; Samadder, A.; Bhattacharyya, S.S.; Das, D.; Khuda-Bukhsh, A.R. Biosynthesized silver nanoparticles by ethanolic extracts of Phytolacca decandra, Gelsemium sempervirens, Hydrastis canadensis and Thuja occidentalis induce differential cytotoxicity through G2/M arrest in A375 cells. *Colloids Surfaces B: Biointerfaces* **2013**, *101*, 325–336. [CrossRef]
356. Alt, V.; Bechert, T.; Steinrücke, P.; Wagener, M.; Seidel, P.; Dingeldein, E.; Domann, E.; Schnettler, R. An in vitro assessment of the antibacterial properties and cytotoxicity of nanoparticulate silver bone cement. *Biomaterials* **2004**, *25*, 4383–4391. [CrossRef]